ANTIOXIDANTS & REDOX SIGNALING
Volume 31, Number 3, 2019
© Mary Ann Liebert, Inc.
DOI: 10.1089/ars.2018.7617

COMPREHENSIVE INVITED REVIEW

Redox Homeostasis in Photosynthetic Organisms: Novel and Established Thiol-Based Molecular Mechanisms

Mirko Zaffagnini,[1] Simona Fermani,[2] Christophe H. Marchand,[3] Alex Costa,[4] Francesca Sparla,[1] Nicolas Rouhier,[5] Peter Geigenberger,[6] Stéphane D. Lemaire,[3] and Paolo Trost[1]

Downloaded by LI CO SA/50127/MI from www.liebertpub.com at 07/22/19. For personal use only.

Abstract

Significance: Redox homeostasis consists of an intricate network of reactions in which reactive molecular species, redox modifications, and redox proteins act in concert to allow both physiological responses and adaptation to stress conditions.

Recent Advances: This review highlights established and novel thiol-based regulatory pathways underlying the functional facets and significance of redox biology in photosynthetic organisms. In the last decades, the field of redox regulation has largely expanded and this work is aimed at giving the right credit to the importance of thiol-based regulatory and signaling mechanisms in plants.

Critical Issues: This cannot be all-encompassing, but is intended to provide a comprehensive overview on the structural/molecular mechanisms governing the most relevant thiol switching modifications with emphasis on the large genetic and functional diversity of redox controllers (*i.e.*, redoxins). We also summarize the different proteomic-based approaches aimed at investigating the dynamics of redox modifications and the recent evidence that extends the possibility to monitor the cellular redox state *in vivo*. The physiological relevance of redox transitions is discussed based on reverse genetic studies confirming the importance of redox homeostasis in plant growth, development, and stress responses.

Future Directions: In conclusion, we can firmly assume that redox biology has acquired an established significance that virtually infiltrates all aspects of plant physiology. *Antioxid. Redox Signal.* 31, 155–210.

Keywords: redox homeostasis, cysteine, photosynthetic organisms, thiol switching, redox proteomics, redox sensors

Table of Contents

Reviewing Editors: *Plamena Angelova, Monica Balsera, Maria Borisova-Mubarakshina, Christine Foyer, Christian Gruber, Jean-Pierre Jacquot, Robert Hancock and Thomas Kieselbach*

Departments of [1]Pharmacy and Biotechnology and [2]Chemistry Giacomo Ciamician, University of Bologna, Bologna, Italy.
[3]Laboratoire de Biologie Moléculaire et Cellulaire des Eucaryotes, UMR8226, Centre National de la Recherche Scientifique, Institut de Biologie Physico-Chimique, Sorbonne Université, Paris, France.
[4]Department of Biosciences, University of Milan, Milan, Italy.
[5]Inra, IAM, Université de Lorraine, Nancy, France.
[6]Department Biologie I, Ludwig-Maximilians-Universität München, LMU Biozentrum, Martinsried, Germany.

Downloaded by LI CO SA/50127/MI from www.liebertpub.com at 07/22/19. For personal use only.

I. Introduction

THE RESEARCH FIELD OF REDOX regulation and signaling in aerobic organisms, including humans and microbes, has received a great impetus from early studies conducted on plants. During the 60s and the 70s of the past century, a decade after the discovery of the photosynthetic CO_2 fixation cycle, now known as the Calvin–Benson (CB) cycle, it was observed that some CB cycle enzymes were activated in the light and inactivated in the dark, indicating that the CB cycle was temporally coupled to the light reactions of photosynthesis (397) [for a recent review see (339)]. Light activation *in vivo* was first demonstrated for chloroplast glyceraldehyde-3-phosphate dehydrogenase (GAPDH) (13, 595), and in the next years for phosphoribulokinase (PRK) (279), and the two phosphatases, namely fructose-1,6-bisphosphate phosphatase (FBPase) (23) and sedoheptulose-1,7-biphosphate phosphatase (SBPase) (12). A mechanistic explanation of these results was essentially provided by Bob Buchanan and collaborators (Peter Schürmann and Ricardo Wolosiuk *in primis*) in a series of articles that marked the birth of the plant redox field (57, 58, 455, 457, 538, 540, 541). Light activation of CB cycle enzymes was proposed to depend on a novel electron chain made by the interaction of three types of stromal proteins: ferredoxin (FDX, an iron–sulfur [Fe-S] protein, where electrons come in from photosystem I [PSI]), FDX:thioredoxin reductase (FTR, a protein containing an Fe-S cluster functionally and physically connected with a disulfide), and thioredoxin (TRX), which also contains two cysteines (Cys) able to reversibly form a disulfide bond (Fig. 1A). By means of this transduction chain, target enzymes are reduced and hence activated in the light (Fig. 1B). In the absence of light, electrons were believed to return to oxygen leaving oxidized enzymes in the inactive form (456). Interestingly, at that time, TRX was only known as a protein involved in ribonucleotide reduction in bacteria and the demonstration of its role in the regulation of chloroplast metabolism opened a wide array of possibilities for the development of redox biology concepts in all aerobic organisms (54).

Once established the FDX–FTR–TRX system (hereafter named FDX–TRX system) in plants, new discoveries in the field were obtained in the following decades. By the end of the century, the targets of the system approached the number 25, including 4 enzymes and 2 regulatory proteins of the CB cycle (529, 539, 587), several other metabolic enzymes including NADP-malate dehydrogenase (NADP-MDH) (240, 448) and glucose-6-phosphate dehydrogenase (G6PDH), the

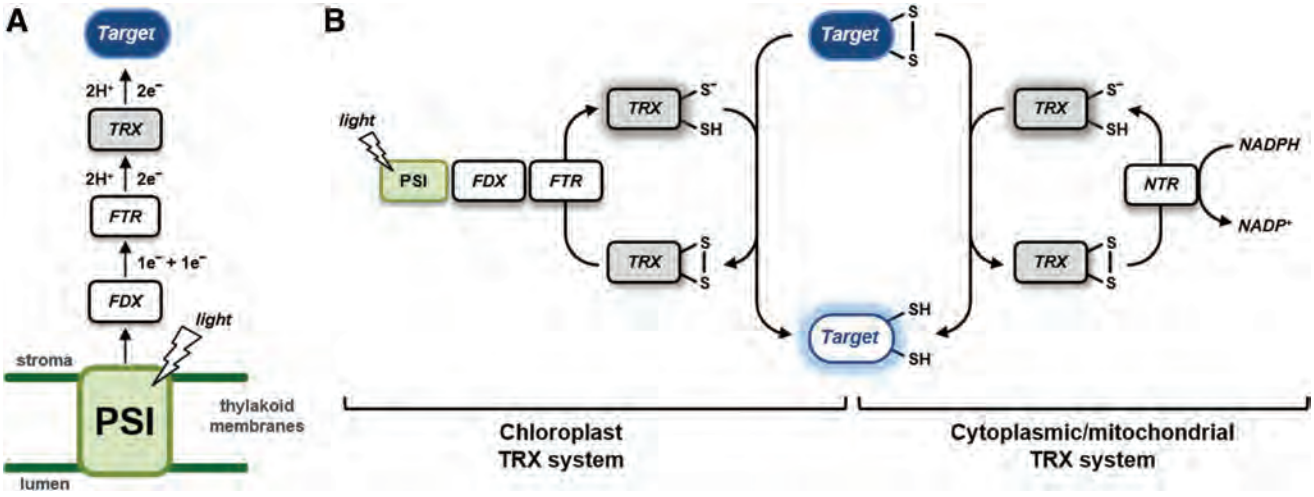

FIG. 1. TRX-dependent redox systems. (A) Schematic representation of the FDX–TRX system of oxygenic photosynthetic organisms. In illuminated chloroplasts, FDX distributes PSI-driven electrons ($1e^-$ plus $1e^-$) to oxidized TRX in a reaction catalyzed by FTR ($2e^-$ plus $2H^+$). In turn, TRX reduces target proteins *via* a dithiol–disulfide exchange reaction ($2e^-$ plus $2H^+$). **(B)** Dithiol–disulfide interchanges of chloroplastic and cytoplasmic/mitochondrial TRX systems. Chloroplastic TRXs are reduced as described previously, whereas cytoplasmic/mitochondrial TRXs are reduced by NTR that uses NADPH as electron donor. Once reduced, TRX catalyzes the reduction of regulatory disulfides on target proteins. FDX, ferredoxin; FTR, ferredoxin:thioredoxin reductase; NTR, NADPH:TRX reductase; PSI, photosystem I; TRX, thioredoxin. Color images are available online.

latter remaining the prototypical example of enzymes that are inhibited, rather than activated, by disulfide reduction in plants (448). Moreover, the FDX–TRX system was found to be operative also in amyloplasts (nonphotosynthetic plastids) where FDX is reduced by metabolically produced NADPH rather than by light (25). Knowledge on TRX diversity was limited to chloroplastic TRX *f* and *m*, with the addition of cytoplasmic TRX *h*, which can be reduced by NADPH:TRX reductase (NTR) using NADPH as electron donor (Fig. 1B). The first structural studies on TRX-regulated enzymes (FBPase and NADP-MDH) appeared in the late 90s providing nice explanations of how redox regulation could operate at the atomic level, at least in these proteins (55, 286, 339, 456). NADP-MDH, in particular, constituted an interesting case. Its mechanism of regulation, based on C- and N-terminal extensions containing Cys pairs able to form internal disulfides under the control of TRXs, was found to be similar to other proteins such as GAPDH (143) and CP12 (144). Another important achievement of the recent past was the ability to determine, *in vitro*, the redox potential of the different dithiol–disulfide interchange reactions (223), which allowed the development of hypotheses concerning the reciprocal influence between TRX and target proteins redox states *in vivo* (92, 93, 222, 223, 266, 267, 322).

Besides the chloroplast pathway for regulatory disulfides reduction, mechanisms of disulfides formation were also investigated. Current knowledge suggests that formation of regulatory disulfides in chloroplasts may involve particular types of TRXs (111, 133, 561) that shuttle electrons from reduced target proteins to 2-Cys peroxiredoxin (2-Cys PRX) and then to hydrogen peroxide (H_2O_2) (see section VII). These findings imply that H_2O_2, rather than oxygen, may be the terminal electron acceptor used for downregulating the TRX-activated enzymes. This example nicely fits into the general concept, largely developed in the past decades, that the manifold interactions between reactive molecular species (RMS) and active protein thiols often play essential physiological roles. However, protein disulfides may also play structural rather than regulatory roles, and the formation of structural disulfides is a compulsory step in the correct folding of several proteins. Systems controlling the oxidative protein folding generally rely on two types of proteins, isomerase and oxidase, forming an electron chain that connects the target protein (where the disulfide is formed) to the terminal acceptor (430). In plant cells, systems of this type are present, at least, in the lumen of the endoplasmic reticulum (190), in the lumen of thylakoids (256), and in the intermembrane space of mitochondria (72). Different protein components and final electron acceptors are used in different locations. For detailed analyses of oxidative protein folding in plants, the reader might refer to other reviews that cover the subject (7, 192, 334, 384).

At the end of the past century, redox regulation in plants was perceived as an established physiological mechanism somehow limited in scope, as it appeared to be essentially required for separating photosynthetic carbon fixation occurring in the light, from catabolic reactions occurring in the dark in the same organelle, thereby preventing dangerous futile cycles (54). Twenty years later, the concept is still valid and strongly supported by experimental data, but the field of redox regulation in plants has witnessed an incredible expansion in many new directions. In this context, this comprehensive invited review tries to give the right credit to the recent explosion of thiol-based redox regulation and signaling studies in plants.

The review is organized in sections (sections II–VII) focused on the topics that in our view represent most significantly the scientific developments achieved in the plant redox field in recent times. The section on redox biochemistry of protein thiols (Section II) recognizes the recent transition from a redox biology dominated by TRXs and disulfides to a more articulated subject that takes into consideration how reactive oxygen, nitrogen, and sulfur species (ROS, RNS, and RSS, respectively) may induce up to 10 different post-translational

Downloaded by LI CO SA/50127/MI from www.liebertpub.com at 07/22/19. For personal use only.

Downloaded by LI CO SA/50127/MI from www.liebertpub.com at 07/22/19. For personal use only.

modifications (PTMs) of protein Cys, in a complex interplay that involves also glutaredoxins (GRXs) and glutathione, besides classical TRXs. Section III witnesses the impressive development of redox proteomic techniques that occurs during the past two decades. Emphasis is given to the methodological principles and future technical developments in redox proteomics. To date, these approaches have already allowed the list of putative redox targets to include hundreds or thousands of members with different known redox PTMs on specifically identified Cys in different photosynthetic organisms. The biodiversity of plant TRXs and GRXs and their reducing systems is described in Section IV. Note that before the genomic revolution that in plants started with the sequencing of the genome of *Arabidopsis thaliana* in 2000, the different known TRXs could be counted on one hand and GRXs were almost unknown. With 20 classes of TRXs and 6 classes of GRXs, photosynthetic organisms are now believed to contain a potential for redox regulation and signaling that seems to largely exceed that of nonphotosynthetic organisms. The state of the art of the structure–function relationships studies in TRXs and GRXs, including their mechanisms of action and interactions with the targets, are included in Section V. Section VI deals with the determination of redox couples *in vivo* by means of genetically encoded probes and fluorescence microscopy. This section witnesses the adaptation of green fluorescent protein (GFP)-based techniques in the redox field, leading, for the first time, to dynamically determine redox states *in vivo*. Most of the section is dedicated to glutathione and the popular roGFP probes. Finally yet importantly, Section VII shows that only recently the original model of redox regulation of chloroplast enzymes is receiving experimental confirmation by reverse genetic data. These experiments open the new avenue of redox plant physiology *in vivo*, including the role of redox regulatory systems in primary productivity, development, and environmental adaptation.

II. Redox Biochemistry of Protein Thiols

A. Production and detoxification of RMS in plants and algae

Redox regulation mainly occurs through different types of PTMs of Cys residues that may occur either through dithiol–disulfide exchange reactions or through reactions in which particular proteins Cys are attacked by RMS. Biologically relevant RMS are based on oxygen (ROS), nitrogen (RNS), or sulfur (RSS), and plant cells may properly synthesize or accidentally release different RMS types by many different mechanisms, both under stress and nonstress conditions.

1. Reactive oxygen species. Light reactions of photosynthesis constitute a fundamental source of ROS in plants. On the one hand, it is believed to be a consequence of the sessile nature of plants since ROS may be produced when the amount of energy obtained from light harvested by photosystems exceeds the combined capacity of downstream metabolic activities and heat dissipation mechanisms (112, 123, 442). On the other hand, ROS are signals that illuminated chloroplasts continuously produce, even in the absence of stress, as the energetic state of the photosynthetic electron transport (PET) chain is affected by varying environmental or metabolic conditions (184). ROS signals produced by altered states of the PET are involved in controlling nuclear gene expression by chloroplast retrograde signaling, leading to long-term acclimation responses (184).

Photosynthesis can produce different types of ROS with different mechanisms (Fig. 2). When light energy absorbed by chlorophylls is not rapidly dissipated, photo-excited chlorophylls in the triplet state accumulate in photosystems II and may generate singlet oxygen ($^1O_2$) by interacting with molecular (triplet) oxygen (Fig. 2) (148). This reaction is prevented in light-harvesting antennae where chlorophyll triplet states are quenched by xanthophyll-type carotenoids that dissipate the excitation energy as heat (442). Tocopherols and carotenoids provide a primary protection against the destructive action of $^1O_2$, which primarily results in lipid peroxidation, but also oxidative modification of protein residues including Cys (137, 270, 391).

PSI is also a potential source of ROS because it contains low potential Fe-S clusters that easily reduce molecular oxygen to the superoxide ion ($O_2^{-\bullet}$) (Fig. 2), when downstream acceptors of the PET chain are limiting because they are already reduced. This condition notably arises when carbon fixation by the CB cycle is limited by partial activation of its light-dependent regulated enzymes or low CO_2 supply from the atmosphere due to stomata closure. Chloroplast superoxide dismutase (SOD) isoforms guarantee a rapid conversion of $O_2^{-\bullet}$ to H_2O_2 that ascorbate peroxidases (APXs), glutathione peroxidases-like (GPLXs), and PRXs may then reduce to water (Fig. 2) (377). Ascorbate, glutathione, pyridine nucleotides, TRXs, and their reductases constitute an interlinked powerful system of chloroplasts that tries to keep under control the unavoidable production of H_2O_2 during photosynthesis (155, 377). Under particular conditions, H_2O_2 can react with ferrous ion leading to the formation of hydroxyl radical ($^{\bullet}OH$) (Fig. 2), the most reactive and damaging ROS molecule.

Although iron-containing components of PSI are the major source of $O_2^{-\bullet}$ in chloroplasts in the so-called pseudocyclic electron transfer, photosynthetic oxygen reduction may also occur by other mechanisms. These include a long suspected role of the plastoquinone pool in generating ROS signals (524). However, it is still uncertain whether oxygen reduction might depend on the activity of the plastid terminal oxidase (365) or occur at the site of plastohydroquinone oxidation on cytochrome b_6f (31) or even result from the direct reaction between the plastohydroquinone pool and oxygen or $O_2^{-\bullet}$ (516) (Fig. 2).

Another important source of ROS is peroxysomal glycolate oxidase (GOX) that, in the photorespiratory pathway, generates H_2O_2 in stoichiometric amounts with the oxygenase activity of ribulose-1,5-bisphosphate carboxylase/oxygenase (RubisCO) (Fig. 2). Given the relevant share of photorespiration on photosynthetic metabolism in C3 plants [up to half of carboxylation at 30°C (594)], this is arguably one of the most important sources of ROS in green cells, at least in organisms with no CO_2-concentrating mechanisms. Moreover, photorespiration of C3 plants is also another way by which photosynthesis unavoidably produces ROS independently from stress conditions (378). However, huge amounts of catalase (CAT), together with APXs, limit H_2O_2 from escaping peroxisomes (Fig. 2) (337, 377).

Similar to animal systems, mitochondria are also in plants a potential source of ROS (Fig. 2) (230). Complexes I and III are able to transfer single electrons to oxygen, thereby

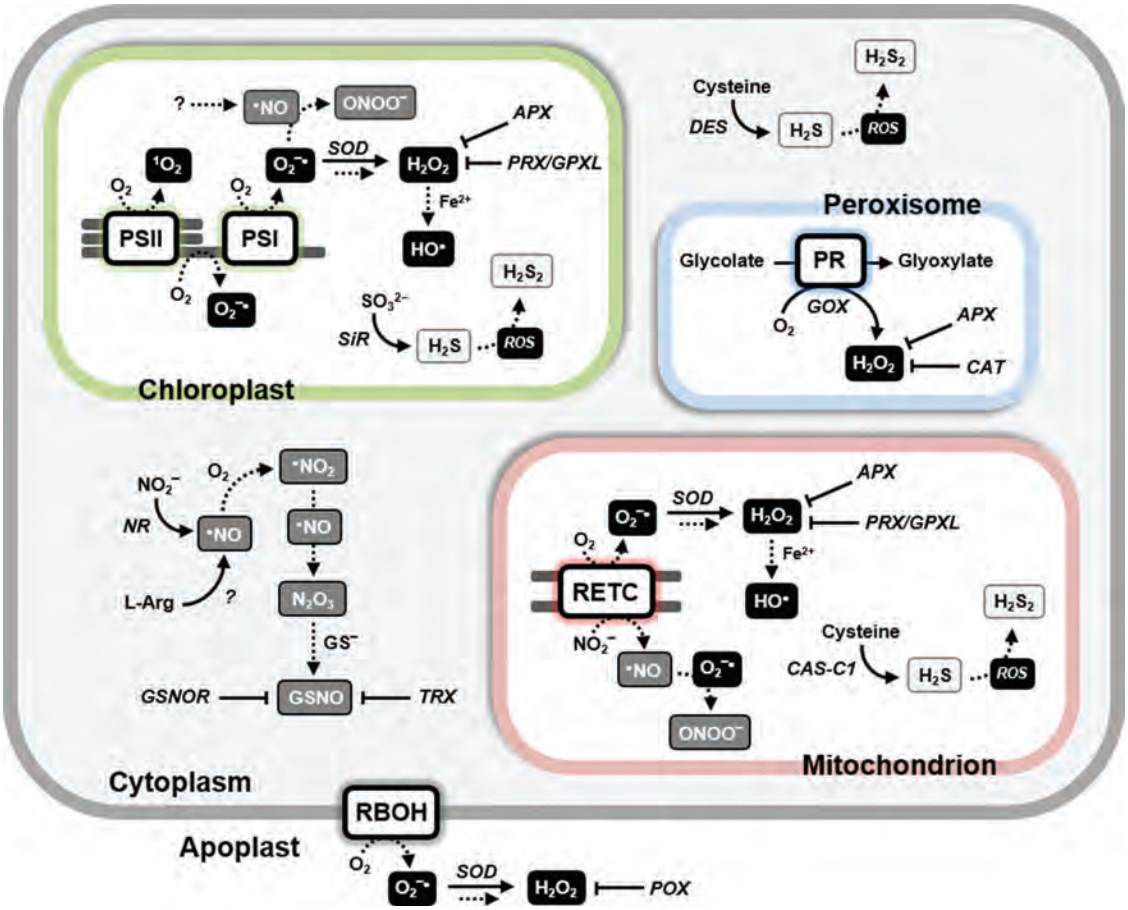

FIG. 2. RMS: production and scavenging systems. Biologically relevant RMS are based on oxygen (ROS, indicated in *white* on *black rectangles*), nitrogen (RNS, indicated in *white* on *dark gray rectangles*), or sulfur (RSS, indicated in *black* on *light gray rectangles*). The generation of RMS occurs through diverse enzymatic and nonenzymatic pathways and involves all subcellular compartments as depicted in the figure (for further details please refer to the text). The scavenging system mainly relies on antioxidant enzymes that are localized in all subcellular compartments including apoplast. APX, ascorbate peroxidase; CAS-C1, *β*-cyanoalanine synthase; CAT, catalase; DES, cysteine desulfhydrase; GPXL, glutathione peroxidase-like; GOX, glyoxylate oxidase; GSNO, nitrosoglutathione; GSNOR, nitrosoglutathione reductase; H_2O_2, hydrogen peroxide; NR, nitrite reductase; POX, peroxidase; PR, photorespiration; PRX, peroxiredoxin; RBOH, respiratory burst oxidase homologue; RETC, respiratory electron transport chain; RMS, reactive molecular species; RNS, reactive nitrogen species; ROS, reactive oxygen species; RSS, reactive sulfur species; SiR, sulfite reductase, SOD, superoxide dismutase. Color images are available online.

Downloaded by LI CO SA/50127/MI from www.liebertpub.com at 07/22/19. For personal use only.

producing $O_2^{-\bullet}$, particularly under conditions of low adenosine diphosphate or low oxygen availability (358, 418). Similar to chloroplasts, mitochondria contain SODs and H_2O_2 detoxifying systems relying on APXs, GPLXs, and PRXs (Fig. 2).

Like H_2O_2, also $O_2^{-\bullet}$ may be enzymatically produced in plant cells. NADPH oxidases of the respiratory burst oxidase homologue (RBOH) family being probably the major source (Fig. 2). A gene family of about 10 members in higher plants encodes these NADPH-dependent flavocytochromes. Some of them at least reside at the plasma membrane and release $O_2^{-\bullet}$ in the apoplast in response to either abiotic or biotic stress and developmental processes (310). In *Arabidopsis*, RBOH is responsible for the oxidative burst triggered by incompatible pathogens. Together with nitric oxide ($^{\bullet}$NO), the resulting superoxide $O_2^{-\bullet}$ orchestrates the hypersensitive response against the pathogens (117). Interestingly, $^{\bullet}$NO is also involved in a feedback loop that inhibits Arabidopsis RBOH subunit D activity *via* S-nitrosylation of Cys-890 (570). Except for the presence of SOD and low concentrations of ascorbate, the apoplast is poor in antioxidant systems (19, 157), suggesting that apoplastic H_2O_2 may accumulate more easily than in other cell compartments.

2. Reactive nitrogen species. Sources of RNS in photosynthetic organisms are diverse and still not fully described. In land plants, reductive pathways converting nitrite (NO_2^-) to $^{\bullet}$NO seem to prevail over oxidative pathways that release $^{\bullet}$NO from arginine (Fig. 2) (21). Nitrate reductase (NR) can slowly produce $^{\bullet}$NO by reducing NO_2^-, instead of its normal substrate nitrate (NO_3^-), using NADH as an electron donor. Since the affinity of NR for NO_3^- is higher than for NO_2^-, and since NO_3^- inhibits the reduction of NO_2^-, $^{\bullet}$NO production by NR is expected to be favored by stress conditions that lead to toxic nitrite accumulation (418). In any case, the role of NR in $^{\bullet}$NO production in *Arabidopsis* is supported by reverse genetic studies (21). Alternatively to

NR, NO_2^- can be also reduced to •NO by components of the mitochondrial electron transport chain (complexes III and IV) (Fig. 2) (196), particularly when oxygen is scarce. Recently, a complex involving NR and NO-forming nitrate reductase (NOFNiR) was shown to constitute a new •NO biosynthetic system in the green microalga *Chlamydomonas reinhardtii* (74). The role of NR in the complex is to transfer electrons from NAD(P)H to NOFNiR. Whether a similar complex also exists in land plants is currently unknown.

Oxidative pathways for •NO production from arginine seem to be operative in plants (Fig. 2), but the proteins involved remain to be identified. An ortholog of animal NO synthases is found in the alga *Ostreococcus tauri* (151) but not in other algae and higher plants, where the oxidative release of •NO from arginine may involve distinct mechanisms (21).

Similar to biogenesis, regulation of intracellular •NO levels may also follow different pathways. Nonsymbiotic hemoglobins convert •NO to NO_3^- (356), but as part of •NO in the cell is bound to reduced glutathione (GSH) to form nitrosoglutathione (GSNO), the activity of GSNO reductase (GSNOR) that releases ammonia from GSNO (300, 575) is potentially very relevant to modulate •NO availability and also the levels of GSNO, an important transnitrosylating agent (see section II.C.4).

3. Reactive sulfur species. In plants, hydrogen sulfide (H_2S) generation occurs through three pathways that differ in the underlying mechanisms and the subcellular compartments in which they take place. The primary source of H_2S is the chloroplast where it is produced in the reductive sulfate-assimilation pathway through the action of sulfite reductase (SiR, Fig. 2) (488). Alternative pathways occur in both mitochondria and cytoplasm. β-Cyanoalanine synthase (CAS-C1), catalyzing the conversion of cyanide and Cys to β-cyanoalanine and H_2S, is found in mitochondria (Fig. 2) (11). In the cytoplasm, the enzyme L-Cys desulfhydrase (DES1) catalyzes the desulfuration of Cys yielding sulfide, ammonia, and pyruvate (Fig. 2) (9, 10, 185). In any case, the production of H_2S in subcellular compartments where ROS or RNS may also be produced can result in nonenzymatic reactions, including the one-electron oxidation of H_2S to hydrogen disulfide (H_2S_2) (Fig. 2), which may lead to persulfidation of protein Cys (see section II.C.5).

B. Reactivity of Cys is strictly controlled by the protein microenvironment

In plants, RMS (including ROS, RNS, and RSS) actively participate in redox homeostasis. In this context, proteins play an essential role as central mediators of RMS-dependent signaling events. Many of these proteins rely on modifications of Cys residues for modulating their redox activity, whereas a few of them use other residues (*e.g.*, methionines or tyrosines) for the same purpose, but knowledge on methionine- and tyrosine-dependent signaling pathways is still limited to a few studies (35, 237, 238, 265, 327).

Cys-based redox modifications have been extensively investigated and they are widely accepted to play a prominent role in regulatory and signaling networks that support plant development, metabolic functions, and responses to varying environmental conditions. The functionality of Cys residues in redox biology depends on the chemical reactivity and structural flexibility of their sulfur atom. Sulfur can form covalent bonds with different types of atoms present in living organisms (C, H, O, P, and N) and establish stable complexes with transition metals (Zn, Fe, and Cu). In addition, being weak acids, Cys thiols (–SH) are found in equilibrium with the deprotonated thiolate form ($-S^-$) over a physiological range of pH to flexibly optimize the function of specific protein Cys (Fig. 3A). Compared with the protonated forms, Cys thiolates are more sensitive to the intracellular redox environment and susceptible to RMS-dependent oxidative modifications. Altogether, these features allow Cys residues to play fundamental structural and catalytic roles, and to function in RMS-mediated redox signaling as reversible molecular switches (321, 508, 537).

The acid dissociation constant (pK_a) of a Cys designates its tendency to dissociate. The pK_a of the sulfhydryl groups of free Cys is $\sim$8.3 (395, 434, 502). A slightly higher pK_a value [8.8, (440)] is attributed to the Cys thiol of GSH. These pK_a values imply that these Cys thiols are largely found in the protonated form at neutral pH, whereas thiolate forms might progressively accumulate only at alkaline pH values. For example, the percentage of GSH thiolate (GS^-) at pH 7 is only 2%, but this value increases to 14% when the pH raises to 8. This variability is particularly important in subcellular compartments that experience a shift from neutral to slightly alkaline pH as observed in the chloroplast stroma during dark to light transitions (215, 221, 503).

Although the vast majority of protein Cys harbors a pK_a >8, some of them are acidic due to the microenvironment in which they are located (395, 508). Selected protein Cys involved in thiol switching reactions have pK_a values ranging between 3 and 6.5 (508), allowing these residues to be predominantly or fully deprotonated at physiological pH (Fig. 3B). The structural features that contribute to modulate the acidity of Cys thiols mainly include the proximity of amino acids such as lysine, histidine, or arginine, which by attracting the proton of the thiol become positively charged and form an ion pair with the negatively charged thiolate (Fig. 3C) (96, 508). These types of interactions are found in enzymes such as GAPDH (36, 576), isocitrate lyase (37),and PRXs (368). In other proteins, hydrogen-bonding networks may also be relevant (Fig. 3C); in TRXs and GRXs, for instance, the hydrogen-bonding network is believed to be the major structural determinant of the acidity of the catalytic Cys (434). Finally, the location of the Cys residue at the N-terminus of an α-helix generating an electric macrodipole may also contribute to its acidity (Fig. 3C) and, in general, desolvation can also have an impact on thiol pK_a by decreasing the dielectric constant of water and thus enhancing electrostatic interactions that occur in catalytic sites (146). In many other cases, the relative influence of each structural factor to the thiol pK_a is still undefined and difficult to derive from the protein tridimensional structure, such that it needs to be determined experimentally (508).

Although thiolates are stronger nucleophiles than thiols, it should be remembered that the nucleophilicity of a thiolate actually decreases with decreasing pK_a of the Cys. In other words, the most reactive Cys are often Cys that are acidic enough to be largely deprotonated at neutral pH, but not too acidic to lose completely their nucleophilicity (146, 508). Moreover, the protein microenvironment affects the reaction between Cys and RMS also in other ways, not directly dependent on Cys pK_a.

Downloaded by LI CO SA/50127/MI from www.liebertpub.com at 07/22/19. For personal use only.

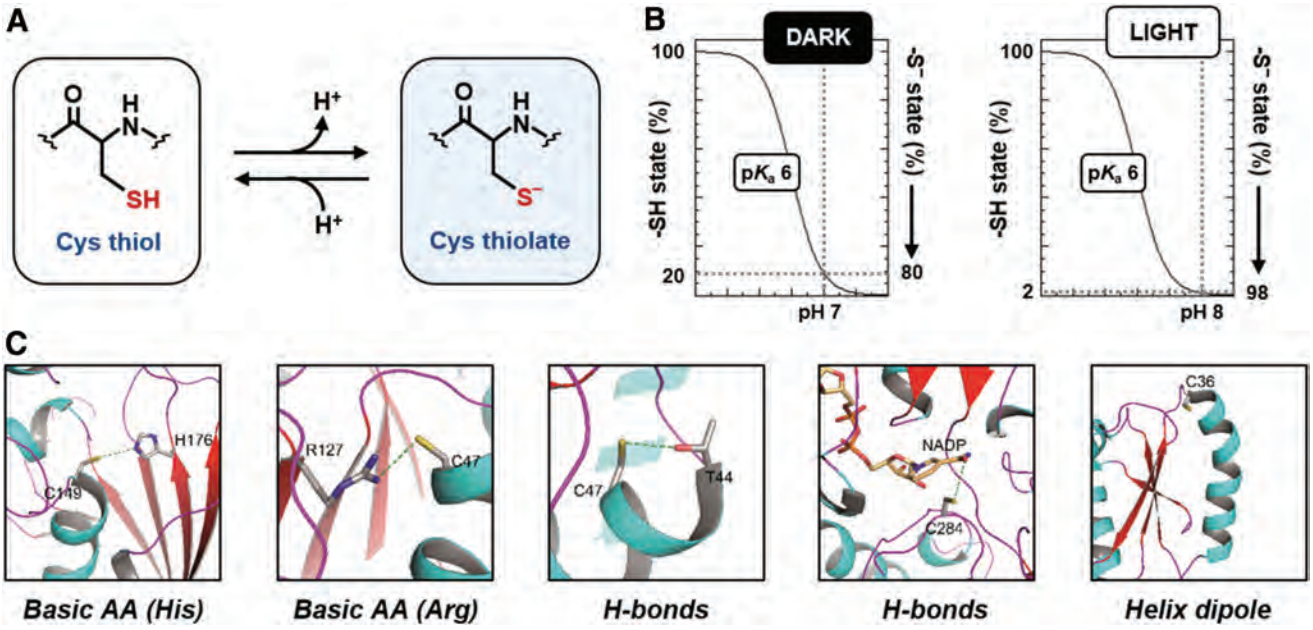

FIG. 3. Biochemical and structural features of protein Cys. (A) Representation of a protein Cys in equilibrium between its thiol form (–SH, *left panel*) and thiolate form ($–S^-$, *right panel*). **(B)** Estimation of thiol/thiolate percentage of the catalytic Cys of photosynthetic GAPDH ($pK_a = 6$) at the indicated pH values (7.0 and 8.0 for stromal pH under dark and light conditions, respectively). **(C)** Examples of the main structural determinants of the Cys thiol reactivity by known protein crystal structures. From *left* to *right*: interactions with basic amino acids (His and Arg; PDB IDs: 4Z0H (576) and 1HD2 (114), H-bond networks (PDB IDs: 1HD2 (114) and 2EUH (91), and positioning of reactive Cys at the N-terminus of an α-helix (helix dipole; PDB ID: 1EP7 (329). Cys, cysteines; GAPDH, glyceraldehyde-3-phosphate-dehydrogenase. Color images are available online.

The H_2O_2-dependent oxidation of Cys thiolate nicely exemplifies the latter point. By comparing the reactivity toward H_2O_2 of two thiolate-containing proteins, namely PRX and GAPDH (pK_a values of ~5 and ~6, respectively), it was observed that PRX reacts with H_2O_2 10^4–10^5 times faster than GAPDH (508, 536). Since the catalytic Cys of both PRX and GAPDH are fully or almost fully deprotonated at neutral pH, other factors than thiolate availability and exposure should be taken into account to explain the vastly different reactivity. Indeed, the stabilization of the transition state (–S···O···O···H) by active-site residues was recently proposed to sustain the catalytic power of PRX (207, 362). A counter example is given by GRX S12, which contains a highly acidic catalytic Cys [pK_a value <4.0; (102, 573)] but exhibits a reactivity toward H_2O_2 that is comparable with GAPDH [pK_a ~6; (508, 573, 576)]. Based on these observations, we can conclude that although oxidation mainly affects acidic Cys, the Cys microenvironment can control the reaction kinetics with H_2O_2 and possibly other RMS, as detailed in the following subsections.

C. Cys residues may be modified in many different ways by RMS or enzymes

The cellular capacity for RMS-mediated regulatory pathways depends on different types of Cys modifications that allow oxidant signals to be transduced into biological responses. In the following subsections, the chemistry and mechanisms of oxidative modifications induced by each class of RMS molecules, namely ROS, RNS, and RSS, are discussed. Alternative mechanisms of protein Cys oxidation catalyzed by enzymatic systems or mediated by intermediate Cys oxoforms (*i.e.*, sulfenic acids and nitrosothiols) or oxidant molecules (*e.g.*, oxidized glutathione, GSSG) are also described.

1. ROS-dependent redox modifications of protein thiols. Protein Cys thiol can be oxidized by both radical ($O_2^{-\bullet}$, $^\bullet OH$) and nonradical ROS molecules ($^1O_2$, H_2O_2). Singlet oxygen is a nonradical molecule that can react with sulfur-containing amino acids (*i.e.*, Cys and methionine) but also with histidine, tryptophan, and tyrosine residues (391). The oxidation of Cys thiols by $^1O_2$ occurs *via* formation of a short-lived zwitterionic intermediate ($RS^+(H)–OO^-$), which decomposes yielding oxidized sulfur species such as sulfonic acids ($–SO_3H$) or alternatively, disulfides if another Cys residue is able to react with the initial intermediate (Fig. 4) (360, 391). Although $^1O_2$ is believed to play a signaling role in chloroplasts (276), the molecular bases of its action are not fully understood.

The radical superoxide ($O_2^{-\bullet}$) is a relatively unreactive radical and its preferential targets appear to be other radical species such as $^\bullet NO$ (395). In proteins, $O_2^{-\bullet}$ can react with Fe-S clusters and some transition metals (113, 537), and shows low reactivity toward protein side chains, Cys being one of the less sensitive amino acids (113). However, if this reaction occurs, Cys may undergo cysteinyl (thiyl) radical ($–S^\bullet$) formation and possibly peroxidation (*i.e.*, thiol peroxide formation) (Fig. 4) (169, 454). In contrast to $O_2^{-\bullet}$, $^\bullet OH$ is highly reactive and is capable to oxidize nearly all protein residues with second order rate constants near the diffusion

Downloaded by LI CO SA/50127/MI from www.liebertpub.com at 07/22/19. For personal use only.

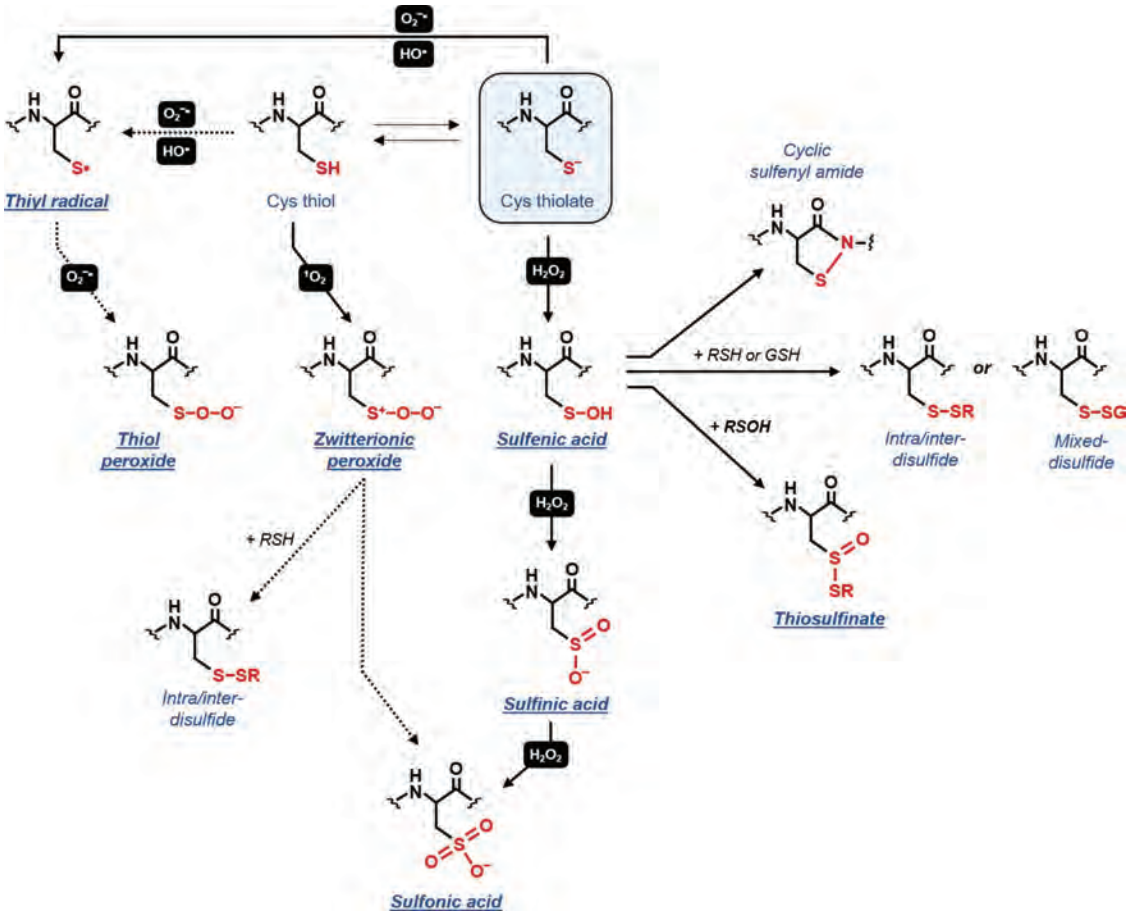

FIG. 4. ROS-dependent thiol-based redox modifications. Biologically relevant ROS-dependent Cys modifications are depicted (*underlined*) together with secondary redox modifications. For further details, please refer to the text. ROS are indicated in *white* on *black rectangles*. *Continuous* and *dotted lines* indicate recognized and possible reactions, respectively. Color images are available online.

limit (*i.e.*, 10^9–10^{10} $M^{-1}s^{-1}$) (113). Protein Cys oxidation mediated by $^{\bullet}OH$ is postulated to occur through hydrogen atom abstraction from S–H bonds yielding thiyl radicals (–$S^{\bullet}$, Fig. 4) (15, 113, 477, 519).

The aforementioned reactions are likely to occur under physiological conditions but their relevance in thiol-based redox signaling networks might be limited. These ROS molecules ($^1O_2$, $O_2^{-\bullet}$, and $^{\bullet}OH$) have high reactivity with biological macromolecules other than proteins. The abundance of these targets *in vivo* results in very short lifetimes and limited diffusion from the sites of generation. Therefore, oxidation by these ROS is restricted to proteins located at the proximity of production sites. In addition, they react with diverse protein side chains and display no specificity for reactive Cys.

Among ROS, H_2O_2 has the longest lifetime and is highly selective toward sulfur-containing residues, Cys thiolates being the most sensitive (226, 395, 453). The H_2O_2-dependent two-electron oxidation of reactive Cys leads to the formation of a sulfenic acid (–SOH) (Fig. 4). Sulfenic acids are emerging as redox signaling hubs implicated in different types of secondary modifications. Owing to their reactive nature, sulfenic acids are often considered as an unstable intermediate subjected to several alternative fates (Fig. 4). In the presence of excess H_2O_2, sulfenic acids can act as a nucleophile and be further oxidized to sulfinic (–SO_2H) and sulfonic acid (–SO_3H) Fig. 4), with reaction rates that are generally slower (0.1–10^2 $M^{-1}s^{-1}$) than the primary oxidation event (10–10^7 $M^{-1}s^{-1}$) (395, 508). Sulfinic and sulfonic acids are usually considered irreversible forms except for sulfinated 2-Cys PRX (PRX-SO_2H), which can be reversibly reduced to the thiol form by sulfiredoxin (243). Sulfenic acids can alternatively serve as electrophiles reacting with the backbone amide group of a neighboring residue forming a reversible cyclic sulfenamide or condensate with an interfacing additional sulfenic acid to generate a thiosulfinate (Fig. 4). In most cases, however, sulfenic acids react with a proximal thiol from a protein Cys or a GSH (Fig. 4) leading to the formation of intra-/intermolecular disulfide bonds (–S–S–) or a mixed disulfide (–S–SG, S-glutathionylation). Besides protein Cys, H_2O_2 can also react with GSH yielding glutathione sulfenate intermediates (GSOH) but, owing to its pK_a, this reaction proceeds very slowly ($\sim$1 $M^{-1}s^{-1}$) (395).

2. Plant cysteine oxidases catalyze the enzymatic oxidation of protein Cys to sulfinic acids. Besides protein disulfides, other oxidative modifications are found to be catalyzed by specific enzymes. Indeed, Cys oxidation to sulfinic acids can occur in the presence of plant Cys oxidases (PCOs). These enzymes are nonheme Fe^{2+}-dependent

Downloaded by LI CO SA/50127/MI from www.liebertpub.com at 07/22/19. For personal use only.

dioxygenases catalyzing an essential step of the N-end rule pathway in plants that controls, for example, the stability of group VII ethylene response factors (ERF-VIIs). Whereas ERF-VIIs are rapidly degraded in normoxia, flooding-induced hypoxic conditions reduce the activity of PCOs allowing ERF-VIIs stabilization and consequently transcriptional adaptative responses (509, 531, 533). The molecular mechanisms underlying PCO activity have been recently established and Cys sulfinic acids are generated *via* an oxygen-dependent reaction (532, 533). Besides oxygen, ROS and likely $^{\bullet}NO$ are postulated to be involved in such reactions but the mechanisms are still not clarified (418).

3. RNS-dependent redox modifications of protein thiols. In biological systems, $^{\bullet}NO$ and derived compounds [*i.e.*, nitric dioxide ($^{\bullet}NO_2$), dinitrogen trioxide (N_2O_3), and $ONOO^-$] can also induce oxidative modifications of protein residues including Cys thiols (Fig. 5). Similar to $O_2^{-\bullet}$, $^{\bullet}NO$ is a relatively unreactive radical and preferentially reacts with other radical species and with metals. By reacting with $O_2^{-\bullet}$, $^{\bullet}NO$ generates $ONOO^-$. Besides binding to heme-containing proteins (395), $^{\bullet}NO$ is involved in a covalent modification of protein Cys termed S-nitrosylation (575). This reversible modification does not directly involve $^{\bullet}NO$ and three major mechanisms have been proposed to account for S-nitrosothiol (–SNO) formation (575). The reaction of $^{\bullet}NO$ with transition metals of metalloproteins yields unstable metal–nitroxyl complexes that can then transfer the NO moiety to a Cys residue that generally belongs to the same protein (Fig. 5). Alternatively, $^{\bullet}NO_2$, which is spontaneously generated by the reaction of $^{\bullet}NO$ with molecular oxygen, can induce the one-electron oxidation of Cys thiolates (Fig. 5). This reaction leads to the formation of thiyl radicals that can undergo radical–radical combination with $^{\bullet}NO$ to yield S-nitrosothiols. S-nitrosothiols formation can also be generated by the nitrosating compound N_2O_3 that is spontaneously formed by the radical reaction between $^{\bullet}NO$ and $^{\bullet}NO_2$ (107, 395). N_2O_3 can subsequently transfer its nitrosonium group (^{+}NO) to proteins or low-molecular weight thiolates generating S-nitrosothiols and releasing NO_2^-.

Owing to its high intracellular concentration [1–5 m*M*, (156, 373, 440)], GSH might be a primary target of N_2O_3-dependent nitrosylation yielding GSNO (Fig. 6). This molecule along with S-nitrosylated proteins can transfer the NO moiety to another Cys in a process termed trans-nitrosylation (Fig. 5). Within cells, the equilibrium between GSH and GSNO controls the level of S-nitrosylation in some proteins at least (Fig. 6) (43, 580). TRXs efficiently reduce GSNO *in vitro* [(369); Zaffagnini *et al.*, personal communication] and catalyze protein denitrosylation of specific targets *in vivo* (262). However, TRX-dependent reduction of GSNO or protein-SNO releases a nitroxyl (HNO) that is highly reactive and still able to interact with Cys residues (49). To date, the foremost enzyme known to control the intracellular concentration of GSNO is GSNOR (300, 575) (see Section II.C.4).

The sensitivity of a particular Cys thiolate to trans-nitrosylation seems to depend on different factors including Cys reactivity, the accessibility to NO donors and the local Cys microenvironment (*e.g.*, acid–base motif and hydrophobic residues) (129, 153, 304, 320, 469, 579). In general, trans-nitrosylation is considered not only as a prominent mechanism of protein S-nitrosylation but also as a mechanism that allows propagating the NO signal far away from the site of $^{\bullet}NO$ production (395). Compared with sulfenic acids, nitrosothiols cannot further react with oxidants but can generate sulfenic acids by spontaneous hydrolysis (Fig. 5) or, alternatively, form disulfides in the presence of protein or GSH thiolates (Fig. 5).

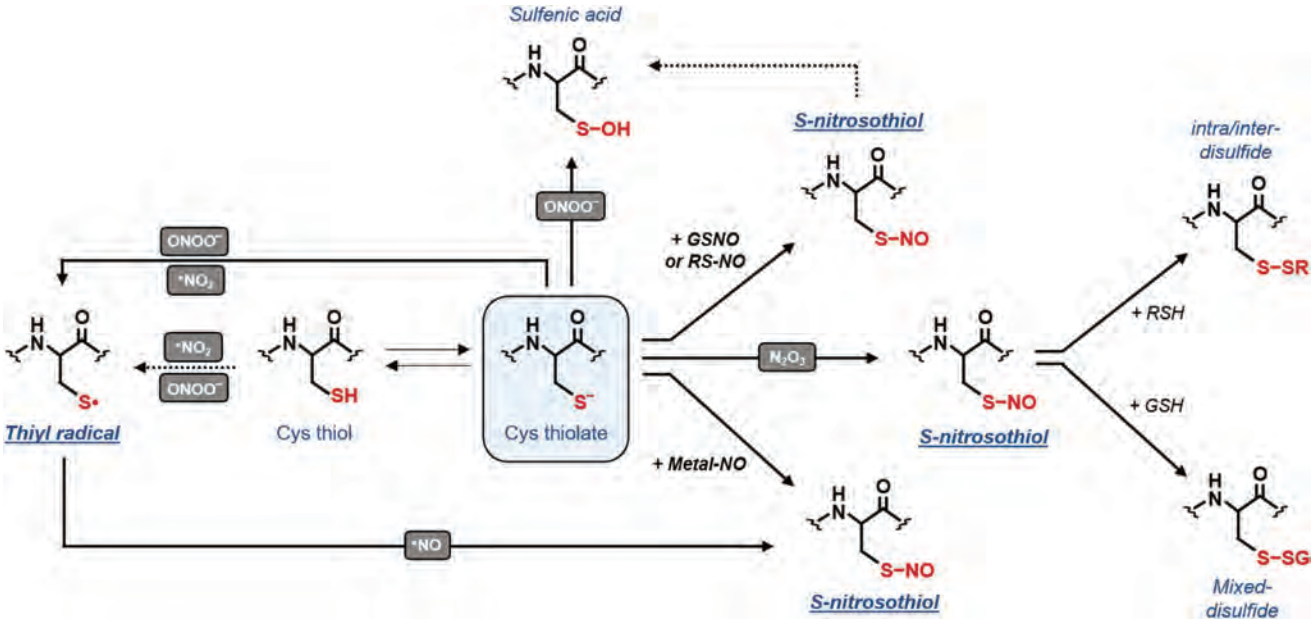

FIG. 5. RNS-dependent thiol-based redox modifications. Biologically relevant RNS-dependent Cys modifications are depicted (*underlined*) together with secondary redox modifications. For further details, please refer to the text. RNS are indicated in *white* on *dark gray rectangles*. *Continuous* and *dotted lines* indicate recognized and possible reactions, respectively. Color images are available online.

Downloaded by LI CO SA/50127/MI from www.liebertpub.com at 07/22/19. For personal use only.

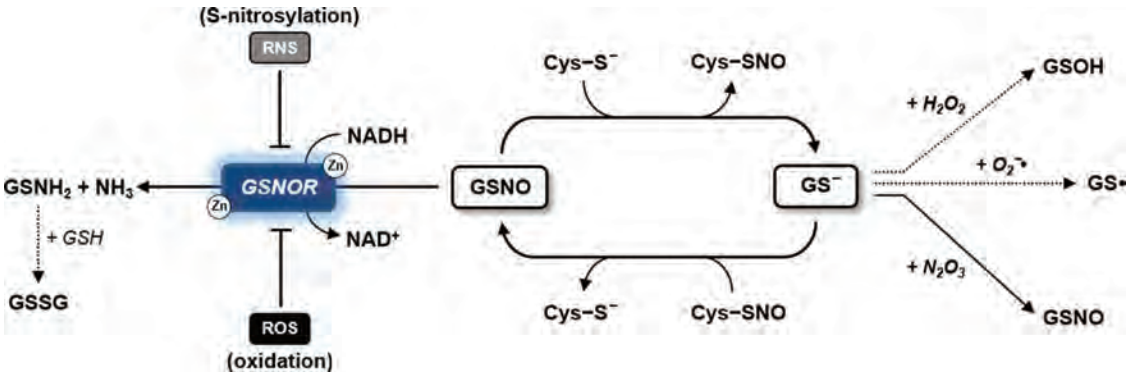

FIG. 6. Redox homeostasis of protein and low-molecular S-nitrosothiols. Protein S-nitrosylation is generally induced by GSNO-dependent trans-nitrosylation with concomitant release of GSH. The reduction of protein S-nitrosylation is mainly controlled by GSH leading to the formation of GSNO. Once formed, GSNO is reduced to NH_3 and GSSG (if GSH is present) by the Zn-containing GSNOR using NADH as electron donor. The reactivity of GSH thiolate (GS^-) with H_2O_2, $O_2^{-\bullet}$, and N_2O_3 is also represented and indicated by *continuous* and *dotted lines* for established and hypothetical reactions, respectively. GSH, reduced glutathione; GSSG, oxidized glutathione; H_2O_2, hydrogen peroxide. Color images are available online.

Downloaded by LI CO SA/50127/MI from www.liebertpub.com at 07/22/19. For personal use only.

Peroxynitrite ($ONOO^-$) and its protonated form (ONOOH) are highly reactive nonradical species that can cause oxidation of several protein residues including Cys, methionine, tryptophan, and tyrosine. The most relevant peroxynitrite-mediated reaction is tyrosine nitration but its physiological relevance in signaling pathways still requires further confirmation. Similar to $^{\bullet}OH$, the reaction of $ONOO^-$ with protein Cys yields thiyl radicals (Fig. 5) (113, 486) but other oxidation products such as sulfenic acids are also generated (Fig. 5) (584).

4. GSNO reductase controls the level of nitrosothiols in plants. GSH can efficiently reduce protein S-nitrosothiols (181, 433, 575). However, although this nonenzymatic reaction restores reduced proteins, it also generates GSNO (Fig. 6), which can further react with reactive Cys thiols yielding *de novo* S-nitrosothiols (97, 575). Consequently, GSH by acting as an efficient reducing system can also promote further S-nitrosylation *via* GSNO. To date, the foremost enzyme known to control the intracellular concentration of GSNO is GSNOR (300, 551, 575). This enzyme is highly conserved in most bacteria and all eukaryotes including plants (303). GSNOR belongs to the class III alcohol dehydrogenase family and catalyzes the reduction of GSNO using NADH as an electron donor (268, 271, 303). The effective contribution of GSNOR in degrading GSNO relies on its catalytic ability to reduce GSNO into glutathione sulfenamide ($GSNH_2$), which spontaneously forms GSSG and NH_3 in the presence of GSH (Fig. 6). Consequently, GSNOR acts as a specific scavenging system for GSNO and indirectly controls the extent of GSNO-dependent protein S-nitrosylation.

In plants, the role of GSNOR in S-nitrosothiols metabolism was demonstrated by Loake and colleagues (139). *Arabidopsis* mutants that do not express GSNOR (*gsnor*) have more low-molecular weight nitrosothiols (*e.g.*, GSNO) and high-molecular weight nitrosothiols (*e.g.*, S-nitrosylated proteins). The function of GSNOR was also associated with various physiological processes including pathogen response, thermotolerance, plant growth, flowering, hypocotyl elongation and germination, and resistance to cell death. Whether these effects are also mediated by S-nitrosylation, however, still need to be clearly established (139, 272, 281, 300, 443).

The activity of plant GSNOR itself has been recently reported to be altered by redox modifications (Fig. 6). *Arabidopsis* and poplar GSNOR were found to undergo S-nitrosylation *in vivo* under conditions of increased endogenous NO availability (83, 162). Intriguingly, this modification causes partial inhibition of GSNOR activity (162, 193). More recently, AtGSNOR was also found to be negatively affected by *in vitro* treatment with H_2O_2 or exposure of *Arabidopsis* plants to paraquat (268). Altogether, these pieces of evidence suggest that the transient inhibition of plant GSNOR by oxidative modifications might reinforce NO signaling by favoring GSNO accumulation (193, 268, 300).

5. RSS-dependent redox modifications of protein thiols. The prototypical inorganic RSS is H_2S, which is the most stable RMS with a half-life in the minute time scale (485). Based on its chemical properties [$pK_{a1} = 7$ and $pK_{a2} = 12–15$; (80, 343)], H_2S can easily dissociate under physiological conditions and it is, therefore, assumed that H_2S pools mainly include H_2S and HS^-. In plants, the involvement of H_2S as a signaling molecule is receiving growing attention because of its ability to interact with proteins and possibly with other RMS (16, 17, 79). Given its nucleophilic properties, H_2S can scavenge reactive intermediates including $^{\bullet}NO$, $O_2^{-\bullet}$, $ONOO^-$, or H_2O_2, suggesting that it can play protective effects against oxidative stress (249, 534). However, a biological relevance for this activity is largely speculative because of its limited reactivity compared with GSH and its intracellular concentration, which is considered low (174, 249, 485). With proteins, H_2S can interact with some heme groups but also with Cys residues in a process called persulfidation. This oxidative modification consists in the conversion of a protein Cys into a persulfide (–S–SH) and it is suggested to modulate protein functions (259, 361, 392, 393) by increasing the nucleophilicity of the Cys (106, 392). Noteworthy, this reaction can involve both Cys thiolates and oxidatively modified Cys intermediates such as sulfenic acids

Downloaded by LI CO SA/50127/MI from www.liebertpub.com at 07/22/19. For personal use only.

(395). Although persulfidation has been proposed as a new key player in redox signaling, the underlying mechanisms are poorly understood and the physiological relevance of H_2S-related mechanisms in plants is still largely unknown.

Three major mechanisms for protein persulfidation have been postulated (Fig. 7), none of which involves a direct reaction between H_2S and Cys residues (249, 505). The first two mechanisms involve a nucleophilic attack of H_2S on oxidized protein Cys, either present as sulfenic acid or engaged in disulfide bonds (*i.e.*, intra/inter or mixed disulfide) (Fig. 7). However, disulfide-mediated persulfide formation is uncertain mainly because H_2S is a poor reductant compared with GSH and this reaction may proceed very slowly *in vivo* (70, 395). Another possibility is that alternative intermediate Cys oxoforms (*e.g.*, S-nitrosothiols or sulfenylamides) can react with H_2S yielding persulfides. The third mechanism involves the ROS-mediated oxidation of H_2S to H_2S_n ($n=2$ or higher), which can subsequently undergo a nucleophilic attack by a protein thiolate to give rise to a persulfide (Fig. 7).

Similar to nitrosothiols and sulfenic acids, persulfides contain two electrophilic centers and can react with another protein thiol yielding a disulfide or facilitating transpersulfidation (Fig. 7). The latter route is reminiscent to transnitrosylation and is likely to be highly protein specific (395).

6. S-glutathionylation as a special type of disulfide formation. Disulfide bond formation is the best characterized Cys-based redox modification. It consists in the covalent bonding between two Cys residues belonging to the same or different polypeptides. Besides the well-known role of TRXs in dithiol–disulfide interchange reactions (see section I) (Fig. 8A), disulfide formation may also involve RMS. One possible route relies on the primary oxidation of a Cys to sulfenic acid or S-nitrosothiol, followed by thiol condensation with an additional Cys (Fig. 8A; see sections II.C.1 and II.C.3).

Protein S-glutathionylation has emerged as a widespread oxidative modification involved in the modulation of protein function but also in the protection of protein Cys from irreversible oxidation (*i.e.*, sulfinic and sulfonic acid formation) (572, 574). As already mentioned, one potential mechanism of protein S-glutathionylation is the condensation of GSH with an intermediately oxidized Cys (*i.e.*, sulfenic acid or S-nitrosothiol; see sections II.C.1 and II.C.3, respectively). The electrophilic nature of these oxidative intermediates favors the nucleophilic attack of GSH thiolates, leading to the formation of protein mixed disulfides (Fig. 8B).

Another mechanism of protein S-glutathionylation involves a thiol–disulfide exchange between GSSG and a protein Cys thiolate (Fig. 8B). Typically, this reaction proceeds very slowly and is supposed to be thermodynamically prevented by the high GSH/GSSG ratios of most plant subcellular compartments (see section VI) (155, 157, 458). Nevertheless, we cannot exclude *a priori* the possibility that specific proteins might undergo GSSG-dependent glutathionylation as a consequence of limited fluctuations (*i.e.* oxidation) of the glutathione redox pool. Plastidial GRXS12 for instance is glutathionylated *in vitro* at GSH/GSSG ratios of 10^2–10^3 that fully prevent the glutathionylation of other targets such as cytoplasmic GAPDH (36, 573).

As an alternative to GSSG, protein glutathionylation can occur in the presence of GSNO (Fig. 8B). This molecule can allow the formation of S-nitrosothiols but can also transfer its GS moiety to a target Cys. The structural features controlling one reaction over another are still uncertain and are likely related to the local environment surrounding the target Cys

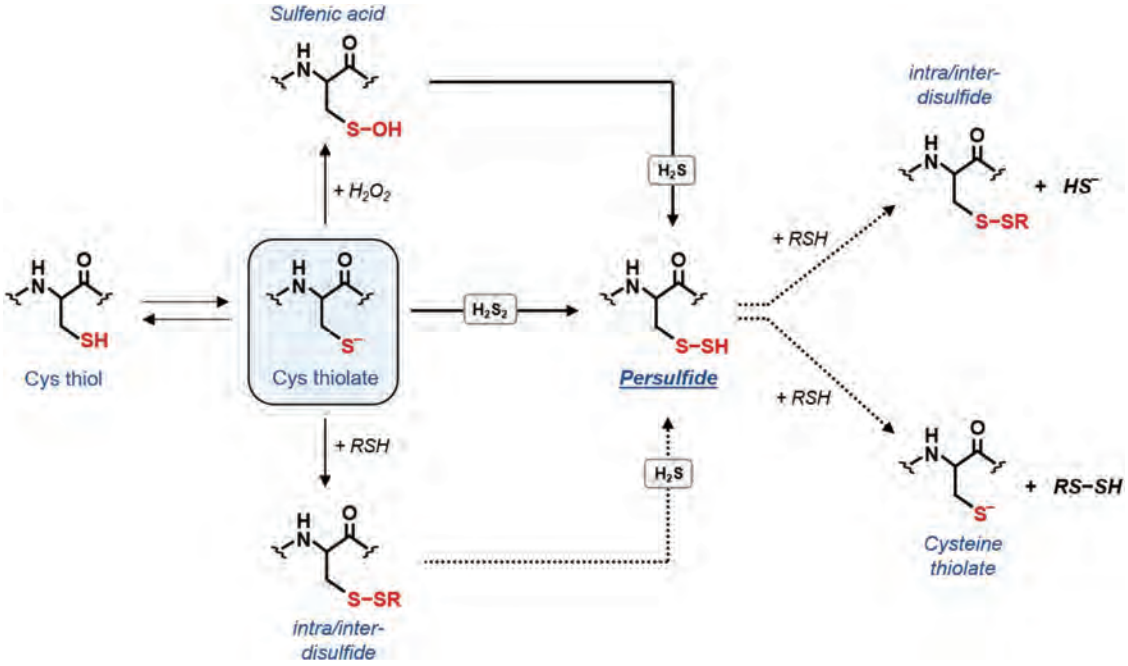

FIG. 7. RSS-dependent thiol-based redox modifications. Biologically relevant RSS-dependent Cys modifications are depicted (*underlined*) together with secondary redox modifications. For further details, please refer to the text. RSS are indicated in *black* on *light gray rectangles*. *Continuous* and *dotted lines* indicate recognized and possible reactions, respectively. Color images are available online.

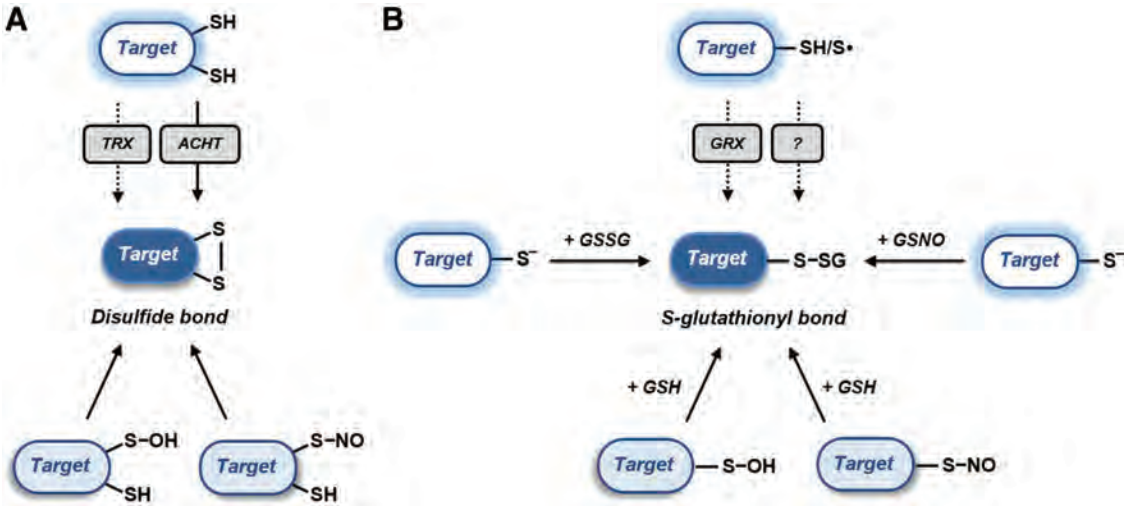

FIG. 8. Major mechanisms of protein disulfide formation. (A) Enzymatic (*upper panel*) and nonenzymatic (*lower panel*) mechanisms of disulfide formation involving diverse enzymes (TRX or ACHT) or Cys oxoforms (sulfenic acid or S-nitrosothiol). *Continuous* and *dotted lines* indicate recognized and possible reactions, respectively. **(B)** Enzyme-catalyzed protein S-glutathionylation (–SSG, mixed disulfide formation) involving GRX or other not identified enzymes (*upper panel*). Nonenzymatic mechanisms (*side* and *lower panels*) of protein S-glutathionylation involving diverse oxidizing molecules (GSNO, GSSG) or Cys oxoforms (sulfenic acid or S-nitrosothiol). *Continuous* and *dotted lines* indicate recognized and possible reactions, respectively. ACHT, atypical Cys histidine-rich thioredoxin; GRX, glutaredoxin. Color images are available online.

Downloaded by LI CO SA/50127/MI from www.liebertpub.com at 07/22/19. For personal use only.

residue. GRXS12 is an example of a protein that is glutathionylated by GSNO, rather than nitrosylated (573).

Finally, in addition to nonenzymatic mechanisms, protein glutathionylation might also be catalyzed by specific oxidoreductases (Fig. 8B). This was shown for human GRX2 that appears to promote protein S-glutathionylation after a reaction mediated by either GSSG or $GS^{\bullet}$ radical (38, 163). Both mechanisms rely on the formation of glutathionyl GRX intermediates and the ability of GRX to transfer the glutathionyl adduct to an acceptor protein thiolate in a trans-glutathionylation reaction. To date, no evidence suggests the ability of plant GRXs to catalyze such reactions *in vivo*. However, a remarkable example of enzyme-assisted glutathionylation occurring in plants involves the genetically encoded probe roGFP2 fused to human GRX1 [GRX1–roGFP2; (333, 458)]. This chimeric protein has been developed to monitor the glutathione redox state and its functioning is specifically related to reversible trans-glutathionylation reactions between the probe and GRX1.

III. Redox Proteomics: Methodological Principles and Future Developments in the Plant Field

Despite the latest improvements of mass spectrometry (MS) in terms of sensitivity and resolution over the past decade, direct analysis of redox-modified proteins remains highly challenging. As shown in Figure 9 (see also section II), >10 thiol-based redox PTMs are currently known (101, 182, 395). Owing to their lability, their low stoichiometry, and their possible interchange during sample processing as exemplified in Figure 9 (black and gray boxes corresponding to primary and secondary modifications), the redox proteomics field has to face different biochemical, methodological, and instrumental challenges to get insights about the *in vivo* dynamics of redox PTMs. In complex systems, redox proteomic strategies currently rely on the differential labeling of Cys according to their modification state followed by MS analyses at the peptide level after an affinity enrichment step.

Nontargeted quantitative strategies, such as OxICAT (283, 470) and OxiTMT (474), were developed to determine oxidation levels of hundreds of Cys upon oxidative treatments. To date, these approaches have been applied to quantitatively identify oxidative-prone Cys in the marine diatom *Phaeodactylum tricornutum* (436) and the cyanobacteria *Synechocystis* sp. PCC 6803 (194). In the latter organism, 20% to 40% of proteins were found to contain oxidized Cys in the dark. Nevertheless, these strategies are unable to distinguish which reversible redox PTM is at the origin of the modification of the Cys. In this section, we focus on approaches trapping selectively the different reversible redox PTMs with a special emphasis on their advantages, drawbacks, and limitations, and their use in photosynthetic organisms.

A. Thioredoxome

Two main proteomic strategies have been employed to identify hundreds of proteins containing disulfide bonds reduced by TRX (56, 299). The first and most common approach takes advantage of the ability of a monocysteinic TRX variant (Fig. 10), where the C-terminal active site Cys is replaced by serine or alanine, to covalently bind oxidized target proteins (for the mechanism, see section V). The monocysteinic TRX is most often grafted on a chromatographic resin and TRX-bound targets are eluted with a chemical reductant such as dithiothreitol (DTT). This type of column has been applied to numerous protein extracts from the cyanobacterium *Synechocystis* sp. PCC 6803 (298, 402, 404) and also different photosynthetic eukaryotes (6, 24, 27, 28, 32, 187, 208, 227, 285, 317, 319, 353, 543, 552, 565). This approach has several drawbacks. First, it lacks specificity as

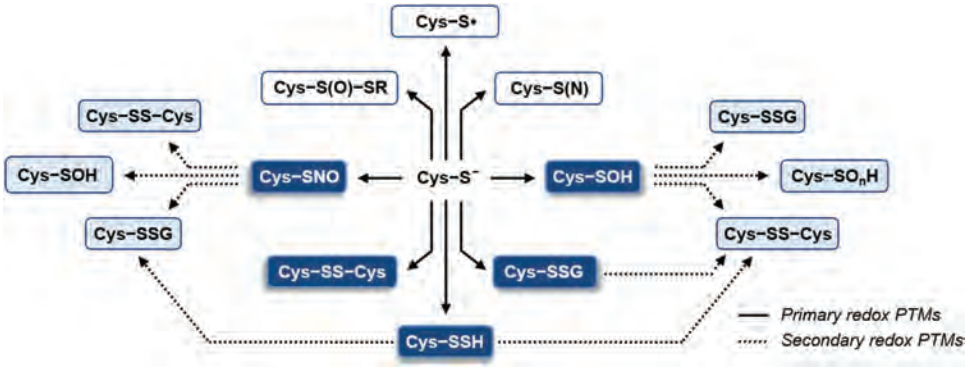

FIG. 9. Primary and secondary thiol-based redox modifications. Biologically relevant RMS-dependent Cys PTMs (*i.e.*, redox PTMs) are represented as follows: proteomic-suited primary redox modifications (*white on dark blue rectangles*), nonproteomic-suited primary redox modifications (*black on white rectangles*), and secondary redox modifications (*black on light blue rectangles*) occurring through further oxidative reactions of primary Cys oxoforms (S-nitrosothiols, sulfenic acid, S-glutathionyl, and persulfide). *Continuous* and *dotted lines* indicate primary and secondary redox reactions, respectively. PTM, post-translational modification. Color images are available online.

Downloaded by LI CO SA/50127/MI from www.liebertpub.com at 07/22/19. For personal use only.

several TRX classes (*f*, *m*, *y*, *h*) immobilized to the resin retain the same targets while they have distinct specificities in solution at more diluted conditions (see section IV). This may be due to the high concentration of TRX or to peculiar properties of the monocysteinic variants (339). Moreover, depending on the washing conditions, proteins interacting with TRX targets may be eluted together with genuine TRX targets, thereby increasing false-positive rates. Nevertheless, the major drawback of the column approach is that it only identifies the target protein, whereas the exact Cys targeted by TRX remains unknown.

The second main strategy, named ''reductome'' approach, is based on the *in vitro* reconstitution of the enzymatic TRX system (NADPH, NTR, and TRX) within a cell-free protein extract followed by labeling of newly exposed Cys with fluorescent (311, 559), radioactive (318), or biotinylated probes (317) (Fig. 10). This strategy was applied to total or subcellular soluble protein extracts from different land plants (6, 26, 27, 208, 311, 312, 325, 542, 543, 558). Biotinylated tags allow enrichment of Cys-containing peptides by affinity purification and allow identification of TRX-targeted Cys, a major advantage of the reductome approach. Unfortunately, to increase the number and diversity of targets, the *in vitro* reduction has to be performed using relatively high TRX concentration for which isoform specificity is mostly lost. Therefore, the lack of specificity is common to both the affinity column and reductome approaches. The two approaches are complementary as the targets identified only partially overlap (317, 405, 543).

Recently, quantitative adaptations of the reductome approach were developed for MS analyses based on chemical labeling with cleavable isotope-coded affinity tag reagents (cICAT) (205, 206) or with Cys-reactive tandem mass tag (Cys-TMT) (588). The most recent study combined the column with the quantitative reductome approach to investigate the thioredoxome of the unicellular green alga *C. reinhardtii* and identified 1188 proteins and 1052 Cys regulated by TRX. The quantitative approach based on differential cICAT labeling allowed to decrease false positives by filtering out the noise due to incomplete thiol blocking of the protein extract and thereby retain only proteins that are effectively reduced by TRX (405). Nevertheless, the targets identified remain putative and the presence of a TRX-reduced disulfide bond needs to be confirmed experimentally. Some TRXs were also shown to function, on specific targets, as denitrosylase (41, 42, 46, 487) and deglutathionylase (36, 189, 482). However, such activities should not impact the identification of TRX targets in both approaches as the vast majority of nitrosylated proteins are denitrosylated by GSH rather than TRX (44, 388, 433, 580), and TRX targets were analyzed in conditions wherein S-nitrosylation and S-glutathionylation are limited or absent (350, 571). Moreover, the reduction of S-nitrosylated or S-glutathionylated proteins by monocysteinic TRX is considered to yield nitrosylated or glutathionylated TRX rather than mixed disulfide with the target (36, 262, 405). Finally, both the proteomic identification of already established TRX targets and the biochemical confirmation of targets previously identified by proteomics strongly support the reliability of proteomic approaches to identify TRX targets. Biochemically confirmed TRX targets previously identified by proteomic studies include at least 2-Cys PRX (187, 353), phosphoglycerate kinase (349) magnesium chelatase CHLI subunit (232), β-amylase 1 (478), methionine sulfoxide reductases (494, 517), glucan water dikinase (342), uricase (130), and cytosolic NAD-MDH (212).

B. Nitrosylome

The identification and the quantification of S-nitrosothiols and S-nitrosylated proteins in biological samples remain highly challenging due to the lability of the –SNO bond (242) whose stability is strongly influenced by multiple factors, including light, metals, and reducing compounds such as GSH or TRXs. Such an instability of S-nitrosothiols precludes their direct detection by matrix-assisted laser desorption-ionization MS (250) and even by electrospray ionization MS (211) unless ionization parameters are carefully optimized (525). Therefore, high-throughput analysis of nitrosylated proteins is based on indirect methods for which the NO moiety is replaced by a more stable tag that allows an enrichment step.

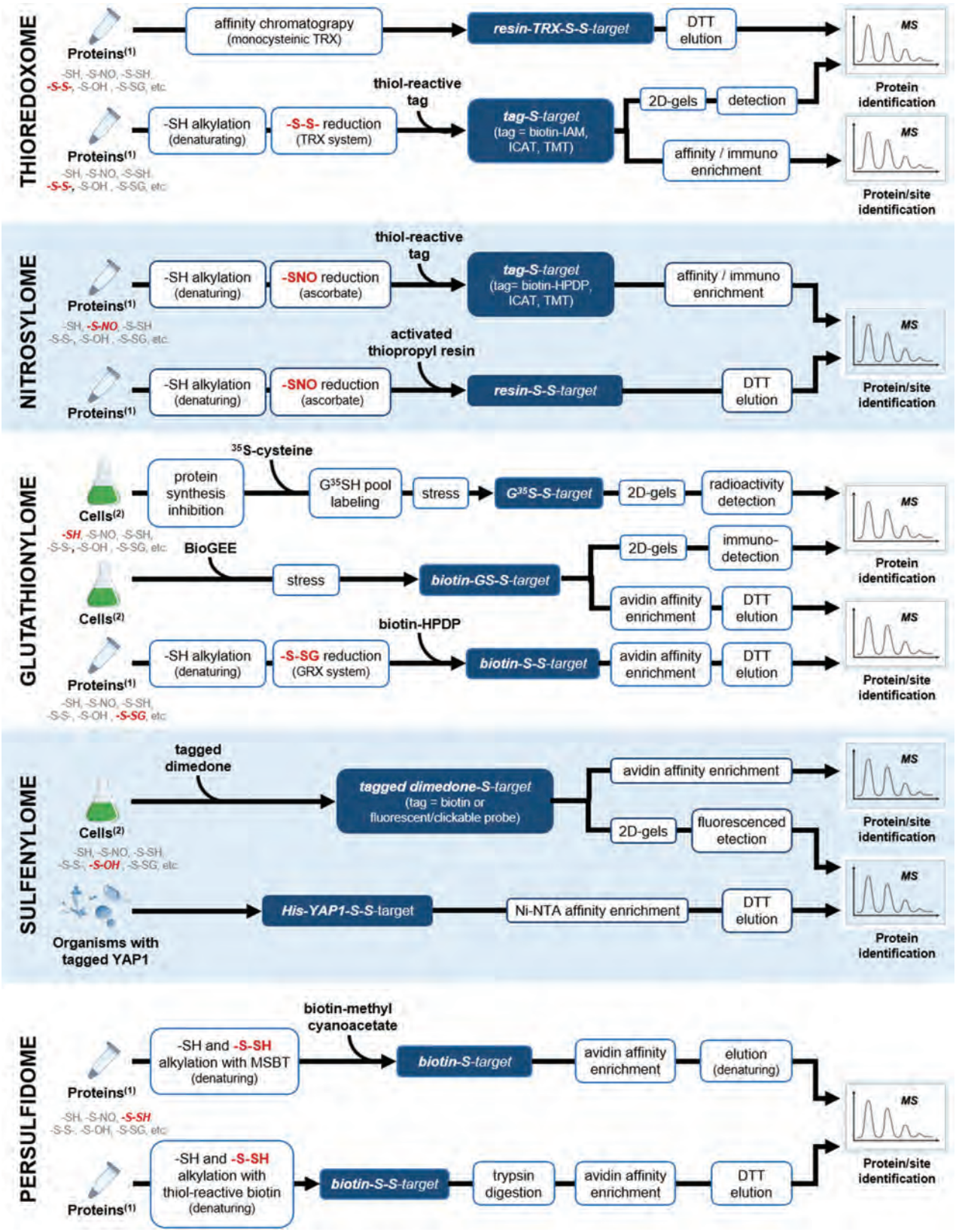

FIG. 10. Methodological principles of redox proteomic-based approaches. Workflows of current redox proteomic strategies are depicted according to the targeted redox PTM. The starting material (proteins, cells, or organisms) is indicated at the beginning of each workflow. The main steps are indicated in *black/white* on *white/blue boxes*, and the information level obtained by MS (identification of the modified protein and/or the modified Cys) is indicated at the end of each workflow. The initial modification state of Cys (–SH: reduced Cys; –S–S–: disulfide bond; –S–NO: nitrosylated Cys; –S–SG: glutathionylated Cys; –S–OH: sulfenylated Cys; –S–SH: persulfidated Cys) subjected to the redox proteomic strategy is indicated in bold. (1), proteins: cell-free protein extracts; (2), cells: intact cells. DTT, dithiothreitol; GRX, glutaredoxin; MS, mass spectrometry; MSBT, methylsulfonyl benzothiazole; TMT, tandem mass tag. Color images are available online.

Downloaded by LI CO SA/50127/MI from www.liebertpub.com at 07/22/19. For personal use only.

Downloaded by LI CO SA/50127/MI from www.liebertpub.com at 07/22/19. For personal use only.

Most studies rely on the biotin switch technique (BST) developed in 2001 (241) that was the first approach allowing detection and identification of S-nitrosylated proteins at the proteome scale (Fig. 10). This method consists in the replacement of the NO moiety of S-nitrosylated Cys residues by a disulfide-bonded biotin tag in a three step process: (i) initial blocking of unmodified Cys thiols under denaturing conditions, (ii) ''specific'' reduction of –SNOs by ascorbate, and (iii) labeling of the nascent thiols with the biotinylating reagent N-[6-(biotinamido)hexyl]-3′-(2′-pyridyldithio)-propionamide (biotin-HPDP). The replacement of the –SNO moiety by a disulfide-bonded biotin tag allows detection of previously S-nitrosylated proteins by immunoblotting or purification by avidin-based affinity chromatography and DTT elution for MS-based identification (301). Many variants of the original BST approach have been proposed such as the –SNO site identification (SNOSID) approach that includes a trypsin digestion step before enrichment (210) or the –SNO resin-assisted capture (SNO-RAC) method that takes advantage of a thiol-reactive resin for capturing nascent thiols after ascorbate reduction (Fig. 10) (152). The two methods allow identification of both the modified proteins and the modified Cys. The BST was applied to a wide range of photosynthetic organisms [reviewed in (269, 420, 463, 575)] and allowed identifying nitrosylated proteins in different organs and subcellular compartments (73, 385, 389, 463), in mutant lines (229, 296), and in plants exposed to exogenous NO donors (301, 350, 389) or affected by biotic (20, 432) or abiotic stresses (1, 64, 136, 217, 296, 421, 462, 463, 491, 492, 512). The most extensive studies identified 492 proteins and 392 sites in *C. reinhardtii* cells subjected to 15 minutes GSNO treatment (350) and 926 proteins and 1195 sites in *Arabidopsis* Col-0 and KO mutants for GSNOR [*gsnor1-3* lines; (229)].

Despite its popularity, BST is a very difficult technique with inherent limitations and biases that are not sufficiently taken into account. A major drawback relies on the identification of false positives due to incomplete blocking and loss of targets due to spontaneous denitrosylation during sample handling. Moreover, the specificity of the ascorbate-dependent reduction step is difficult to establish unambiguously toward either disulfide bonds (105) or by-products of reactions of classical thiol blocking agents with other species such as sulfenic acids (426). Overall, the signal-to-noise ratio is low and variable due to differences in biological material, growth conditions, experimental design, sample handling, instrument setup, and bioinformatic data analysis. This strongly decreases the reproducibility and sensitivity of the method.

Several quantitative BST approaches allowing quantification of nitrosylation levels have been proposed. They are based on the combination of BST with chemical labeling strategies such as ICAT or related molecules (136, 167, 388, 421), Cys-TMT (359), iodo-TMT (422) or isobaric tag for relative and absolute quantification (iTRAQ) using the SNO-RAC method (152), stable isotope labeling with amino acids in cell culture (593), or label-free spectral counting (589). Such quantitative approaches will certainly improve the confidence into data generated by BST-based studies and allow uncoupling protein levels from nitrosylation levels. We believe that a method more reliable than BST is probably required for analysis of nitrosylation at a dynamic level. More direct and promising approaches based on direct capture of S-nitrosocysteine residues have been proposed but need further confirmation of their potential for quantitative proteomic studies (129, 135, 520).

C. Glutathionylome

Proteomic analysis of S-glutathionylated proteins has been initially performed using radiolabeling of the glutathione pool in cell cultures in the presence of ^{35}S-cysteine and protein synthesis inhibitors (Fig. 10). Radiolabeled proteins are visualized by fluorography after separation on 2D gels. The spots disappearing in the presence of reducing agent, which correspond to S-glutathionylated proteins, are then identified by MS. Originally developed for human cells (160), this method allowed identification of 25 proteins in *C. reinhardtii* (340) but proved unsuccessful in *Arabidopsis* due to low levels of radiolabeling (126). This method has numerous drawbacks: (i) the protein synthesis inhibitors perturb cell physiology; (ii) this method cannot distinguish S-glutathionylated proteins (protein-SSG) from other forms of S-thiolation such as S-cysteinylation; (iii) it is limited by the necessity to perform 2D gels; (iv) it can only be used with cell cultures, thereby precluding studies on whole plants; (v) it can only detect proteins undergoing glutathionylation during treatment excluding proteins already glutathionylated under basal conditions; and (vi) finally it precludes high-throughput identification of glutathionylated sites.

An alternative method is based on biotinylated glutathione (BioGSH/BioGSSG) or the membrane permeant biotinylated glutathione ethyl ester (Fig. 10). The presence of the biotin tag allows detection of S-glutathionylated proteins by immunoblotting or enrichment by affinity chromatography. The latter can be coupled to MS for identification of not only S-glutathionylated proteins but also S-glutathionylated Cys if proteins are trypsin-digested before enrichment, as in the SNOSID approach (see section III.B). The major drawback of such methods is that proteins are not S-glutathionylated by the cellular GSH itself but by an exogenous sterically different molecule. The presence of the biotin tag on the glutathione molecule might perturb the function of glutathione-dependent enzymes and especially GRXs (Zaffagnini *et al.*, personal communication). Another drawback, shared with the ^{35}S labeling method, is that proteins glutathionylated under basal conditions are not detected. Originally used in mammals (483), this approach allowed identification of >70 S-glutathionylated proteins in *Arabidopsis* (126, 236), 225 proteins and 56 S-glutathionylation sites in *Chlamydomonas* (571), and 349 proteins and 145 sites in *Synechocystis* sp. PCC 6803 (76).

Several additional methods have been employed but not yet used in photosynthetic organisms. Commercial antiglutathione antibodies that can be useful for analysis of isolated proteins lack specificity and sensitivity, precluding application for high-throughput proteomics. S-glutathionylation can also be studied using an adaptation of the BST where the reduction step is performed with GRXs instead of ascorbate (Fig. 10) (175, 209, 253, 297). This approach has roughly the same drawbacks as the BST. In addition, the blocking of free thiols under denaturing conditions is difficult to combine with the enzymatic reduction of S-glutathionylated proteins by the GRX system (NADPH, glutathione reductase, GRX; see section V) that has to be performed in the absence of detergents.

Overall, despite the fact that S-glutathionylation is more stable than S-nitrosylation, the methods currently employed have numerous caveats and drawbacks, and the development of new approaches is most probably required for proteome-wide quantitative analysis of glutathionylation. A ''chemo-biology'' approach based on click chemistry (417) may be possible since biosynthesis of a click analogue of glutathione seems experimentally feasible (141, 254, 445, 446). Such approaches have proven very efficient for proteomic analysis of S-palmitoylation (323, 592), N-myristoylation (545), or glycosylation (292, 496).

D. Sulfenylome

Proteomic analysis of sulfenic acids follows two major strategies that are based on either chemical or genetically encoded probes (4, 413, 554). Current chemical probes are mostly based on 1,3-carbonyl scaffold such as the cyclic dimedone (5,5-dimethyl-1,3-cyclohexanedione) (198, 424). At physiological pH, dimedone is in equilibrium with its enolic form that itself performs a nucleophilic attack on sulfenic acid. Dimedone tagged peptides can be detected by MS, and due to the generated mass increase, the involved Cys can be easily characterized. Nevertheless, dimedone has limited application for complex samples as it lacks a functional group for enrichment. Therefore, molecules harboring a dimedone conjugated with a fluorescent tag (DCP-Rho and DCP-FL series) or a biotin tag (DCP-Bio series) have been developed (Fig. 10) (77, 415). These probes have proven efficient but the presence of a bulky tag may alter cell permeability or prevent interaction with sulfenic acids that are not fully solvent accessible (413, 466).

Recently, small biorthogonal probes derived from dimedone have been developed such as DAz-1/DAz-2 (289) and DYn-1/DYn-2 (396). These probes can be biotinylated through click chemistry allowing enrichment of sulfenylated peptides. Used at lower concentrations than the classical dimedone, they are nontoxic and do not influence the intracellular redox balance (396, 555). Analysis of sulfenylated Cys with dimedone-based probes is compatible with classical quantitative MS-based strategies such as iTRAQ or TMT, which introduce reporter tags on tryptic peptides. Another way consists in synthesizing light and heavy isotope-coded forms of DYn-2 (556). Such a strategy allowed identification, in human cells, of 1000 sulfenylated Cys in 700 proteins (555). Despite their selectivity, these probes suffer from poor reaction kinetics under physiological conditions compared with biological reactions of sulfenic acids (197). New probes with faster reaction rates are, therefore, being considered to further expand our ability to monitor the sulfenome (198, 199, 302, 416). Biotinylated strained bicyclo[6.1.0]nonyne derivatives appear promising tools as they show reaction rates two orders of magnitude higher than dimedone even at low concentrations (μM range) (416).

The second approach is based on the yeast transcription factor Yap-1 that naturally interacts with the sulfenic acid formed on the Orp1 protein through formation of a transient mixed disulfide (Fig. 10) (116, 544). An engineered monocysteinic His-tagged version of Yap1 has been developed and shown to covalently trap sulfenylated proteins in *Escherichia coli* (489) and *Saccharomyces cerevisiae* (490). The major advantage of this type of probe is that their reaction kinetics is, at least theoretically, faster than dimedone-based chemical probes (4). Moreover, since they are genetically encoded, they can be controlled through genetic circuits and can be targeted to explore the sulfenylome of diverse subcellular compartments. Yap1-based methods also have several drawbacks, including a low efficiency that may be linked to *in vivo* reduction of Yap1 target mixed disulfides and a selectivity bias due to the Yap1 protein backbone and its steric effects.

In photosynthetic organisms, few studies addressed the question of the sulfenylated proteome *in vivo*. A combination of DCP-Bio and Yap1 probe allowed identification of 91 proteins in *Medicago truncatula* and 20 in its symbiont *Sinorhizobium meliloti* (381). More recently, the YAP1 probe was combined with a tandem affinity purification tag to detect 97 sulfenylated proteins in *Arabidopsis* cell suspensions under H_2O_2 stress (527). The DYn-2 probe was also recently employed in *Arabidopsis* and allowed identification of 226 sulfenylated proteins (3). Interestingly, a low overlap (17%) was observed between the two *Arabidopsis* sulfenylomes obtained by the same groups, suggesting that both approaches are highly complementary.

E. Persulfidome

Persulfides exhibit a reactivity similar to thiols, rendering their analysis at a proteome scale challenging. Some BST-based proteomic strategies aiming at unravelling persulfidation in complex samples have been recently developed. In the pioneering method, free thiols are blocked by methyl methanethiosulfonate (MMTS), whereas unblocked persulfides are subsequently biotinylated by HPDP-Biotin before enrichment by avidin-based affinity chromatography (361). Nevertheless, the assumed selectivity of the strong thiol-alkylating agent MMTS is questionable as it was shown to react indifferently with thiols and persulfides (390). Another approach combines initial blocking of all free thiols and persulfides with N-ethyl maleimide (NEM), DTT reduction, and labeling of nascent thiols with NEM-biotin (511). This strategy should be used with care as many proteins can undergo multiple DTT-reducible redox PTMs (186, 405).

A more innovative proteomic approach, called Tag-switch, allows persulfide biotinylation without the use of any reductant (585). In this strategy, both thiols and persulfides are first blocked with the alkylating reagent methylsulfonyl benzothiazole (MSBT), but only the activated disulfide bond of MSBT-derivatized persulfides is able to react in a second step with the biotinylated electrophile methyl cyanoacetate (Fig. 10). After enrichment using avidin-based affinity purification, persulfidated proteins are eluted under nonselective denaturing conditions that may lead to contaminations with proteins tightly bound to avidin such as endogenously biotinylated proteins. Another issue is linked to the selectivity of the Tag-switch approach as methyl cyanoacetate can cross-react with other forms of protein oxidations (sulfenic acid, sulfenylamide, and carbonyls) (585).

The last strategy recently developed consists in the direct alkylation of persulfidated proteins with biotinylated cysteine alkylating reagents (127, 165). In this case, both persulfides and thiol groups are indiscriminately biotinylated and persulfidated proteins retained on avidin affinity columns are specifically eluted in the presence of DTT. Nevertheless, to avoid that true persulfidated proteins remain linked to the

Downloaded by LI CO SA/50127/MI from www.liebertpub.com at 07/22/19. For personal use only.

column due to the presence of other biotinylated surface-exposed Cys in their sequence, low concentration (50 μM range) of biotinylated alkylating reagents should be employed as these conditions are known to promote alkylation of hyper-reactive thiols such as persulfides and thiolates rather than thiols (165, 530). The persulfide site identification approach, which is equivalent to the SNOSID approach, circumvents these pitfalls by identifying persulfidated peptides and thus Cys instead of proteins (165). Moreover, it remains compatible with classical quantitative MS techniques to compare persulfidomes (307).

In photosynthetic organisms, data about protein persulfidation are limited. Only two studies attempted to characterize the persulfidome in the model plant *A. thaliana*. By using either the pioneering approach (17) or the Tag-switch assay (16), these studies allowed the identification of 106 and 2015 persulfidated proteins, respectively. These proteins are localized in different subcellular compartments but mainly reside in chloroplasts and cytoplasm (65%) and are involved in a wide variety of pathways and processes, suggesting that persulfidation may be an important thiol switching mechanism as other redox PTMs in photosynthetic organisms.

F. The Cys proteome: a complex dynamic network

Before the advent of omics strategies, research in cell signaling has been conducted using ingenious analytical approaches. It is becoming clear now that proteomes are so intricate that we cannot understand the cellular functional organization using only a reductionist approach studying a limited number of cellular components. This is especially relevant for redox signaling that coordinates large number of redox elements involved in a multitude of pathways and cellular processes to allow resistance and adaptation to environmental challenges (182). This Cys proteome can be considered as an interface between the functional genome and the external environment (183). This highly dynamic network probably involves spatial and temporal regulation of multiple interconnected redox PTMs on hundreds of protein thiols with flexible reactivities (395, 414, 530). Therefore, global approaches are required to fully understand the entire molecular complexity of redox signaling pathways and their links with numerous pathophysiological features. Among global approaches, MS-based strategies have benefited lately from tremendous technological improvements, and are now ready to face the challenge of comprehensive and quantitative proteomic approaches at the level of protein expression, protein interactions, or PTMs (372).

Combinations of multiple redox PTMs act as a cellular network rather than as insulated elements. Understanding the organization of these networks will require to unravel the determinants of the specificity of the diverse redox PTMs for proteins and Cys. Indeed, it remains unclear whether multiple redox PTMs occur on a limited number of proteins containing reactive Cys or whether each modification targets a distinct redox network. Recently, the identity of redox-modified Cys belonging to proteins undergoing at least two different redox PTMs (among targets of TRX, S-glutathionylation, and S-nitrosylation) was compared in Chlamydomonas (405). This analysis revealed that 86% of these Cys were modified by only one type of redox modification. This comparison indicates, on one hand, that the Cys proteome does not represent a subset of highly reactive Cys that are modified indiscriminately, and highlights, on the other hand, a strikingly high specificity of each modification for distinct Cys residues (405). A similar high specificity with a limited overlap between Cys targeted by multiple PTMs was also reported in human and mouse (186, 289). These results indicate that the Cys proteome does not represent a small subset of highly reactive Cys that are modified through indiscriminate interaction with the molecules they encounter but represent a complex system of redox PTMs that are specific toward distinct interconnected protein networks (405).

The complexity of the network likely provides the robustness and specificity required to allow simple molecules such as ROS, RNS, and RSS to play a signaling role. This redox network is presumably a major component of signal integration and constitutes the molecular signature of the ROS/RNS/RSS cross talk whose importance in cell signaling has been recognized (158, 161, 191, 347, 471).

Understanding this complex network will require to determine the stoichiometry and dynamics of multiple redox PTMs under diverse physiological conditions or in different genetic backgrounds, and at different time scales. This should be favored in the future by the development of sensitive and accurate redox quantitative MS approaches combined with the development of new chemospecific probe molecules (554). These chemical probes will have to (i) be specific for a given modification with no interference with other biological molecules, (ii) be compatible with quantitative MS, (iii) be nontoxic and membrane permeable to allow *in situ* or *in vivo* labeling, (iv) be highly sensitive to allow detection of low abundant proteins or low levels of modifications, (v) allow efficient enrichment methods using, for example, click chemistry, and (vi) exhibit fast reaction rates compatible with the half-life and reactivity of the species studied. New types of modifications may also become amenable to proteomic analysis with the development of new probes such as NO-Bio, a recent biotin-tagged probe for proteomic analysis of sulfinic acids (306). Future redox proteomic studies will have to take advantage of isotope-coded multiplex reagents such as TMTs to monitor multiple modifications or multiple samples simultaneously. Progress in the sensitivity of MS instruments and proteomic methods will allow analyses on limited amounts of biological samples and thus foster the development of single cell redox proteomic approaches to decipher the redox signaling network rather than unravel averaged redox signals from multiple cells. In other words, temporal quantitative redox proteomics on limited number of cells is certainly the grail that will allow us to discriminate redox modification events from noise and thus shed light on the functioning of the redox network.

In addition, computational structural genomic approaches will be required to integrate the Cys proteome at the structural level. Finally, besides redox PTMs, the integration of the signal implicates a myriad of other molecules and processes acting at multiple levels (326). In photosynthetic organisms, several redox PTMs are linked to signaling pathways controlled by hormones (140, 262, 497, 522, 528, 567) or calcium (506), and in mammals, nitrosylation was shown to interfere with signaling processes mediated by phosphorylation, ubiquitylation, sumoylation, acetylation, or palmitoylation (214). Therefore, a strong effort is required to integrate redox networks with other signaling pathways and to analyze their impacts on the cellular responses at multiple levels. This will certainly be crucial to unravel how

Downloaded by LI CO SA/50127/MI from www.liebertpub.com at 07/22/19. For personal use only.

environmental challenges are encoded into a biochemical signal than can be exploited to trigger the appropriate responses in terms of localization, duration, and intensity, at the genome, transcriptome, proteome, and metabolome levels to allow adaptation and survival.

IV. The Remarkable Diversity of Redoxins in Photosynthetic Organisms

A. A general introduction on plant TRX superfamily (redoxins)

The TRX superfamily encompasses several protein families (notably TRXs, GRXs, protein disulfide isomerases [PDI], and glutathione-S-transferases [GSTs]), the members of which have in common a specific structural arrangement named the TRX fold (see Section V) and often a typical XCXXC/S signature containing the redox active Cys pair.

The number of PDI genes found in plant genomes is comparable with that in mammals and higher than that in fungi (465). For the TRX, GRX, and GST gene families, algae and terrestrial plants have an expanded number of representatives, which is explained, in part, by the existence of additional classes (87, 100, 274, 286, 287, 336). Hence, in the next subsections, we focus our attention on the remarkable diversity found in TRX and GRX families, describing their subcellular distribution and how comparative genomics led to a rather exhaustive and refined classification of these genes/proteins and to a better understanding of their evolution.

B. Classification and evolution of redoxins and their reductases

TRXs and GRXs were initially defined by quite strict signatures, for example, WC[G/P]PC and YCP[F/Y]C, respectively, but the sequencing of numerous genomes pointed to the existence of a large variety of other combinations. These variations are usually still compatible with an oxidoreductase activity, although some are associated with the capacity to bind Fe-S clusters as observed initially for GRXC1, which possesses a slightly divergent YCGYC active site signature and then with several other GRXs (441). In the PDI family, the majority of plant isoforms possess a WCGHC signature, but variations also appeared in some representatives (465). There is no such universal signature for GSTs and actually only a very few of them have conserved both Cys. An important number has even lost the first catalytic Cys that has been replaced by a serine. This has led to a change in the type of activity catalyzed by GSTs. Those that kept the catalytic Cys have glutathione-removing activities, whereas those possessing a serine have glutathione-conjugating activities, this residue serving for the activation of the thiol group of the glutathione molecule. Besides, GSTs have a particular structural arrangement with the existence of an all-helical domain fused at the C-terminus of the TRX domain. We invite the reader to refer to the following reviews for detailed information about phylogenomic analyses of PDIs (287, 465) and GSTs possessing the catalytic Cys (274). From now, this section uniquely focuses on the TRX and GRX systems that primarily control the RMS-dependent PTMs of protein Cys.

1. Phylogenetic and sequence diversity within the TRX and TRX reductase families. The TRX family is split into 21 well-defined classes including the NADPH–TRX reductase C (NTRC) fusion proteins that contain a TRX domain and a TRX reductase (TR) domain (Table 1 and Fig. 11). Some TRX family members can unequivocally be distinguished by the active site signature and domain organization. Typical TRX isoforms (TRX *f*, *m*, *x*, *y*, *z*, *o*, and *h* classes) are formed by a single domain with regular tryptophan-cysteine-glycine-proline-cysteine (WCGPC) or tryptophan-cysteine-proline-proline-cysteine (WCPPC) active site signatures corresponding to that found in ancestral TRXs (Fig. 11). In addition, there are larger proteins that contain either two or more TRX domains (chloroplast drought-induced stress protein of 32 kDa, CDSP32, or nucleoredoxins, NRX) or a TRX domain fused to a domain with other functions (TR domain in NTRC, tetratricopeptide repeat domain in tetratricopeptide domain-containing TRXs (TDXs) (Fig. 11). The active site signatures of the TRX domain(s) are also usually regular or with little variations. In CDSP32, the first domain has lost the Cys, whereas the signature of the C-terminal domain is of the HCGPC type (Fig. 11). Among NRXs, three groups can be distinguished. In NRX1 and NRX3 members, both TRX domains have generally WCGPC or WCPPC active site signatures, whereas in NRX2 members, only the C-terminal domain conserved the Cys and the consensus signature has significantly diverged being of the [W/R]C[L/A]P[C/G] form (Fig. 11). The C-terminal TRX domains in NTRC and TDX have a TCGPC and WCGPC signature, respectively (Fig. 11). Finally, there are atypical TRXs formed by a single domain and divergent active site motifs: CLOT (WCPDC), HCF164 (WCEVC), TRX-like1 (most often WCRVC), TRX-like2 (WCRKC), TRX-lilium1 (GCGGC), TRX-lilium2 (WC[G/A]SC), TRX-lilium3 (SCGSC), TRX *s* (no conserved signature), and TRX CxxS (often WC[M/I]PS), which are included in the TRX *h* class (Fig. 11). Lilium-type TRXs are also known as atypical Cys histidine-rich TRXs [ACHT, (110, 111, 133)] because they contain several conserved Cys and histidine residues outside the active site. These chloroplast atypical TRXs are proposed to play a role in the inactivation of light-activated redox targets (see section VII). It is worth mentioning that HCF164 possesses an N-terminal anchoring domain to the thylakoid membrane (Fig. 11). The TRX *s* class is not presented in Table 1 because it is only found in some *leguminosae*. There are four members in *M. truncatula* (428) and they likely possess specific functions for the establishment of symbiotic interactions between plants and bacteria of the rhizobia genus. Interestingly, the TRX *s1* is secreted into the microsymbiont although it seems that it derived from plastidial TRX *m* (428). Therefore, it may be that the plastid targeting sequence evolved into a secretory signal.

When considering two angiosperms, the dicot *A. thaliana* and the monocot *Oryza sativa*; a lycophyte, the fern *Selaginella moellendorffii*; a bryophyte, the moss *Physcomitrella patens*; a green alga, *C. reinhardtii* and a cyanobacterium, *Synechocystis* sp. PCC 6803, the minimal TRX equipment in photosynthetic organisms, as found in this cyanobacterium and conserved in all other organisms, appear to be formed by four members belonging to the HCF164, TRX *m*, TRX *x*, and TRX *y* types (Table 1) (87). This number increases to 20 in *C. reinhardtii* with the appearance of TRX *f*, *h*, *o*, *z*, CDSP32, CLOT, TRX-like, TRX-lilium, NRX, and NTRC. Another increase occurred in terrestrial plants, both nonvascular (mosses) and vascular (ferns and angiosperms) plants. So far, in land plants, the lowest and highest number of reported TRXs have been found in *S. moellendorffii* (22 isoforms,

Downloaded by LI CO SA/50127/MI from www.liebertpub.com at 07/22/19. For personal use only.

Table 1. Gene Content in the Glutaredoxin and Thioredoxin Families in Representative Organisms of the Green Lineage

	At	*Os*	*Sm*	*Pp*	*Cr*	*Synsp6xxx*
GRXs	33	29	17	15	7	3
Class I	6	5	4	5	2	2
C1	1	0	0	0	—	—
C2	1	2	2	3	—	—
C3	1	1	0	1	—	—
C4	1	1	1	0	—	—
C5	1	0	0	0	—	—
S12	1	1	1	1	—	—
Class II	4	5	9	8	4	1
S14	1	1	3	2	1	—
S15	1	2	3	2	1	—
S16	1	1	1	1	1	—
S17	1	1	2	3	1	—
Class III	21	17	3	2	0	0
Class IV	2	2	1	0	1	0
TRXs	37	30	22	28	20	4
TRX f	2	1	2	3	2	0
TRX h	11	7	5	5	2	0
TRX m	4	4	2	6	1	1
TRX o	2	1	0	1	1	0
TRX x	1	1	1	2	1	1
TRX y	2	1	1	1	1	1
TRX z	1	1	1	2	1	0
TRX-like 1	1	1	2	1	1	0
TRX-like 2	2	1	2	2	0	0
TRX-lilium 1	3	2	0	0	0	0
TRX-lilium 2	1	1	2	1	1	0
TRX-lilium 3	1	1	0	1	1	0
TDX	1	1	0	0	0	0
CDSP32	1	1	1	1	1	0
CLOT	1	1	1	1	1	0
HCF164	1	1	1	1	1	1
NRX1	1	2	0	0	5[a]	0
NRX2	0	1	1	0	0	0
NRX3	1	1	0	0	0	0
TR	4	4	3	6	4	2
NTRA/B	2	2	1	2	3[b]	0[c]
NTRC	1	1	1	2	1	0
FTR-b	1	1	1	2	1	1

Sequences from *Oryza sativa* (*Os*), *Selaginella moellendorffii* (*Sm*), *Physcomitrella patens* (*Pp*), *C. reinhardtii* (*Cr*), and *Synechocystis* sp. PCC 6803 (*Syn*) have been retrieved from genomic data available through Phytozome V12 portal or cyanobase by BLAST-p analysis using *Arabidopsis thaliana* (*At*) sequences as references. The classes in the GRX and TRX families have been previously defined (87, 100).

[a]The five NRXs found in *C. reinhardtii* have been arbitrarily classified as NRX1 but they group independently from land plant NRXs.

[b]This indicates the existence among NTRA/B from *C. reinhardtii* of a mammalian-type selenocysteine-containing NTR.

[c]*Synechocystis* sp. PCC 6803 does not possess an authentic NTR, but another type of diflavin protein of unknown function (59).

CDSP32, chloroplastic drought-induced stress protein; GRX, glutaredoxin; FTR, ferredoxin:thioredoxin reductase; NRX, nucleoredoxins; NTR, NADPH:thioredoxin reductase; NTRC, NADPH:thioredoxin reductase C; TDX, tetratricopeptide domain-containing thioredoxin; TR, thioredoxin reductase; TRX, thioredoxin.

Table 1) and in *Eucalyptus grandis* (45 isoforms) (412). This rise is mostly linked to duplications within existing classes, as the sole innovation specific to angiosperms is the TDX class that contains one or two members. These substantial differences in the TRX content among terrestrial plants are appealing although some cautions may be needed for recent automatically annotated genomes.

Why the evolution positively selected complexity in the plant TRX system (on average in the human genome 1 TRX-coding gene is found for every 10,000 protein-coding genes *versus* 1350 protein-coding genes in *Arabidopsis*) is unknown. Reasonably more than a single evolutionary cause has contributed to positive selection. In fact, it is generally accepted that in plants several physiological processes are under the control of the TRX-mediated redox mechanisms. Whether as a result of the sessile lifestyle of photosynthetic organisms or due to the greater permissiveness to genome doubling events as well as arising from the existence of three evolutionary distinct genomes (nuclear, mitochondrial, and plastid genome) inside a cell, plant TRX system is indeed more complex and versatile than that of prokaryotes (*e.g.*, bacteria) and heterotrophic organisms (*e.g.*, animal and fungi).

On the contrary, there are only minimal variations concerning the TRs along the green lineage (Table 1). The FTR is

Downloaded by LI CO SA/50127/MI from www.liebertpub.com at 07/22/19. For personal use only.

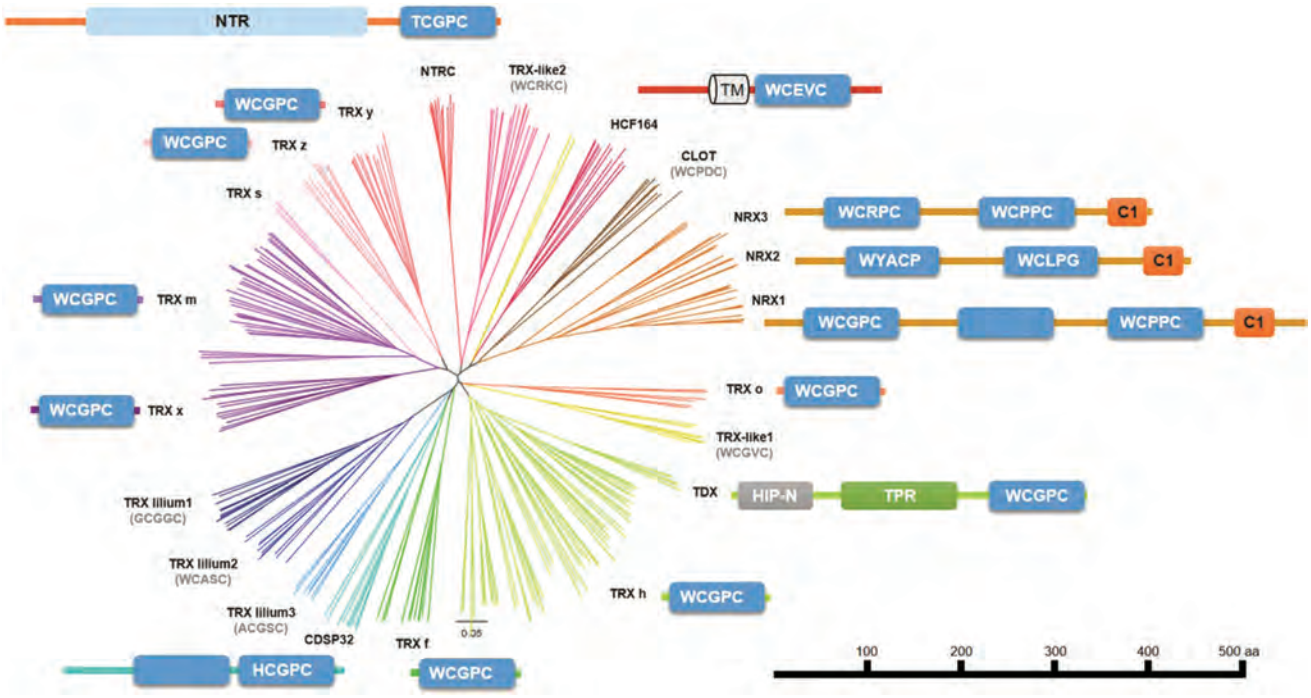

FIG. 11. Phylogenetic analysis of plant TRXs and schematic representation of the architecture of TRX members. A total of 267 sequences have been retrieved by blastp analyses from 10 genomes found in the cyanobase for cyanobacterial genomes and from the version 12 of the Phytozome portal for algal and terrestrial plant genomes. Sequences were aligned using ClustalOmega and the phylogenetic tree was constructed with BioNJ (168) in Seaview using the observed distance methods and ignoring all sequence gaps. The robustness of the branches was assessed by the bootstrap method with 1000 replications. The scale marker represents 0.1 substitutions per residue. The tree was then edited using Figtree software. The names of individual sequences have been indicated and proteins possessing classical or additional domains as predicted by the pfam or NCBI conserved domain tools are represented with the exception of TRX lilium1-3, CLOT, TRX-like1-2, and TRX *s*. The TRX domain of a chosen *Arabidopsis thaliana* representative is in *light blue* with the active site signature in *white*. The TRX domains without active site signatures have lost both catalytic cysteines. Among additional domains, NTR stands for NADPH thioredoxin reductase, HIP-N for N-terminal domain of HSP70-interacting proteins, C1 for C1 domain (short domain rich in cysteines and histidines), and TPR for tetratricopeptide repeat. The only protein with a membrane-anchoring domain, represented as a cylinder, is HFC164. The size of the boxes and strings is proportional to the length in amino acids. Note that TRX *s* and NRX2 are absent in *A. thaliana* and that poplar NRX2 was used as the plant representative. NRX, nucleoredoxins; WCGPC, tryptophan-cysteine-glycine-proline-cysteine; WCPCC, tryptophan-cysteine-proline-proline-cysteine. Color images are available online.

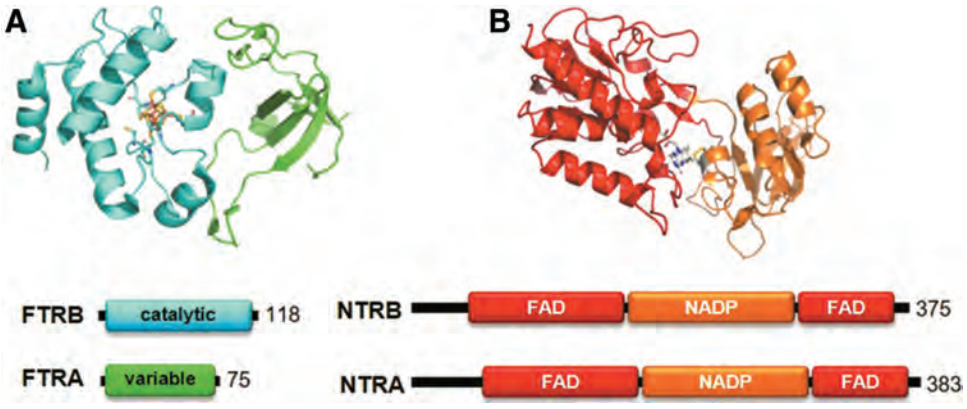

FIG. 12. Structural and schematic representation of the architecture of plant TRs. (A) The catalytic (FTRB) and variable (FTRA) subunits of FTR from *Synechocystis* sp. PCC 6803 are represented (*upper panel*: ribbon, PDB ID: 2PVD; *lower panel*: schematic subunits), and in *cyan* and *light green*, respectively. Accession numbers: catalytic FTR subunit, Q55389; variable FTR subunit, Q55781. **(B)** The FAD- and NADP(H)-binding domains of NTRB/A from *A. thaliana* are represented as *ribbon* (*upper panel*, PDB ID for *Arabidopsis* NTRB: 1VDC) and schematic domains (*lower panel*), and in *red* and *orange*, respectively. Accession numbers: NTRB, Q39243; NTRA, Q39242. For both panels, the size of the boxes is proportional to the length in amino acids. Color images are available online.

Downloaded by LI CO SA/50127/MI from www.liebertpub.com at 07/22/19. For personal use only.

Downloaded by LI CO SA/50127/MI from www.liebertpub.com at 07/22/19. For personal use only.

composed of a catalytic and a variable subunit (Fig. 12), which is, by definition, difficult to identify based on sequence homology. Hence, concentrating on the FTR catalytic subunit, all analyzed genomes contain a single gene except *P. patens* that has two genes (Table 1). Concerning NTRs, there is usually a single NTRC isoform and one to two NTRA/B members (Table 1, Figs. 11 and 12). A large number of NTRA/B genes (six) is found in the genome of *Quercus robur* but the same caution as before applies for this first assembled genome version (412). One particularity is the presence of a mammalian-type NTR in some green algae such as *C. reinhardtii* (239). These are remnant selenoproteins common to many eukaryotes but not terrestrial plants, since they lost the system for selenocysteine insertion.

The subcellular localization of most *Arabidopsis* TRXs and TRs has been determined experimentally. The mitochondrion is likely the less rich compartment containing only TRXs *o* and a TRX *h*2 in some organisms as poplar and *Arabidopsis* (172, 275, 330). They should be maintained reduced *via* NTRA or NTRB, both isoforms having been detected, although NTRB may be more abundant (425). Both TRXs *o*1 and *o*2 show double localization, the former in mitochondria and nucleus, the latter in mitochondria and cytoplasm (118, 171). Both NTRA and NTRB are also found in the cytoplasm, whereas NTRA may also be in the nucleus (316, 425). In these compartments, they might reduce a certain number of cytoplasmic TRXs (Clot, TRX-like 1, TRX *h*1, *h*3 to *h*8, TRX CxxS1, and TDX) and nuclear proteins (NRX1, NRX2, and NRX3) (85, 316) but also some membrane-bound TRXs (TRX *h*9, TRX CxxS2) owing to the existence of N-terminal glycine and Cys residues promoting membrane anchoring through N-myristoylation and palmitoylation, respectively (330, 507). The employed reduction system has not been validated for all of them but TRX CxxS and TRX *h*9 (or TRX *h*4 in poplar) use a GSH/GRX system (173, 264, 330). Besides, a myristoylated glycine in *A. thaliana* TRX *h*7 and TRX *h*8 promotes their attachment to the ER/Golgi endomembrane system (507). An orthologous tobacco TRX *h* is secreted, which raises the question of its reduction (247).

The chloroplast possesses by far the largest TRX equipment. In *A. thaliana*, there are 20 TRXs taking into account NTRC (52, 61, 92, 110, 288, 330, 468). All regular/typical TRXs (*i.e.*, TRX *m*, *f*, *x*, *y*, *z*) are reduced by FTR (87, 564) and some of them, such as TRX *z*, may be reduced by NTRC as well (563). It is not yet clear how CDSP32 is recycled upon oxidation, whereas poplar TRX-like 2.1 and TRX-lilium2 were shown to be reduced by a GSH system (85). ACHT1 and ACHT4 were proposed to be reduced by TRX-regulated ADP-glucose pyrophosphorylase, thereby contributing to its downregulation (133) (see section VII). HCF164 is attached to thylakoids, likely facing the luminal side (288) and would relay the reducing equivalents from stromal TRXs into the lumen (352), where proteins regulated by disulfide formation are present (475).

As far as their reducing activity is concerned, TRX *m* and *f* reduce disulfides on several metabolic targets, including enzymes of the CB cycle, oxidative pentose phosphate pathway, starch metabolism, ATP synthase, and malate valve (68, 92, 200, 349, 367, 478–480). TRX *x* and *y*, together with CDSP32 and ACHT1/4, are more specific for antioxidant enzymes, for example, PRXs and methionine sulfoxide reductases (93, 111, 124, 147, 164, 225, 494, 495).

2. Phylogenetic and sequence diversity within the GRX family. The GRX family can be split into six classes (see below in this section for further details; Fig. 13). Classes I and II are shared by eukaryotes and cyanobacteria (Table 1). Classes III and IV are specific to eukaryotes (Table 1 and Fig. 13). Classes V and VI are specific to cyanobacteria, although they are not present in *Synechocystis* sp. PCC 6803 (Table 1 and Fig. 13). Therefore, both photosynthetic eukaryotes and cyanobacteria contain GRXs belonging to up to four classes (eukaryotes: classes I, II, III, and IV; cyanobacteria: classes I, II, V, and VI). As for the TRX family, members of these GRX classes differ notably by their active site signature and domain organization (Fig. 13). The nomenclature established previously using *A. thaliana* members relies on the presence of a Cys or a serine at the last position of the active site signature (439). Therefore, they were named from GRXC1 to C14 and from GRXS1 to S17, although AtGRXS13 possesses a CPLG motif and at the time, the two class IV members (see this section) were not included. The presence of a residue different from Cys or serine at the last position is also observed in a limited number of GRX members in some other species (*e.g.*, *O. sativa* or *Sorghum bicolor*).

Except for the specific case of the PRX-GRX fusion proteins found in some cyanobacteria, class I GRX isoforms (GRXC1-C5, GRXS12, and cyanobacterial GRX I) are formed by a single domain with a quite regular YC[P/S/G][Y/F]C active site signature with some exceptions as GRXC5 (WCSYC) and GRXS12 (WCSYS) (Fig. 13). The phylogenetic analysis reveals that cyanobacterial and algal GRXs form independent clades, whereas terrestrial plants can be further divided into GRXC1/C2, GRXC3/C4, and GRXC5/S12 subgroups (Fig. 13), and these subgroups also differ in their biochemical and redox properties (100–102, 104, 573). Only two class I isoforms are found in model nonphotosynthetic organisms such as *E. coli* and *Homo sapiens*, but four in *S. cerevisiae*.

The class II GRXs are typified by their extremely conserved CGFS signature. They can also be further divided into four subclasses (GRXS14, S15, S16, and S17) in eukaryotic photosynthetic organisms according, in particular, to the existence of multidomain proteins, whereas cyanobacterial GRX II isoforms systematically grouped independently (Fig. 13). The GRXS14 and S15 members are only formed by a single GRX domain, as are cyanobacterial orthologs (Fig. 13). The GRXS16 and S17 have a modular organization (Fig. 13). The former possesses an N-terminal domain with some similarity with a certain type of endonuclease and the latter is formed by an N-terminal TRX-like domain with a distorted active site signature fused to one to three GRX domains. It is extremely interesting to point out how the GRXS17 fusion appeared and evolved during evolution. Indeed, haptophytes such as *Emiliania huxleyi* have isoforms with only one GRX domain, heterokonts and green algae with two GRX domains, sequenced mosses (*P. patens* and *Sphagnum fallax*), liverwort (*Marchantia polymorpha*), and fern (*S. moellendorffii*) possess isoforms with two and/or three GRX domains, and gymnosperms (*Picea abies*) and angiosperms have isoforms with three GRX domains (100). Since GRXS16 prototypes are specific to the green lineage, only one to three class II isoforms are found in model nonphotosynthetic organisms, one in *E. coli*, three in *S. cerevisiae*, and two in *H. sapiens*.

The class III GRXs are characterized by the presence of two adjacent Cys forming CCxC, CCxS, or CCxG signatures

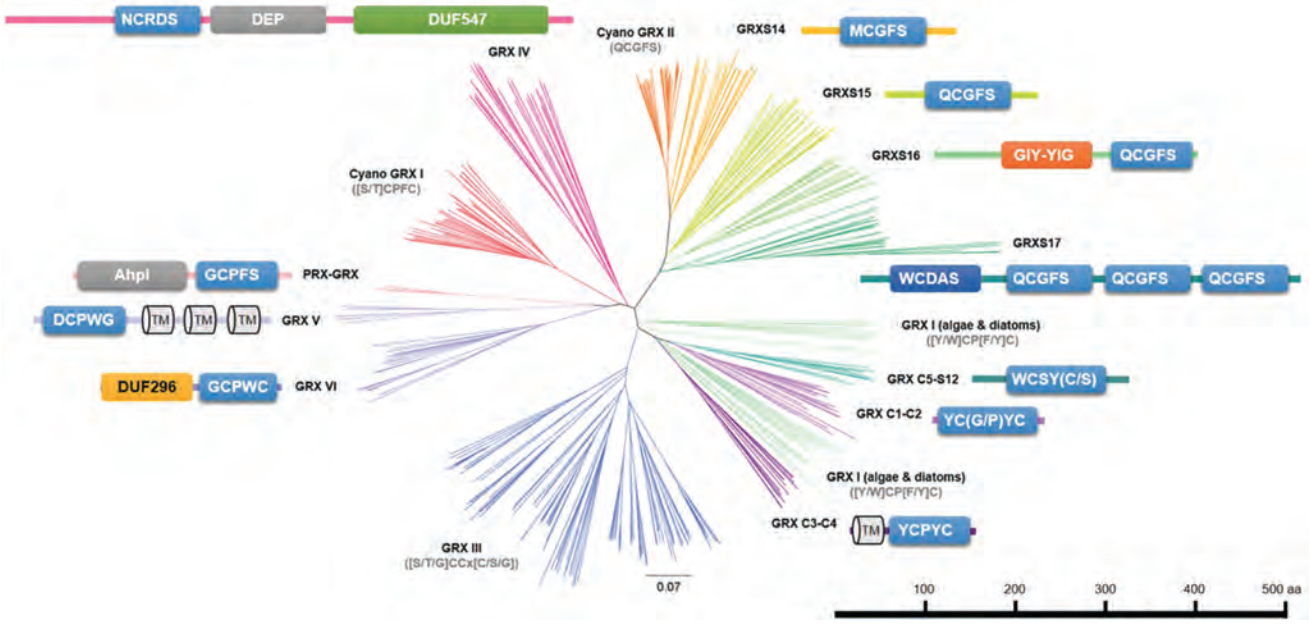

FIG. 13. Phylogenetic analysis of plant GRXs and schematic representation of the architecture of GRX members. The retrieval and alignment of amino acid sequences (415 from 58 organisms) and the building of the phylogenetic tree were achieved exactly as described in the legend of Figure 11. The names of individual sequences are indicated and proteins possessing classical or additional domains as predicted by the pfam or NCBI conserved domain tools are represented. The GRX domain is in *light blue* with the active site signature of a chosen *A. thaliana* representative shown in *white*, except when there was no Arabidopsis representative, which is the case for the PRX-GRX, GRX V, and GRX VI clades specifically found in cyanobacteria. Among additional domains, DEP stands for domain found in Dishweller, Egl10 and Pleckstrin, DUF547 for domain of unknown function 547, GIY-YIG for domain similar to the catalytic domain of I-Tev and UvrC endonucleases, DUF296 for domain of unknown function 296 and AhpI for an alkyl hydroperoxide/PRX domain. Membrane-anchoring domains are represented as *cylinders*, when the predicted score using the TMpred server was >1000. The size of the boxes and strings is proportional to the length in amino acids. Color images are available online.

(Fig. 13). They are uniquely found in terrestrial plants, ranging from 2 isoforms in *P. patens* to 24 isoforms in *Populus trichocarpa* (100, 412). The expansion of class III GRXs in angiosperms occurred mainly through paleopolyploidy duplications shortly after the monocot–eudicot split (201) and then proceeded by species-specific duplication, leading to the existence of multiple tandem duplication.

The class IV GRXs (also referred to as GRX-like) are only present in terrestrial plants and they are rarely represented by more than two isoforms in a given species. These proteins have a particular domain organization with the presence of a long N-terminal extension followed by a GRX domain with a quite divergent active site signature (although green algal ancestors have CPYC/CPHC motifs), and two additional domains with unknown function, named DEP (domain found in Dishweller, Egl10, and Pleckstrin) and DUF547 (domain of unknown function 547) (Fig. 13). There are in fact two clades, the first containing sequences with an NCRD[C/S] signature, the second comprising sequences with a GCE[E/D]C signature.

As mentioned previously, the classes V and VI GRXs are found uniquely in cyanobacteria but not in all of them. They are for instance absent in *Synechocystis* sp. PCC 6803 and thus not included in Table 1. On the contrary, a few species have both of them (100). Members of class V are formed by a GRX domain with a highly conserved CPWG followed by a C-terminal extension predicted to form three to five transmembrane domains (Fig. 13). Members of class VI are formed by an N-terminal DUF296 domain, followed by a C-terminal GRX domain with a CPW[C/S] signature (Fig. 13). From the presence of this DUF296 domain in proteins that contain AT-hook motifs and the conservation of metal-binding histidines, it is predicted that these proteins have DNA-binding properties.

When considering the same set of representative organisms as before, the basal common GRX equipment in photosynthetic organisms as found in *Synechocystis* sp. PCC 6803 is formed by three members, two belonging to class I and one to class II (Table 1). This number increases to seven in *C. reinhardtii* because of duplications occurring for class II GRXs and of the appearance of class IV GRXs (Table 1). Another increase occurred in nonvascular plants (mosses) and in ferns with further duplications occurring for class II GRXs and with the appearance of class III GRXs (Table 1). Finally, class III GRX has strongly expanded in seed plants, from 9 in *Carica papaya* to 24 in *P. trichocarpa* (Fig. 13) (201, 412). To date, in terrestrial plants, the lowest and highest number of reported GRXs are found in *P. patens* (15 isoforms) and in *P. trichocarpa* (38 isoforms), respectively (Table 1) (412).

The subcellular localization of many poplar and *Arabidopsis* GRXs has been determined experimentally. First, it is important to point out that there might be a single GRX in mitochondria, which is the class II GRXS15 (30, 351). This is extremely surprising because it has no or extremely poor oxidoreductase activity (39, 351), whereas there is an intense

Downloaded by LI CO SA/50127/MI from www.liebertpub.com at 07/22/19. For personal use only.

GSH-dependent metabolism in this compartment suggesting that a catalyst of protein deglutathionylation is required. In chloroplasts, there are three GRXs in most photosynthetic organisms, GRXS12 (class I) and GRXS14 and S16 (class II) (30, 104). A variation is observed in brassicaceae including *A. thaliana* due to existence of the close GRXS12 paralog, GRXC5, and in algae, because they have only the two class II GRXs (102, 104, 284). It is again surprising that there is no class I GRX with regular GSH-dependent activity in algal plastids. The fourth class II GRX, GRXS17, is found both in the cytoplasm and in the nucleus as do GRXC1 and C2 and most class III GRXs (30, 228, 263, 366, 431, 441, 549, 550, 553). In fact, there are still some uncertainties about several class III GRXs, for which the targeting has not been experimentally verified or which have N-terminal extensions (104, 439). Interestingly, GRXC3 and C4 have also short N-terminal extensions, which may represent either a signal peptide for secretion or a membrane-anchoring sequence.

In conclusion, the genomic and phylogenetic analyses indicate that the TRX and GRX families constitute a largely diversified group of proteins in plants with numerous plant-specific isoforms or classes, which appeared during evolution, whereas this expansion/diversification did not occur in bacterial, fungal, and animal kingdoms. Although this classification is quite robust, relying on the use of specific motifs for protein identification (for instance, the presence of glutathione-binding residues in the case of the GRX family) (100), one could wonder whether all these proteins adopt a TRX fold and have oxidoreductase activity. Hence, having systematic activity and structural information for isoforms belonging to each class would be mandatory in assessing to which extent the electrostatic surfaces are crucial in determining the specificity of TRXs and GRXs toward their targets as proposed in the case of *E. coli* 3'-phosphoadenosine-5'-phosphosulfate reductase (48). This may provide clues to refine the classification on an activity/structure basis. Besides this is not detailed at all in previous paragraphs, the presence of extra-Cys residues in some specific GRXs or TRXs is known to interfere with their activity and recycling. To cite only two examples, some TRX *h* having an additional Cys at position 4 become dependent on GSH and GRX instead of NTR (264), and the glutathionylation of Cys67 of *A. thaliana* TRX *f*1 inactivates the protein, preventing its regeneration by FTR (338). Finally yet importantly, besides the punctual changes in key amino acids, many proteins have additional domains, the function of which is often not yet determined although it could considerably affect their localizations, protein–protein interactions, or activities. It would be expected that these protein innovations modify for instance the set of partner proteins. In this regard, it is interesting to see the intricate relationship between class III GRXs and TGACG motif-binding (TGA) transcription factors, sustaining the role of these GRXs in plant stress response and development (notably floral development) (201).

V. Structures and Catalytic Mechanisms of Redoxins

A. The TRX fold and the structural determinants of redoxin reactivity

The TRX fold, common to all TRXs and GRXs, is composed of a central core made of a four to five stranded mixed beta-sheet, flanked by three to four alpha-helices (Fig. 14A, B). The residues forming the typical CXXC/S signature containing the catalytic Cys are positioned at the N-terminus of one of the alpha helices. Another important structural feature of the TRX superfamily members is the presence of an invariant cis-Pro residue that is found about 40 amino acids on the C-terminal side of the CXXC/S motif and, in the tridimensional structures, faces the catalytic Cys in the active site. This fold was first identified in the crystal structure of oxidized *E. coli* TRX1 (224). Since then, several structures of TRXs and GRXs from different photosynthetic organisms have been solved (Table 2).

The catalytic site containing the redox active Cys is located in a hydrophobic region quite exposed to the solvent. The thiol group of the first Cys of the generic $C_NX_1X_2C_C$/S signature (where C_N and C_C are the N-terminal and C-terminal Cys, respectively) is accessible and can easily react with disulfides or possibly other forms of oxidized thiols on the target proteins (Fig. 14A, B). On the contrary, the thiol of the second Cys, substituted by serine in some GRX classes (see section IV and Fig. 13), is buried and surrounded by hydrophobic residues. The reactivity of the N-terminal Cys is mainly determined by the pK_a of its thiol group (see section II) ranging from 4.0 to 5.0 in GRX (102, 104, 573) and from 6.3 to 7.1 in TRX [(434), Zaffagnini *et al.*, personal communication], indicating partial or complete deprotonation of the N-terminal Cys at physiological pHs. Despite their acidic Cys, neither TRX nor GRX is particularly prone to oxidation by H_2O_2, confirming that other factors come into play in the thiolate to sulfenic acid conversion [(508, 573), Zaffagnini *et al.*, personal communication]. In contrast, the C-terminal active site Cys, which may be absent or not essential for activity in GRX, shows a pK_a that may even be higher than that of free Cys and, therefore, should be relatively unreactive [(88), Zaffagnini *et al.*, personal communication]. Nevertheless, the C-terminal Cys of TRX is involved in the thiol–disulfide exchange reaction. The mechanism proposed for *E. coli* TRX (89) predicts that a buried and highly conserved aspartic residue (Asp26 in *E. coli* TRX) works as an acceptor for the proton released by the C-terminal thiol when it attacks the N-terminal Cys bonded with the target protein (see section V.B) (65, 329).

The low pK_a of the N-terminal Cys of both TRXs and GRXs is chiefly determined by a hydrogen bond network, whereas the contribution of the helix macrodipole is negligible (150, 435). Crystallographic investigations showed that the N-terminal Cys thiolate is often stabilized by hydrogen bonds with residues belonging to the catalytic sequence $C_NX_1X_2C_C$/S. For example, in barley TRX *h*1 [PDB ID 2VM1; (314)], the sulfur atom of the N-terminal Cys40 is involved in a double hydrogen bond with the sulfhydryl group and the backbone amide group of the C-terminal Cys (Cys43; Fig. 14C). The lower pK_a value of the N-terminal Cys in GRX-like *Arabidopsis* GRXC5 was explained by an additional third H-bond with the backbone amide group of the X_2 residue, which further stabilizes the N-terminal thiolate (Fig. 14D) (104). A similar hydrogen bond network could not be established in most TRX active sites due to the presence of a proline in the X_2 position (150).

B. TRX and GRX: mechanisms of disulfide reduction

Although the large superfamily of TRXs include members that do not appear to be redox active, TRXs and GRXs can be considered anyway typical reducing agents for disulfide

Downloaded by LI CO SA/50127/MI from www.liebertpub.com at 07/22/19. For personal use only.

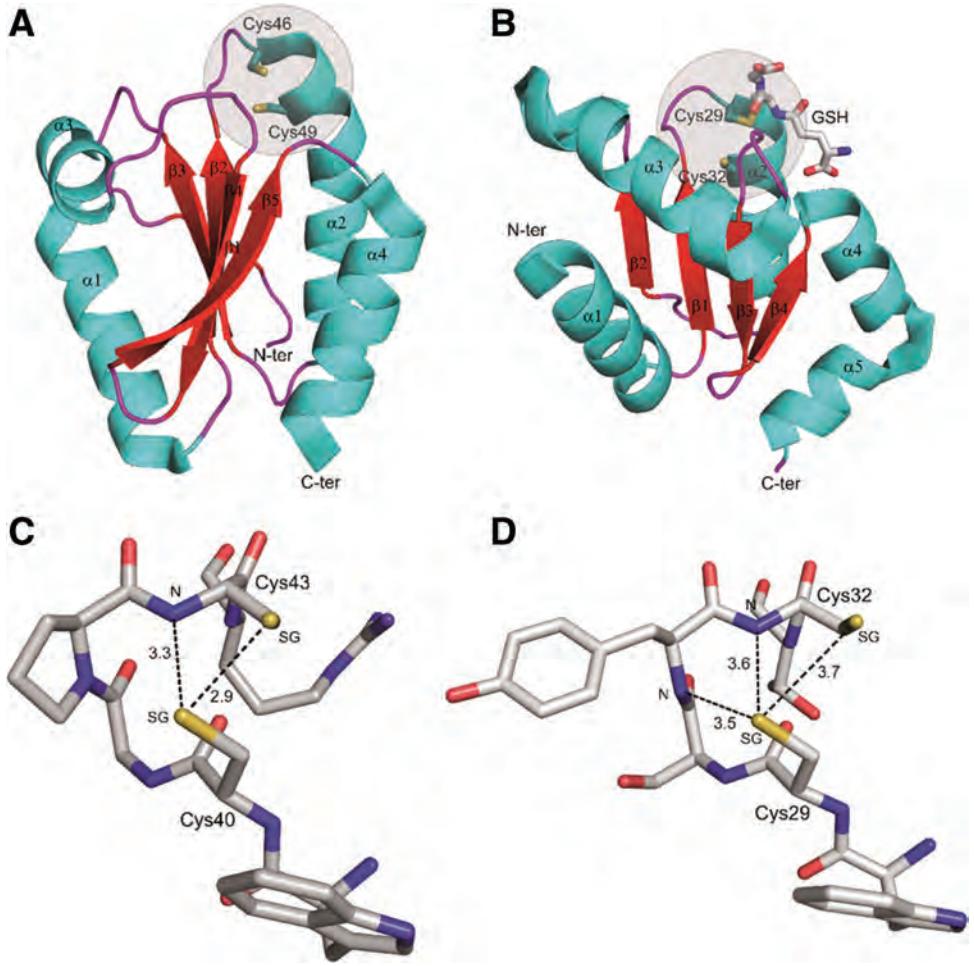

FIG. 14. Structural features of typical TRX (TRX *h*1) and class I GRX (GRXC5). Ribbon representation of the crystal structure of **(A)** reduced TRX *h*1 from *Hordeum vulgare* [PDB ID 2VM1; (314)] and **(B)** GRXC5 from *Arabidopsis thaliana* [PDB ID 3RHB; (104)]. The secondary structure elements are differently colored. The two proteins present a very similar fold, and the active sites formed by two close cysteine residues are located at the N-terminus of helix α2 and quite solvent exposed. Representation of the hydrogen bonds formed by the N-terminal catalytic cysteine in **(C)** reduced TRX *h*1 from *H. vulgare* [PDB ID 2VM1; (314)] and **(D)** GRXC5 from *A. thaliana* [PDB ID 3RHB; (104)]. Color images are available online.

Downloaded by LI CO SA/50127/MI from www.liebertpub.com at 07/22/19. For personal use only.

bonds. The TRX system is older than the GRX system in evolutionary terms (171, 335) and it is more efficient in reducing protein disulfides even under severe oxidative stress, ensuring a reduced environment in the cell. In contrast, GRXs are more versatile being able to reduce protein disulfides compensating if necessary TRXs, but also glutathione-mixed disulfides. Reduced GRXs are regenerated mainly by GSH and in a few cases by TRs (*i.e.*, FTR and NTR), depending on the redox potential and catalytic mechanism of the specific GRX (145, 246, 578). Instead, TRXs are mainly reduced by TRs (FTR and NTR), but a small subgroup of plant TRXs *h* is uniquely reduced by the GSH/GRX system [see section IV.B.1; (173, 264, 330)].

In the catalytic mechanism of TRXs, the exposed N-terminal Cys of the active site $C_NX_1X_2C_C$ signature performs a nucleophilic attack on the disulfide of the target protein forming a mixed disulfide bond with the target protein itself (Fig. 15A). Then, the free C-terminal Cys becomes reactive (deprotonated), thanks to the proton accepting role of a conserved nearby Asp, and attacks the N-terminal sulfur atom involved in the mixed disulfide, generating oxidized TRXs and reduced target proteins (Fig. 15A). The reaction is reversible and its equilibrium is determined by the redox potentials of both TRXs and target proteins (92, 93, 222, 223, 322, 478–480). The midpoint redox potential of TRX *f* and *m* is about −290 mV at pH 7 (223, 339) and several target proteins show midpoint redox potentials that differ from that of these TRXs by $< \pm 30$ mV (92, 93, 222, 223, 322, 478–480), suggesting that fluctuations in TRX redox state may effectively translate in fluctuations of target protein redox states and *vice versa*. An exception to this general view is constituted by lilium/ACHT atypical TRXs that possess redox potential about 50 mV less negative than typical TRX *f* or *m* (85, 110). Indeed these TRXs have been proposed to shuttle electrons from reduced AGPase to 2-Cys PRX in the presence of H_2O_2, possibly constituting a pathway of downregulation of chloroplast starch biosynthesis under low-light intensity. A similar role of TRX in the oxidation of reduced chloroplast targets might be expected for TRX *y* that on one side is less reducing than TRX *f* and *m* (93), and on the other hand is a good reductant for 2-Cys PRX (93, 124).

Although typical of TRXs, the dithiol oxidoreductase mechanism just described is also shared by some GRXs (166, 578). Most GRXs, however, are specialized in protein deglutathionylation. In this reaction, the N-terminal catalytic Cys of GRXs attacks the disulfide of the glutathionylated protein, releases the reduced peptide, and becomes itself glutathionylated (Fig. 15B). Afterward, a second GSH molecule reduces back the glutathionylated thiol of GRX (60, 379) generating GSSG (Fig. 15B), in turn reduced to GSH by NADPH and glutathione reductase (GR), all together forming the GSH/GRX reducing system (100, 574). The C-terminal Cys of

TABLE 2. THREE DIMENSIONAL STRUCTURES OF THIOREDOXINS AND GLUTAREDOXINS FROM PHOTOSYNTHETIC ORGANISMS

Protein (redox state)	*Organism*	*PDB ID (reference)*	*Method*
TRX *h* (ox)	*Chlamydomonas reinhardtii*	1TOF (344)	NMR
TRX *h* (ox)	*C. reinhardtii*	1EP7 (329)	X-ray
TRX *h* D30A (ox)	*C. reinhardtii*	1EP8 (329)	X-ray
TRX *h*1 (red)	*Hordeum vulgare*	2VM1, 2VM2 (314)	X-ray
TRX *h*2 (ox)	*H. vulgare*	2VLT (314)	X-ray
TRX *h*2 (partially red)	*H. vulgare*	2VLU, 2VLV (314)	X-ray
TRX *h*1 (ox)	*Arabidopsis thaliana*	1XFL (410)	NMR
TRX *h*1 (red)	*Populus trichocarpa x Populus deltoides*	1TI3 (98)	NMR
TRX *h*4 (ox)	*P. trichocarpa x P. deltoides*	3D21 (264)	X-ray
TRX *h*4 C61S (red)	*P. trichocarpa x P. deltoides*	3D22 (264)	X-ray
TRX *h* (red)	*Oryza sativa*	1WMJ (/)	NMR
TRX *f* (short form; ox)	*Spinacia oleracea*	1F9M (65)	X-ray
TRX *f* (long form; ox)	*S. oleracea*	1FAA (65)	X-ray
TRX *m* (red)	*S. oleracea*	1FB0 (65)	X-ray
TRX *m* (ox)	*S. oleracea*	1FB6 (65)	X-ray
TRX *m* CH2 (ox)	*C. reinhardtii*	1DBY (277)	NMR
TRX 2 (ox)	*Anabaena* sp. PCC 7120	1THX (444)	X-ray
TRX *o*1 (ox)	*A. thaliana*	6G61 (581)	X-ray
TRX *o*2 (ox)	*A. thaliana*	6G62 (581)	X-ray
TRX-like2.1 (ox/red)	*P. tremula x P. tremuloides*	5NYK, 5NYM (84)	X-ray
GRXC1-Fe_2S_2-GSH (red)	*P. trichocarpa x P. deltoides*	2E7P (441)	X-ray
GRXC1 (red)	*P. trichocarpa x P. deltoides*	1Z7P (142)	NMR
GRXC1 (red)	*P. trichocarpa x P. deltoides*	1Z7R (142)	NMR
GRXC5-GSH (red)	*A. thaliana*	3RHB (104)	X-ray
GRXC5-Fe_2S_2-GSH (red)	*A. thaliana*	3RHC (104)	X-ray
GRXS12-GSH	*P. trichocarpa x P. deltoides*	3FZ9 (102)	X-ray
GRXS12-GSH-BME	*P. trichocarpa x P. deltoides*	3FZA (102)	X-ray
GRXS14 (GRXcp, red)	*A. thaliana*	3IPZ (291)	X-ray
GRXS14 (red)	*P. tremula x P. tremuloides*	2LKU (521)	NMR
GRXS16 (N-terminal endonuclease domain, red)	*A. thaliana*	2LWF (305)	NMR
GRX-GSH	*Fagopyrum tataricum*	5KQA (590)	X-ray
GRX A (red)	*Synechocystis* sp. PCC 6803	3QMX (258)	X-ray

BME, beta-mercaptoethanol; GSH, reduced glutathione.

Downloaded by LI CO SA/50127/MI from www.liebertpub.com at 07/22/19. For personal use only.

GRXs when present is not involved in this mechanism, which is, therefore, called monothiol mechanism. The monothiol mechanism requires a single Cys on GRX (the N-terminal of the active site signature) but two glutathione molecules, one bound to the target protein and the other free (39). This mechanism may be used by class I GRXs bearing one or two Cys in the active site (see section IV.B.2). An example of GRX utilizing a monothiol mechanism for deglutathionylation is poplar GRXS12 found in chloroplasts with a WCSYS active site sequence, unique to plants (102, 573).

Some GRXs such as GRX3 from *Chlamydomonas* (578) use instead a dithiol mechanism for deglutathionylation (Fig. 15C). In this mechanism, the deglutathionylation of the target protein occurs like in the monothiol mechanism. However, the glutathionylated GRX is then deglutathionylated by a second protein Cys that generates an internal disulfide and releases the GSH (Fig. 15C). Depending on the GRX isoform, the second Cys may or may not belong to the active site. The latter is the case of GRX3 from *Chlamydomonas*, a chloroplast class II GRX whose internal disulfide is very efficiently reduced by FTR, thus constituting a potential link between deglutathionylation and photosynthesis (335, 578).

Unlike TRXs, some plant GRXs (GRXC1, GRXC5, GRXS14-S17) have been identified as Fe-S cluster binding proteins ligating [2Fe-2S] clusters (30, 142, 233, 351, 441). Although the Fe-S clusters bound to class I GRXs (GRXC1 and GRXC5) may modulate GRX activity (the holoforms are inactive) under oxidative stress conditions for instance, class II GRXs (GRXS14-S17) are involved in Fe-S cluster biosynthesis and assembly in specific cell compartments (103).

C. Structural basis of TRX–target interaction and specificity

A detailed comparison of the crystal structures of two plastidial TRXs from the same organism (spinach TRX *f* and TRX *m*) showed that despite a quite similar overall structure [rmsd 1.2 Å for 102 superimposed C_a atoms; (65)], they show a different distribution of charges around the active site, with TRX *f* being characterized by a positive region that is less prominent in TRX *m*. In addition, TRX *f* active site is more flexible and the Trp45, the residue preceding the N-terminal Cys, can adopt different conformations. It is plausible that these features contribute to the different specificities shown by these two TRXs toward their targets. Indeed, although many tested targets may be reduced *in vitro* by either TRX *f* or TRX *m*, in some cases a strong specificity for TRX *f* was documented [(339) and references therein].

The crystal structure of TRX–target complexes provide further information on the interaction between plant TRXs and their targets. One study investigated the complex

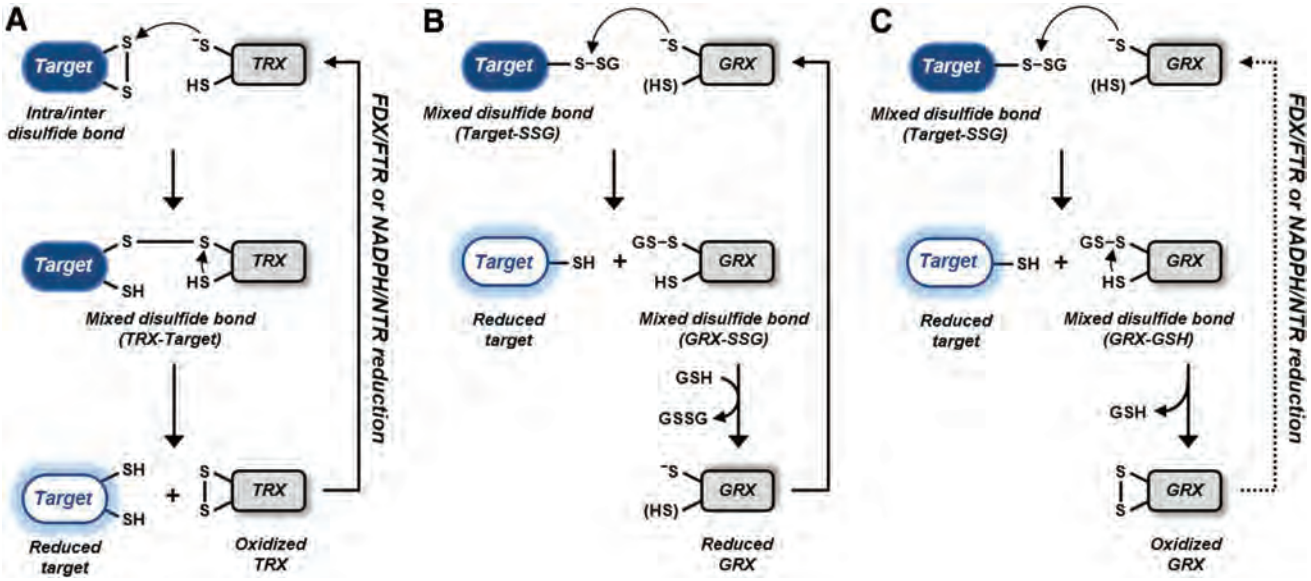

FIG. 15. Schematic representation of TRX and GRX reduction mechanisms. **(A)** TRX-dependent molecular mechanism of protein disulfide reduction. Under physiological conditions, the thiolate form of the N-terminal Cys of the CXXC active site initiates a nucleophilic attack on the disulfide bond in a protein target. Owing to local conformational perturbations, the transient intermolecular disulfide formed is resolved by the C-terminal Cys in TRX, resulting in the formation of an intramolecular disulfide in TRX and the release of reduced target. The reduction of oxidized TRX is then catalyzed by the FDX–FTR or NADPH–NTR systems. **(B)** GRX-dependent monothiol deglutathionylation mechanism. In GRX, the nucleophilic active site Cys forms a mixed disulfide with GSH upon reaction with an S-glutathionylated target. Typically, a second GSH resolves the enzyme-glutathione mixed disulfide bond to generate the reduced GRX. **(C)** GRX-dependent dithiol deglutathionylation mechanism. Some GRXs, such as Chlamydomonas GRX3, can also follow a mechanism in which the mixed disulfide in GRX is resolved by a second nonactive site Cys yielding an oxidized GRX. In chloroplasts, GRX3 is believed to be reduced *via* the FDX–FTR system. Color images are available online.

Downloaded by LI CO SA/50127/MI from www.liebertpub.com at 07/22/19. For personal use only.

between barley TRX *h*2 and barley alpha-amylase/subtilisin inhibitor (BASI) (313). The interface area between the two proteins is quite small (762 $Å^2$). TRX *h*2 recognizes the target by interacting with the exposed Cys (Cys148) with which it forms the mixed disulfide bond, and two preceding residues (Asp146 and Trp147). This short peptide of BASI that is solvent exposed and free of intermolecular contacts forms van der Walls interactions and three backbone–backbone hydrogen bonds with two TRX residues (Met88 and Ala106) both belonging to loop regions. Therefore, the TRX *h*2 active site portion (Trp45-Cys46-Gly47-Pro48) plus two additional segments (Ala87-Met88-Pro89 and Val104-Gly105-Ala106) form the so called substrate recognition loop motif, which is also conserved in several other TRXs, but also in some GSTs, few PDIs, and different proteins such as cytochrome c (313). A similar motif is also observed in the cocrystal structure of the *E. coli* 3′-phosphoadenosine-5′-phosphosulfate reductase covalently bound to *E. coli* TRX1 (78).

VI. Genetically Encoded Sensors for Detection of Redox Couples *In Vivo*

A. Detection of RMS and antioxidants in plant cells

Biochemical techniques have been largely applied to study RMS and the redox status of the most important antioxidant pools in plant cells or tissues (375, 376). In most cases, these are still the only methods available allowing analysis of the general redox state of antioxidant molecules such as ascorbate and glutathione in whole tissues or subcellular compartments (157). Data on the subcellular concentrations of ascorbate and glutathione in plant tissues were also obtained by immunogold electron microscopy, a technique that cannot distinguish between reduced and oxidized forms (582, 583). TRX isoforms, for which the subcellular distribution is usually known, were quantified by proteomic methods and their redox state under light and dark conditions examined by redox Western blots (564). Unfortunately, in most cases biochemical assays require tissue homogenization that, on one side, may dramatically reduce the sensitivity of the analysis and, on the other, can introduce artifacts due to the sample manipulation. Since both RMS and antioxidants are unevenly distributed in different subcellular compartments, the meaning of biochemical determinations of concentrations and redox states in raw extracts is intrinsically limited, independently from the precision of the measurements.

To overcome these problems, in the past 15 years, biologists have started to use new *in vivo* technologies that rely on the use of genetically encoded sensors that enable a real-time monitoring of the dynamics of chemical species and redox couples (333, 458). Although this approach has greatly increased the precision and the flexibility of the measurements that can be performed *in vivo*, the availability of genetically encoded sensors is still restricted to few chemical species and redox couples. Technical developments are urgently needed for expanding the palette of sensors to a larger number of redox compounds.

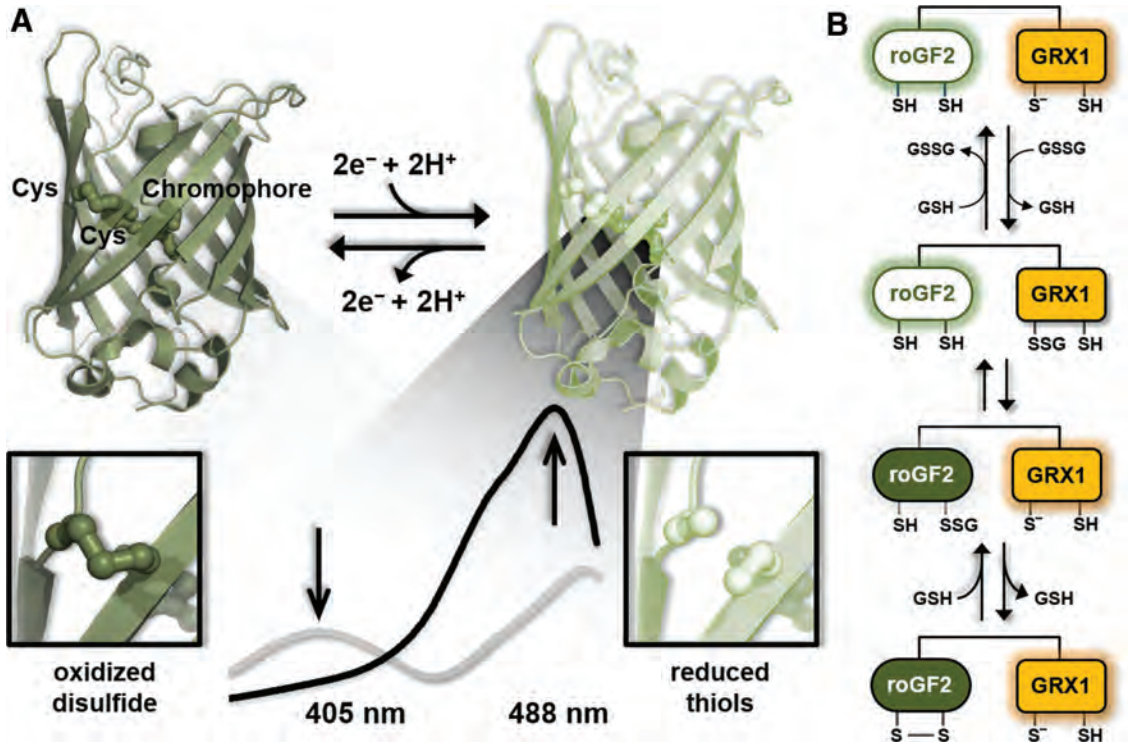

FIG. 16. Spectroscopic and biochemical features of roGFP-based redox sensors. (A) Ribbon representation of roGFP with chromophore and Cys residues involved in the disulfide bond formation represented as *balls* and *sticks*. The change in the oxidation state of the Cys residues affects the spectral properties of the fluorescent protein by inducing a change in its absorption profile. The *gray* and *black lines* correspond to the absorption spectrum of the roGFP2 in the oxidized and reduced form, respectively. Adapted from (348) **(B)** Redox equilibration mechanism of GRX1–roGFP2 sensor. As depicted, each individual reaction step of dithiol–disulfide exchange cascade is fully reversible.Color images are available online.

B. Genetically encoded sensors for glutathione

In the redox field, the most commonly used genetically encoded sensors are RxYFP, roGFP1, and roGFP2 that are based on modified yellow fluorescent protein (YFP) or GFP (128, 333, 386, 458). In these modified versions of the GFP- or YFP-based sensors, two Cys residues have been inserted in adjacent β-strands on the surface of the protein β-barrel making the protein able to make a disulfide in a cellular context (333, 458). The Cys residues, being positioned in proximity to the chromophore, can form a disulfide bond that causes a structural change influencing the light absorption and fluorescence of the sensor (Fig. 16A).

To reveal the formation or reduction of the disulfide bond, it is required to perform a ratiometric imaging by dual and sequential excitation of the sensor, usually with violet ($\sim$405 nm) and blue ($\sim$488 nm) light (Fig. 16A). The emitted fluorescence is then acquired in a 505–540 nm window. Specifically, the disulfide-induced structural change of the fluorescent sensor has the effect of changing the quantum yield (QY) of its two main absorption peaks with an opposite trend: the QY at 405 nm increases, whereas the QY at 488 nm decreases, hence leading to a ratiometric response. The ratio of the light emitted after excitation at 405 and 488 nm (briefly, the 488/405 nm ratio) provides a direct readout of disulfide bond formation in the sensor population. The higher the 488/405 nm ratio is, the higher the oxidation of the sensor (*i.e.*, the percentage of sensor molecules bearing the disulfide). Most importantly, such ratio can be monitored in real time and *in vivo* with different grades of resolution depending on the system used for the acquisition (*e.g.*, wide-field and confocal microscopy or a fluorescent-based plate reader).

The field of application of the system depends on whether the sensor *in vivo* equilibrates with one or more redox couples such that it can be used to measure the redox state of these couples. The sensors of the roGFP family show midpoint redox potentials (E^0_{roGFP}) between −260 and −290 mV and are proposed to provide an accurate determination of the redox potential of glutathione (E_{GSH}) *in vivo* (331, 387, 459). This implies that glutathione is assumed to equilibrate with the sensor *in vivo*. Since the midpoint redox potential of glutathione is less negative (E^0_{GSH} −240 mV), the roGFP sensors are intrinsically more adapted to measure highly reduced than oxidized glutathione redox states. Moreover, since GSH dimerizes upon oxidation (GSSG $+2\ e^- + 2H^+ \rightarrow$ 2 GSH), the E_{GSH} depends on the $[GSH]^2/[GSSG]$ ratio. In other words, it depends on both the GSH/GSSG ratio and the total concentration of GSH+GSSG. Therefore, glutathione redox potentials estimated by the roGFP cannot be translated into GSH/GSSG ratios unless the total concentration of GSH+GSSG is known (157).

Key advantages of the ratiometric nature of these sensors are manifold. First, the sensor readout is largely independent of their concentration in the cell. Second, the ratiometric feature of the sensors allows for the correction of focus changes or moving artifacts when samples are imaged by

Downloaded by LI CO SA/50127/MI from www.liebertpub.com at 07/22/19. For personal use only.

Downloaded by LI CO SA/50127/MI from www.liebertpub.com at 07/22/19. For personal use only.

microscopy. Third, by using different promoters, they can be specifically expressed in different tissues and engineered for their targeting to different subcellular compartments or to modify their properties. Considering all these features, these redox genetically encoded sensors have been shown to be suitable for deriving information on redox conditions prevailing in the cell in different plant species, different cell types, and different subcellular compartments.

Concerns about the specificity of the roGFP for glutathione have long been debated. Peroxidases such as yeast Orp1 and mammalian GPX4 appear to oxidize roGFP2 directly in response to H_2O_2 in HeLa cells, suggesting that the roGFP redox state may be influenced by other factors than glutathione (203). In fact, roGFP is not oxidized by H_2O_2 *in vitro* but is rapidly oxidized by H_2O_2 *in vivo*. Whether this effect is mediated by glutathione or peroxidases is difficult to tell. Anyway, even if different compounds obviously influence the roGFP redox state *in vivo*, it is still possible that roGFP and glutathione reciprocally equilibrate under any condition. As briefly discussed hereunder, experimental evidence acquired so far supports this hypothesis.

The first work reporting the expression of a redox sensor in plants was published in 2006 (244) in a study where the roGFP1 was expressed in the cytoplasm and mitochondria of *A. thaliana* and performed oxidation and reduction treatments with H_2O_2 and DTT (244). This pioneering work showed the possibility to monitor dynamically subcellular redox changes by measuring in real time the sensor fluorescent emission ratio. By carrying out a calibration curve, it was possible to convert the sensor ratios into redox potentials, showing that in mitochondria the E_{roGFP} was more reduced than in the cytoplasm (−362 and −318 mV, respectively). Soon after the development of the rxYFP and roGFP sensors and their first applications in animals and plants, it clearly emerged that both redox sensors equilibrated predominantly with glutathione (331, 387, 459) and that equilibration *in vivo* was accelerated by GRXs that mediated the thiol–disulfide exchange between glutathione and the redox sensor (458). A confirmation of this came in 2007 when Meyer *et al.* expressed the roGFP2 sensor in *Arabidopsis* (GFP2 is an enhanced variant of GFP1, see this section). Also in this case, the roGFP2 reversibly responded to redox changes induced by incubation with H_2O_2 or DTT and, more important, the sensor was severely oxidized in mutants with reduced levels of glutathione and in wild-type plants, in which the glutathione content was depleted by treatments with an inhibitor of glutathione biosynthesis (L-buthionine-sulfoximine, BSO) (332). Soon after, another work confirmed these results in *Arabidopsis* leaves (459). The fact that different laboratories with different imaging techniques, wide-field *versus* confocal microscopy, obtained similar results pointed out the reliability of the roGFP measurements. In addition, Schwarzländer *et al.* showed that, *in vivo*, roGFP1 had a lower dynamic range and was less photostable than roGFP2. Hence, the use of roGFP2 instead of roGFP1 was recommended (458).

As the equilibrium between roGFPs and glutathione was suspected to be mediated by GRXs *in vivo*, it was reasoned that the availability of endogenous GRXs might limit the fast equilibration between glutathione and the sensor. To overcome this problem, human GRX1 was fused to the roGFP2 (202). This new GRX1–roGFP2 was expressed and tested in plants such as *A. thaliana* and tobacco and in the phytopathogenic fungus *Botrytis cinerea* (132, 216, 328). In *Botrytis,* a side by side comparison of GRX1–roGFP2 and roGFP2 revealed that the oxidation of GRX1–roGFP2 was slightly faster than roGFP2, thereby sustaining the hypothesis that GRX could facilitate the equilibrium between glutathione and the sensor (216). The functional interaction between glutathione and GRX1–roGFP2 is proposed to involve first the glutathionylation of GRX1 by GSSG, then the internal trans-glutathionylation of roGFP2 by GRX1, followed by the formation of the disulfide in the roGFP2 (Fig. 16B). All steps are reversible (Fig. 16B). Note that roGFPs do not contain acidic/reactive Cys; therefore, its glutathionylation can proceed *via* GRX1-dependent trans-glutathionylation with no requirement of H_2O_2 and transient sulfenic acid formation (see section II.C.6 and Fig. 8). Neither GRX1 nor roGFP2 is expected to react with H_2O_2 directly.

Altogether, the results obtained with different redox sensors based on roGFP1/2 expressed in different subcellular compartments of different organisms under physiological conditions show that the sensors are always highly reduced in mitochondria, nuclei, peroxisomes, chloroplasts, and cytoplasm and highly oxidized in the ER lumen (458).

Interestingly, the picture changes in stress conditions. For example, drought stress causes oxidation of roGFP1 in the cytoplasm of *Arabidopsis* (E_{GSH} shifted from −311 to −302 mV) with reversion to control values after rewatering (248). Strong oxidation of cytoplasmic roGFP2 was also observed in the root tip of *Arabidopsis* seedlings treated with cadmium (515) and in wounded *Arabidopsis* leaves (40, 332). In the latter case, an oxidation wave propagating from the wound area preceded a reduction wave in the opposite direction, suggesting a systemic signaling response as previously hypothesized for ROS waves (346). Technically, the *in vivo* monitoring of the GSH/GSSG status in real time offered an unprecedented spatial and temporal resolution that may be difficult, if not impossible, to reach with other techniques.

The oxidation of cytoplasmic roGFP2 was also reported in *Arabidopsis* and tobacco leaves infected with the avirulent pathogen *Pseudomonas syringae* DC3000 (328). The mitochondrial version of roGFP1 and roGFP2 sensors was oxidized in response to heat stress, cadmium, and darkness (437, 458, 460). Dark-induced roGFP2 oxidation occurred also in plastids, peroxisomes, and cytoplasm, but in all cases with a different and slower timing than in mitochondria (437), suggesting that mitochondria may represent the origin of the oxidative stress in the dark occurring during the senescence program. In chloroplasts, treatments with electron transport inhibitors (3-(3,4-dichlorophenyl)-1,1-dimethylurea and 2,5-dibromo-6-isopropyl-3-methyl-1,4-benzoquinone) led to stromal roGFP2 oxidation and, in the same organelle, increased formation of stromules (53). The effect is interesting since stromules were shown to play a role in oxidative signaling (66).

As expected for a sensor sensing the glutathione redox potential, roGFP2 was also found more oxidized in *Arabidopsis* mutants [*rml1,* (8); *cad2*, (332)], in which the total glutathione content is strongly diminished (62, 514), and in mutants of glutathione reductase (*gr1, gr2*) in which the GSH/GSSG is more oxidized (324, 569).

C. Other redox sensors

The high sensitivity of thiol peroxidases, including PRXs, for H_2O_2 was exploited to develop a redox sensor with

different specificity than roGFP variants. PRXs bear an extremely reactive catalytic Cys that forms a sulfenic acid upon reaction with H_2O_2. The sulfenic acid is then resolved by a second Cys forming a disulfide. Although in the common catalytic cycle of PRXs, the disulfide is reduced by TRX or GRX, some PRXs harbor an intrinsic and powerful capacity to act as H_2O_2-dependent protein thiol oxidases when they are recruited into proximity of oxidizable target proteins (203). Hence, the idea of fusing the yeast GPLX protein Orp1 to the roGFP2 to get an H_2O_2 sensor came (203). However, this probe cannot be considered as a strict H_2O_2 sensor as the roGFP2–Orp1 is on one side oxidized by H_2O_2, but on the other is likely to be reduced *in vivo* by TRXs that have been shown to directly reduce Orp1 (458). Different from the GRX1–roGFP2 probe whose oxidation by GSSG and reduction by GSH are reversible, the oxidation of the catalytic Cys of Orp1 by H_2O_2 is not reversed by water [(508); sulfenic acids are not easily reduced by water], such that roGFP2–Orp1 cannot equilibrate with the H_2O_2/H_2O redox couple. As a matter of fact, the redox state of roGFP–Orp1 is not only influenced by the level of the oxidant (H_2O_2), but also by the reductants, GRXs and TRXs. This makes the sensor unsuitable to determine absolute H_2O_2 levels (458). Nevertheless, the roGFP2–Orp1 expressed in *Drosophila* showed a different redox state from GRX1–roGFP2 during development and aging (5), suggesting that both sensors provide different information. The roGFP2–Orp1 sensor has been recently used in *Arabidopsis,* revealing that in guard cells treatment with H_2S determines its oxidation *via* activation of NADPH oxidase (H_2O_2 production) (461).

Other relevant redox couples important for redox homeostasis in plants are represented by nicotinamide adenine dinucleotides. *In vivo* monitoring of NADH/NAD^+ ratios was attempted by combining a bacterial NADH-binding protein and a fluorescent protein variant, creating a genetically encoded fluorescent biosensor of the cytoplasmic NADH/NAD^+ redox state, named Peredox (231). The functionality of Peredox was demonstrated in mammalian cells showing that it efficiently reported the cytoplasmic NADH/NAD^+ ratio and that it was sensitive to exogenous administration of lactate and pyruvate (231). Such sensor was also employed in the fungus *Ustilago maydis* to monitor cytoplasmic NAD redox dynamics (213). More recently, a new ratiometric pH-resistant genetically encoded fluorescent indicator for NADPH (iNap) was also generated (493). The iNap sensors have been used to monitor NADPH fluctuations during the activation of macrophage cells or wound response *in vivo* (493). Up to now, there are no reports showing the functionality of such NAD(P)(H) sensors in plant cells.

VII. Redox Plant Physiology *In Vivo*

As outlined previously, plants organize a multiplicity of different low-molecular weight redox couples and redox proteins to regulate cellular redox homeostasis. Whereas research in the past mainly focused on the characterization of these components during *in vitro* studies, recent progress has been made to resolve the organization and biological significance of this complex redox network *in planta.* In the following section, we review the emerging roles of this regulatory network in integrating photosynthesis, growth, development, and stress responses of plants to cope with fluctuating environmental conditions.

A. Redox regulation of light acclimation: the FTR–TRX system and light-responsive control of photosynthesis within the chloroplast

Sunlight represents the source of energy for photosynthesis and plant growth. However, photosynthetic cells have to manage strong fluctuations in light intensities that can occur very rapidly in nature. This requires sensitive and rapid light acclimation mechanisms to maintain photosynthetic performance and chloroplast functions in a dynamic manner and to avoid the generation of potentially harmful ROS.

One pathway to transfer light signals to chloroplast target enzymes is provided by the FDX–TRX system (54). It involves sequential transfer of reducing power from photosynthetic light reactions *via* FDX and FTR to five different TRX classes (*f*, *m*, *x*, *y*, and *z*), which activate specific sets of stromal and thylakoid proteins by reducing their regulatory disulfides (Fig. 17) (564).

Comparative studies using sets of recombinant purified TRX isoforms and target proteins revealed functional specificities of the different classes of TRXs for their targets *in vitro* (92, 322, 500, 562). TRXs belonging to *f* and *m* classes revealed metabolic functions in activating enzymes of the CB cycle, starch synthesis, redox export *via* the malate valve, and ATP synthesis, whereas isoforms belonging to the *x* and *y* classes revealed antioxidative functions in providing reducing power to PRXs. For a comprehensive overview on the TRX target proteins and their regulatory specificities for different TRX isoforms identified during *in vitro* studies, see (171).

Although until recently most of our knowledge on the functional diversity of chloroplast TRXs relied on *in vitro* studies, a boost of genetic studies in the past years specifically in *Arabidopsis* led to a rapid increase in our knowledge on their roles *in vivo*. As outlined in section IV, the plant genome contains a complex gene family of TRXs, with up to 21 different TRX classes, including 7 classes containing typical TRXs because of their conserved active site signature and single domain structure. Typical TRXs from five classes reside in *Arabidopsis* chloroplasts, with different isoforms (TRXs *f*1-2, *m*1-4, *x*, *y*1-2, and *z*). The chloroplasts contain also several atypical TRX isoforms that are often little studied with respect to typical isoforms. A quantification of the protein levels of typical TRX isoforms showed that TRXs *f* and *m* are the major isoforms, accumulating to 22% and 69% of the total level of typical TRXs in the chloroplast stroma, respectively (383). For the sake of simplicity, when not otherwise specified, the term TRX will be used for typical TRXs in the following text.

Arabidopsis mutants deficient in TRX *f*1 (lacking 70%–90% of total TRX *f* proteins) or with combined deficiencies of TRXs *f*1 and *f*2 (*trxf1f2* mutants) revealed that *f* class TRXs are important for the rapid activation of carbon metabolism and photosynthesis in response to light. During rapid dark–light transitions, TRX *f* deficiency led to delayed and incomplete reduction and activation of the CB cycle enzyme FBPase and RubisCO activase, retarded light activation of CB cycle activity, and transient inhibition of PET, whereas thermal dissipation of the absorbed light energy by

Downloaded by LI CO SA/50127/MI from www.liebertpub.com at 07/22/19. For personal use only.

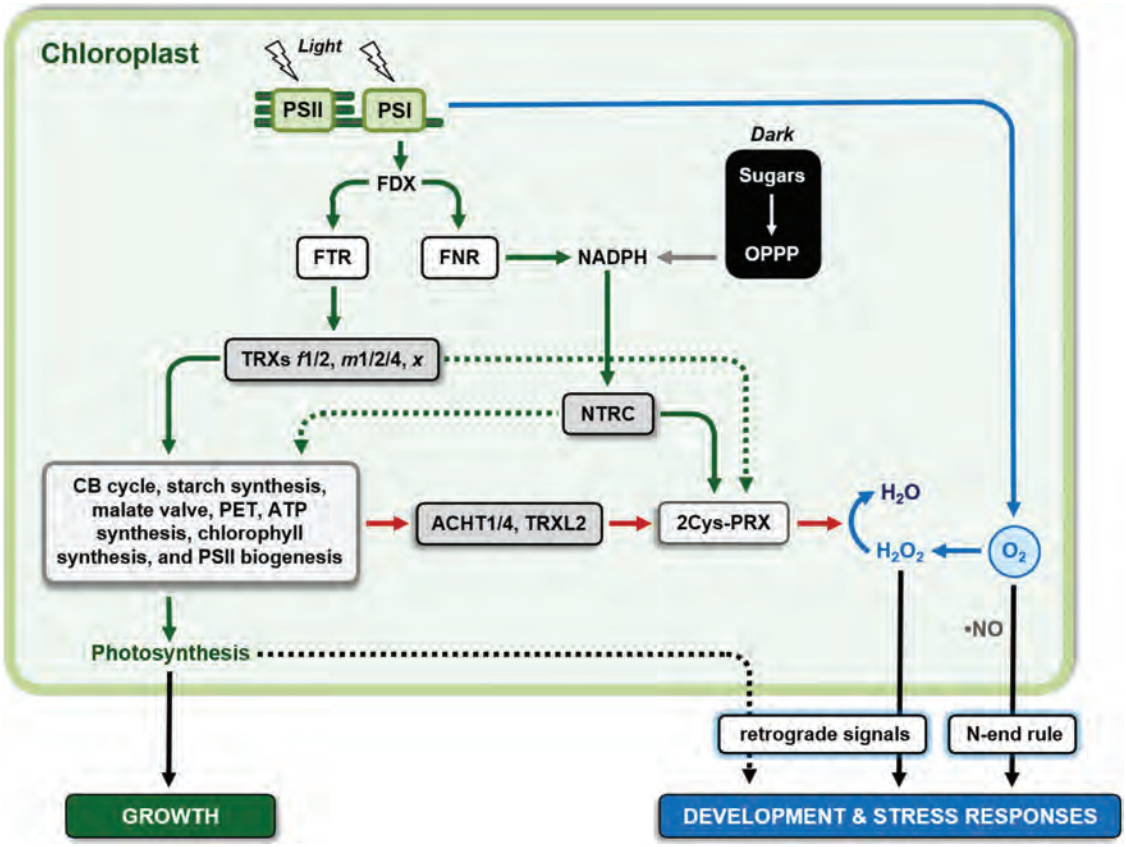

FIG. 17. Proposed model for the *in vivo* role of the chloroplast redox network in light-dependent regulation of photosynthesis, growth, vegetative development, and stress responses. Two different TRX systems coordinately participate to ensure light-responsive control of chloroplast functions by reducing regulatory dithiols in various target enzymes (171). The FDX–TRX system is reduced by electrons provided by PSI in the light, whereas NTRC consists of an NTR and TRX domain providing a separate reduction system that depends on NADPH. Joint operation of these two different reduction systems has been found to be crucial for the regulation of photosynthetic performance, biosynthetic activities, and growth in acclimation to varying light conditions (69, 108, 371, 382, 383, 498, 501, 563). The photosynthetic light reactions also produce O_2 and ROS/NO providing a feedback loop to oxidize the regulatory thiols of TRX target proteins *via* 2-Cys PRX and the atypical TRXs ACHT1/4 (111, 133) and TRXL2 (561), whereas they also serve as retrograde signals to the nucleus regulating leaf development (14) and stress responses (119, 123, 134). NTRC is the major system to provide electrons for reduction of 2-Cys PRXs (419, 563), thereby diminishing the oxidation loop (371, 382) and maintaining the reducing capacity of the pool of FDX–TRXs (408), allowing increased reduction of targets of the FDX–TRX system to promote photosynthesis and growth (408), while it modulates ROS (H_2O_2)-dependent retrograde signals to promote early plant development (382), abiotic stress (257), and immune responses (234). ROS levels and related immune and developmental responses were also found to be affected by chloroplast GPX-like (75); however, the TRXs involved in their reduction have not been identified yet. In addition to ROS, there are also more direct O_2 and NO sensing and signaling pathways *via* cysteine oxidases that lead to proteasomal degradation of transcription factors *via* the N-end rule pathway affecting leaf development and stress responses at the transcriptional level (180, 394, 451). The individual specificities of TRXs *f*1, *f*2, *m*1, *m*2, *m*4, and *x* for the different photosynthetic target processes, as well as the role of TRXs *m*3, *y*1, *y*2, and *z*, are not shown in this figure for clarity (see section VII for further information). Reduction signals are indicated with *green lines* whereas oxidation signals are indicated with *red lines*. *Dotted lines* indicate pathways of minor importance. FNR, FDX:NADPH reductase; NO, nitric oxide; NTRC, NADPH–TRX reductase C; OPPP, oxidative pentose phosphate pathway; PET, photosynthetic electron transport chain; TRXL2, TRX-like2. Color images are available online.

nonphotochemical quenching (NPQ) was transiently increased (363, 383, 498, 501, 562). This shows a role of TRX *f* in short-term light adjustment of photosynthetic carbon fixation to optimize photosynthetic efficiency. Deficiency of TRX *f* also led to an incomplete photoreduction of the small subunit of the key starch synthetic enzyme AGPase resulting in decreased starch accumulation during the day, providing evidence for a role of TRX *f* in regulating diurnal starch turnover in response to dark–light alterations (363, 498, 500). Interestingly, despite the complete lack of *f* class TRXs, FBPase and RubisCO activase became partially reduced during illumination (363, 382, 562), indicating functional compensation by other classes of TRXs or thiol-reduction systems (see sections VII.A, VII.B, and VII.C). In line with this, silencing of TRX *f* did not substantially affect overall rates of photosynthetic carbon fixation and plant growth

Downloaded by LI CO SA/50127/MI from www.liebertpub.com at 07/22/19. For personal use only.

Downloaded by LI CO SA/50127/MI from www.liebertpub.com at 07/22/19. For personal use only.

under long-day conditions, whereas there were only slight growth retardations under short-days or very low light intensities (363, 498).

TRXs of the *m*-class have more diverse *in vivo* functions than TRX *f*. Earlier studies documented a role of the very low abundant TRX *m*3 in symplastic permeability and meristem development (45), see section VII.F). On the other hand, more recent reports revealed photosynthetic functions for the relatively high abundant TRXs *m*1, *m*2 and *m*4, each representing ~23% of the total stromal TRX (99, 383, 501, 523). For TRX *m*4 a role in the regulation of cyclic PET was revealed (99), whereas TRXs *m*1 and *m*2 were found to participate in the rapid light activation of NADP-MDH (501) involved in the export of excess reducing equivalents from the chloroplast *via* the malate valve to prevent photoinhibition (447). This indicates that TRXs *m*1, *m*2 and *m*4 are important to balance the chloroplast ATP/NADPH ratio for optimized photosynthesis. *Arabidopsis* double mutants with combined deficiencies of TRXs *m*1 and *m*2 showed wild-type growth and photosynthesis under constant light conditions, but photosynthetic parameters were strongly modified in fluctuating light environments with rapidly alternating low and high light intensities (501). Combined silencing of TRXs *m*1 and *m*2 led to lower photosynthetic efficiency in high light, but surprisingly had the opposite effect in the low light periods. This indicates that TRXs *m*1 and *m*2 are involved in dynamic acclimation of photosynthesis, being essential for full activation of photosynthesis in the high-light peaks by rapid induction of the malate valve to prevent photoinhibition, whereas there is a trade-off in photosynthetic efficiency during the low-light phases of fluctuating light (501). The reason for the higher photosynthetic efficiency of the TRX*m1 m2* mutants in low light is unclear and requires further investigation.

Interestingly, multiple silencing of TRX *m*1, TRX *m*2 and TRX *m*4 in triple *Arabidopsis* mutants led to more severe phenotypes, depending on the extent of the decrease in total TRX *m* protein (383, 523). A decrease in TRX *m* protein to ~30% of the level found in wild-type plants led to incomplete photo-reduction of FBPase and SBPase from the CB cycle and NADP-MDH from the malate valve in response to light, resulting in decreased CO_2 assimilation rates, inhibition of PET and substantial retardations in plant growth under constant light conditions (383). When compared with *trxf1f2* mutants (see earlier in this section), this reveals a high level of redundancy of *f*- and *m*-class TRXs in the light activation of the CB cycle and photosynthesis being operational *in vivo*, which is unexpected given the predominant role of *f*-class TRXs in regulating enzymes of the CB cycle as proposed by *in vitro* studies (171). When the total amount of TRX *m* proteins was decreased to less than 15% of the level found in wild-type plants, mutant plants displayed very severe growth defects, pale green leaves, strongly decreased *PSI*I activity and impaired *PSI*I assembly (383, 523). In line with this, triple silencing of TRXs *m*1, *m*2 and *m*4 in transgenic *Arabidopsis* led to a decrease in chlorophyll accumulation and in the redox status and activity of Mg-protoporphyrin IX methyltransferase (CHLM), which catalyzes the second step in the chlorophyll synthesizing Mg branch of the tetrapyrrol pathway in the chloroplast (108). Interestingly, studies in pea revealed that simultaneous silencing of TRX *f* and *m* genes is required to decrease the *in vivo* redox status of the Mg chelatase CHLI subunit (CHLI), catalyzing the first step of the Mg branch, as well as chlorophyll content and photosynthetic capacity (309). While interpretation of *in vivo* results is complicated by the fact that genetic removal of part of the TRX pool is likely to affect the redox state of the remnants, overall, these studies suggest redundant roles of *f*- and *m*-class TRXs in, both, rapid light activation of photosynthetic metabolism and more long-term light regulation of the biosynthesis of photosynthetic machineries.

Arabidopsis mutants deficient in the less abundant TRXs *x* or *y* showed wild-type phenotypes, despite their proposed roles in reduction of 2-Cys PRX and PRX Q for peroxide detoxification based on *in vitro* studies (280, 419). This indicates functional compensation by other chloroplast TRX systems *in vivo* (see sections VII.B and VII.C). In contrast to this, deficiency of the low abundant TRX *z* led to an albino phenotype with impaired photoautotrophic growth and disturbed chloroplast development, similar to mutants of chloroplast gene expression (18). In confirmation to this, TRX *z* was found to act as an essential structural component of the plastid-encoded RNA polymerase complex and proposed to be important for the light-dependent expression of photosynthetic genes in the chloroplast. However, the role of TRX *z* in this context seems to be independent of its redox activity (535) and the *in vivo* pathways leading to its reduction are currently unclear (563) because the Arabidopsis isoform does not seem to be reduced by FTR *in vitro* (51) unlike poplar counterpart (86). Further studies will be necessary to elucidate the role of TRX *z* in the chloroplast dithiol/disulfide network.

B. Redox regulation of light acclimation: chloroplast NTRC, 2-Cys PRXs, and photosynthetic performance under low light

In addition to the light-dependent FDX–TRX system described above, the more recently discovered NTRC forms a separate thiol reduction cascade in the chloroplast stroma, combining both NTR and TRX activities on a single polypeptide (Fig. 17) (468). Unlike FTR, NTRC receives its reducing potential from NADPH and provides electrons to target proteins *via* its own TRX domain (47). Biochemical and genetic studies established a major role of NTRC in reducing 2-Cys PRXs involved in the scavenging of H_2O_2 within the chloroplast (409, 563). Comparative studies using *Arabidopsis* mutants deficient in NTRC and TRX *x* identified NTRC as the primary electron donor for 2-Cys PRXs *in vivo*, providing a redox buffer to keep this enzyme in a reduced state for antioxidant functions in the light as well as in the dark (419). Although these studies suggested that NTRC operated as a separate thiol reduction system independently of light, recent work provided *in vivo* evidence for additional functions of NTRC in the light-dependent regulation of photosynthetic metabolism and thylakoid energy transduction similar to the FDX–TRX system. In *Arabidopsis* mutants, deficiency of NTRC led to incomplete photo reduction of regulatory disulfides in enzymes involved in chlorophyll biosynthesis [CHLI, CHLM, and glutamyl-transfer RNA reductase1, GluTR1; (407, 429)], starch biosynthesis [AGPase; (498)], CB cycle [FBPase, SBPase, and PRK (371, 382, 498, 563)], ATP synthesis [γ-subunit of CF1-ATP synthase (69, 371)], and NADPH export [NADP-MDH; (501)] in response to dark–light transitions, resulting in impaired chlorophyll accumulation (429, 468), starch turnover (290, 498), CO_2 assimilation

(498), photosynthetic light energy utilization (69, 364, 371, 498, 501), and plant growth (290, 364, 498). For most of these parameters, silencing and overexpression of NTRC led to opposing effects, indicating that NTRC is limiting for CO_2 fixation, photosynthetic efficiency, and growth in wild-type *Arabidopsis* plants (371) and may be a promising target for biotechnological strategies to improve crops (370). The role of NTRC to optimize photosynthetic efficiency is specifically relevant under constant (69, 364) and fluctuating low light intensities (69, 501). When light availability is limiting, NADPH-dependent NTRC allows efficient redox activation of proton-coupled ATP synthase, leading to lower acidification of the thylakoid lumen and lower energy dissipation by NPQ, resulting in a more efficient utilization of available light energy for photosynthesis and growth (69, 364). In confirmation to this notion, blocking of NPQ in the *ntrc* mutant background led to partial recovery of photosynthetic performance and growth, indicating that NTRC promotes photosynthesis by regulating NPQ (364). Under rapidly alternating low and high light intensities, NTRC is indispensable to ensure the full range of dynamic responses of NPQ to optimize photosynthesis and maintain growth in fluctuating light environments occurring frequently in nature (501).

C. Redox regulation of light acclimation: cooperation of FTR–TRX and NADPH–NTRC systems for photoautotrophic growth

The participation of NTRC in the light activation of enzymes known to be regulated by the FDX–TRX system suggests that chloroplast redox regulation depends on the cross talk between both thiol–redox systems *in vivo*. To dissect the relationship of NTRC with the other TRXs, recent studies investigated *Arabidopsis* mutants with combined deficiencies of NTRC and TRXs. When the deficiency of NTRC was combined with those of TRX *f*1/2 (382, 498) or TRX *x* (382), double/triple mutants showed severe growth retardation phenotypes, almost abolished light activation of FBPase from the CB cycle, severely impaired CO_2 assimilation, starch turnover, photosynthetic efficiency, and chlorophyll accumulation, whereas single mutants were hardly affected. Severe growth retardation and severely impaired chlorophyll synthesis were also revealed when NTRC deficiency was combined with deficiencies of TRXs *m*1, *m2*, and *m*4 in quadruple mutants (108). A double mutant combining the deficiency of NTRC and of the catalytic subunit of FTR was not viable under photoautotrophic conditions (563). This suggests that NADPH-dependent NTRC acts concertedly with diverse other classes of TRXs of the light-dependent FDX–TRX system in photosynthetic redox regulation, with TRXs *f*1/2, *m*1/2/4, and *x* showing a high degree of functional redundancy. A cooperation of both thiol–reduction loops is, therefore, indispensable to sustain light acclimation of photosynthetic metabolism, photosynthetic efficiency, and photoautotrophic growth of plants.

Different mechanisms have been proposed to explain the functional integration of NTRC and FDX–TRX systems. The phenotypic recovery of the *ntrc Arabidopsis* mutant by overexpression of redox-inactive forms of NTRC together with bimolecular fluorescence complementation assay-based protein–protein interaction studies provided evidence that NTRC physically interacts with the FDX–TRX system and its targets *in vivo* (371). However, the functional role of this interaction is still unclear. *In vitro* studies show that NTRC is very inefficient in reducing TRXs *f*1, *f*2, *m*1, *m*4, x, and *y*1 (51, 563) and is not able to reduce the regulatory disulfides of the TRX target enzymes FBPase, SBPase, and NADP-MDH directly (382, 563). This puts forward indirect effects to explain why light activation of the CB cycle and export of excess reducing equivalents require NTRC. Recent studies show that decreased levels of 2-Cys PRX suppress the phenotype of the *ntrc* single and *ntrc-trxf1-trxf2* triple *Arabidopsis* mutants, indicating that FDX–TRX and NTRC redox systems are integrated *via* the redox balance of 2-Cys PRX (408). As NTRC is the major system to provide electrons for the reduction of 2-Cys PRXs (419, 563), it will indirectly maintain the reducing capacity of the pool of FDX–TRXs (408) and restrict reoxidation of their targets *via* an oxidation loop involving H_2O_2, oxidized 2-Cys PRX, and the atypical TRXs ACHT1/4 (111, 133, 371) and TRX-like2 (TRXL2) (561) to finally increase the reduction state of disulfides in target proteins of the FDX–TRX system (Fig. 17).

D. Redox regulation of light acclimation: integration of redox signals at the cellular level

In addition to intraorganellar cross talk of redox systems within the chloroplast, light acclimation of photosynthesis also requires interorganellar redox communication (380, 449). During acclimation to fluctuating light intensities, chloroplasts communicate information by retrograde signaling to the nucleus, leading to rapid changes in the transcription of nuclear genes coding for proteins involved in light harvesting, electron transport, stromal metabolism, and antioxidant systems to balance input of light energy with photosynthetic capacity (122, 184). There is *in vivo* evidence that H_2O_2 acts as an important retrograde signal in this response, sensing excess excitation energy in the chloroplast rather than being a toxic by-product of aerobic metabolism (134, 159, 345). Elevated light leads to increased reduction of oxygen to superoxide radicals at the acceptor side of PSI, leading to increased production of H_2O_2 *via* SOD within the chloroplast (134, 355). The elevated level of H_2O_2 is subsequently transferred from the chloroplast into the nucleus (50, 134, 355), where it leads to induced expression of high light responsive nuclear genes (134, 510) *via* redox sensitive transcription factors (473). As H_2O_2 movement from chloroplast to nucleus does not involve the cytoplasm (134), its transfer most likely involves a close physical association of the two organelles (464), allowing efficient aquaporin-mediated transmembrane diffusion (50), or the formation of stromules as direct stroma-filled interorganellar connections (53). In confirmation, stromule formation between chloroplasts and nucleus is specifically increased in response to light and chloroplast ROS production (53). This retrograde signaling pathway will (i) be attenuated by light-dependent reductive signals mediated by chloroplast TRXs and NTRC, which will diminish the production of H_2O_2 by decreasing acceptor limitation at PSI (501), (ii) increase the scavenging of H_2O_2 by activation of PRXs in the chloroplast stroma (563), and (iii) restrict the transport of H_2O_2 to the nucleus by inhibiting stromule formation (53). This is consistent with recent studies on *Arabidopsis* mutants with combined deficiencies of chloroplast 2-Cys PRXs and APXs revealing

Downloaded by LI CO SA/50127/MI from www.liebertpub.com at 07/22/19. For personal use only.

Downloaded by LI CO SA/50127/MI from www.liebertpub.com at 07/22/19. For personal use only.

increased H_2O_2 levels and upregulation of H_2O_2-responsive marker genes in the nucleus (22).

Interorganellar redox signaling also involves the exchange of reducing equivalents *via* metabolite shuttles, including the triose-P/3PGA shuttle at the chloroplast envelope (518) and the malate/oxaloacetate shuttles at the chloroplast (260, 447), mitochondrial (447), and peroxysomal (219) envelopes/membranes. This allows high light acclimation responses at the cellular level by sensing acceptor limitation at PSI *via* an increase in the chloroplast NADPH/$NADP^+$ ratio, which is transmitted to cytoplasm, mitochondria, and peroxisomes *via* a combination of the different redox shuttles. Recent studies suggested that this redox signaling system affects light acclimation responses by (i) translational inhibition of photosynthetic gene expression *via* TRX-*h*-dependent regulation of denitrosylation of the repressor protein NAB1 in the cytoplasm (46), (ii) inhibition of protein uptake into chloroplasts *via* redox regulation of chloroplast envelope translocons (29, 586), (iii) inhibition of CAT in peroxisomes to modulate H_2O_2 signaling responses (219), and (iv) dissipation of excess reducing equivalents *via* alternative oxidase in mitochondria (149, 566), probably involving regulation by mitochondrial TRXs (109) to prevent an over-reduction of the photosystems in the chloroplast (malate valve) and to modulate ROS responses. Although direct evidence for the light dependency of mitochondrial TRXs is largely lacking, there is *in vivo* evidence that the malate valve can act in the reverse direction by transmitting mitochondrial redox signals to the chloroplasts, leading to redox regulation of chloroplast metabolism (71) and import of chloroplast precursor proteins (586) *via* alterations in the chloroplast NADPH/$NADP^+$ ratio. This implies cross talk of chloroplast, cytoplasmic, and mitochondrial TRX systems to integrate redox signals at the cellular level. Further work is required to resolve the network of interorganellar redox communication and the *in vivo* roles of its components, ensuring photosynthetic light acclimation and redox balancing at the cellular level.

E. Redox control of abiotic and biotic stress responses: integration of multiple signaling pathways

In addition to its role in light acclimation of photosynthesis, redox regulation is also involved in the control of various abiotic and biotic stress responses. As reviewed recently, ROS and RNS play critical and integrative roles in multiple stress signaling (34, 377, 472), controlling pathogen defense (282, 450), and abiotic stress tolerance of plants (Fig. 17) (138, 423). The complexity in ROS responses to various environmental stimuli is attributable to the intrinsic chemical properties of different ROS, different sites and mechanisms of ROS production, the spatial and temporal coordination of ROS signals, and their integration with other signals related to metabolites, antioxidants, redoxins, hormones, and genetic control elements [reviewed in (34, 218, 251, 341, 374, 377, 423)]. In this context, different subcellular sites of ROS production may define specificity in signaling (341, 377). ROS are produced in the apoplast by activation of plasmalemma RBOHs (484) or cell wall peroxidases (315) and in chloroplasts (123), peroxisomes (115), and mitochondria (230), as a by-product of aerobic metabolism (see section II). It is proposed that specific sets of environmental stress conditions, such as pathogen infection, ozone, UV-B, excess irradiation, salinity, drought, temperature, or low oxygen, will result in specific subcellular ROS, RNS, and redox signatures that will, in turn, lead to the activation of specific defense and acclimation responses (90, 119, 403, 423). However, little is known on the underlying mechanisms allowing subcellular changes in ROS and RNS levels to be sensed and the signal being transduced to specific downstream response elements (158, 377, 423). In yeast and Chlamydomonas, the induction of autophagy in response to numerous stress conditions is associated with ROS production and is regulated by TRX-dependent activation of the ATG4 cysteine protease (398–401, 406). In plants, recent studies indicate that defense responses to abiotic and biotic stresses involve an interplay between salicylic acid (SA), ROS, RNS, GSH, and TRXs (218, 499). Different environmental stimuli lead to ROS production in different subcellular compartments that precedes SA signaling, causing transcriptional reprogramming of gene expression (218). The ROS–SA interaction is modulated by GSH, which leads to increased SA production, whereas SA causes increased GSH levels and reducing power, which, in turn, is involved in ROS scavenging (131). Upon pathogen infection, ROS is produced in the apoplast (315) leading to elevated SA levels and a subsequent more reduced cellular redox state (or at least glutathione redox state), which is sensed by the NPR1 protein, a master regulator of pathogenesis-related (PR) gene expression (354). Redox regulation involves NTRA-dependent TRX *h*5, leading to monomerization of the NPR1 oligomer in the cytoplasm to allow its translocation into the nucleus (487), where it activates the expression of PR genes *via* its interaction with TGA transcription factors, which are also modulated by redox conditions (262). In this context, TRX *h*5 is facilitating NPR1 monomerization by catalyzing the direct reduction of intermolecular disulfide bonds linking the NPR1 monomers (487) and by denitrosylation of the regulatory Cys156 in antagonistic action to GSNO and NO (262).

A further cytoplasmic mediator of redox signal transduction is the highly conserved glyceraldehyde-3-phosphate dehydrogenase C (GAPC), a key glycolytic enzyme with important noncatalytic functions for various abiotic and biotic stress responses [reviewed in (220, 557, 577)]. Plant GAPCs act as common target proteins of ROS and RNS with their catalytic Cys being subjected to diverse reversible modifications, such as S-nitrosylation, sulfenylation, and S-glutathionylation, which can be reversed/reduced by GSH, TRX, and GRX (36, 46, 102, 166, 575, 577, 580). During cadmium-induced oxidative stress, NO accumulates and GAPC1 is translocated from the cytoplasm to the nucleus, where its role remains to be established (515). Whereas in mammalian cells nuclear relocalization of GAPC depends on nitrosylation of its catalytic Cys, mutation of this residue (Cys155) in *Arabidopsis* plants led to a stimulation of relocalization, rather than an inhibition (515).

With respect to transcription factors, ERF-VII have emerged as novel regulators of abiotic and biotic stress responses involved in oxygen- and NO-dependent signal transduction in plants (177, 560). Molecular oxygen and NO lead to oxidation of the conserved N-terminal Cys of ERF-VIIs to Cys sulfinic and sulfonic acids facilitated by PCOs targeting ERF-VII proteins to the N-end rule pathway of proteasomal degradation (176, 178, 179, 294, 531, 533). This

provides a sensing mechanism for oxygen and NO mediating ERF-VII degradation and reprogramming of gene expression (178, 294, 560), allowing an efficient regulation of central metabolic processes to optimize hypoxic resistance (394) and immune responses of plants (394, 591). Although the N-end rule pathway has emerged as an important regulator of environmental stress responses, further studies are necessary to identify N-end rule substrates beyond ERF-VII and their role in the plant signaling network (125, 176).

Recent studies provide evidence for an emerging role of chloroplasts as integrators of plant stress signals specifically in plant immunity against pathogens [reviewed in (119, 154, 252, 467]. Chloroplasts are important as sensors of available photosynthetic energy to fuel immune responses and serve as major production sites of prodefense molecules such as phytohormones (including SA and jasmonic acid) and ROS providing retrograde signals to modulate nuclear gene expression and plant resistance to pathogens. This involves the chloroplast redox status as a major regulator of defense responses (Fig. 17). Manipulation of ROS buildup in chloroplasts by expression of a plastid-targeted flavodoxin (411), silencing of FTR (295), deficiency of NTRC and PRX (234, 235), and depletion of chloroplast forms of GPLX, GPXL1, and GPXL7 (75), led to changes in the expression of PR genes and pathogen resistance in diverse plant species. Although the interplay between plastidial and extraplastidial ROS sources during plant immunity is still unclear (341), the specificity of chloroplast ROS signaling may be attributable to pathogen-induced formation of stromules, providing physical connections to transport ROS and other prodefense molecules from the chloroplast directly to the nucleus (66). This will allow the transport of chloroplast-derived signaling proteins such as NRIP1 involved in pathogen recognition (67) or WHIRLY1 involved in redox sensing (154) to the nucleus to trigger PR gene expression. As NTRC acts a master regulator of chloroplast redox homeostasis (408), it will affect pathogen-related responses by modulating H_2O_2 production *via* 2-Cys PRXs (234) and light-dependent stromule formation (53).

GRXs, represented by members belonging to four different classes in terrestrial plants (see section IV), are also emerging as important redox-active players of plant responses to stress. For example, GRXS12 positively correlates with brassinosteroid accumulation and antioxidant responses under chilling conditions in tomato plants (548). Although poplar GRXS12 is very active in protein deglutathionylation *in vitro* (573), the relevance of this activity *in vivo* is still unknown. Class II GRXs are best known for their role in Fe-S cluster biogenesis (30, 351, 481), but they are also implied in stress responses. Class II GRXS14 levels correlate with plant tolerance to abiotic stress conditions in *Arabidopsis* (81, 427) and tomato (195). Plants with altered class II GRXS17 expression were found to be tolerant to drought and oxidative and heat stresses (82, 546, 547). Recently, GRXS17 was found to be associated with components of the cytoplasmic Fe-S cluster assembly pathway and to be demanded for a proper response to iron deficiency stress (233). Members of class III, namely GRXC7 and GRXC8 (ROXY1 and ROXY2, respectively), participate in pathogen responses, overexpressing lines being hypersusceptible to the infection of the necrotrophic pathogen *B. cinerea* with a concomitant accumulation of H_2O_2 (526). Interestingly, plants impaired in class III GRXS13 are less susceptible to *B. cinerea* infection (273). Transgenic plants with reduced level of GRXS13 and GRXC9 showed increased levels of superoxide radical and reduced tolerance to high light and methyl viologen treatments (278). Overexpression of class III GRXC7 and class I GRXC2 confers increased arsenic tolerance, allowing reduced accumulation of this metal pollutant in both seeds and shoot tissues (513). In general, plant *grx* mutant analyses point to a positive role of GRXs of any class in different biotic and abiotic stress responses *in vivo*. Mechanistic models of their function, however, are still largely hypothetical.

F. Redox regulation of plant development: integration of redox signals into molecular networks of developmental control

An increasing number of reports in the literature indicate redox regulation of growth and development as an emerging field in plant biology. This is summarized in many excellent recent reviews documenting emerging roles of oxidation (oxygen, ROS, and RNS) and reduction signals (TRX, GSH, and GRX) in the regulation of the whole plant developmental cycle interfacing with signaling pathways involving phytohormones and transcription factors (95, 377, 438, 451, 452, 504). There is evidence for the role of ROS, GSH, GRX, and TRX in controlling the development of root and shoot apical meristems. ROS production by mitochondria (568) and plasmalemma-located NADPH oxidases (245) together with GRXS17 (263) and ABPH2 (553) are involved in the regulation of transcription factors to determine meristem size and maintenance. Plastid-located TRX *m*3 (45) and plasma membrane-associated TRX *h*9 (330) allow cell-to-cell communication and meristem function. Extraplastidic NTRA/NTRB and GSH (33), and chloroplastic TRXs and NTRC (261, 382) are involved in auxin and redox signaling regulating meristem development. These mechanisms may also influence cell cycle progression and cell differentiation, which are associated with oscillations in cellular redox state, involving bursts of H_2O_2 and subsequent import of GSH into the nucleus, regulating transcription factors through reversible Cys reduction/oxidation *via* nuclear TRXs (63, 120, 121). Thiol-based regulatory mechanisms are also involved in the molecular networks controlling floral development with GSH and class III GRX proteins regulating petal (549) and anther development and pollen formation (357) by interacting with TGA transcription factors in the nucleus (118).

Although research into hypoxia usually emphasized the response to changes in external oxygen supply during stress responses, there is recent evidence for developmental transitions in the oxygen status of meristems and reproductive plant organs [reviewed in (170, 509)], while conversely local hypoxic conditions may contribute to regulate developmental processes in plants (94, 293, 451). Establishment of internal hypoxic environments will contribute to developmental regulation by maintaining reducing conditions in specific plant tissues. In this context, hypoxia arising naturally within growing anther tissue acts as a positional cue to set germ cell fate (255). Changes in oxygen concentrations may also contribute to plant development by affecting the stability of ERF-VII transcription factors *via* the N-end rule pathway. As published recently, the N-end rule pathway controls multiple functions during shoot and leaf development (188), probably

Downloaded by LI CO SA/50127/MI from www.liebertpub.com at 07/22/19. For personal use only.

Downloaded by LI CO SA/50127/MI from www.liebertpub.com at 07/22/19. For personal use only.

via its function to sense gaseous signals such as oxygen and NO (179, 294). This may partly involve regulation of ERF-VII by protein degradation, as *Arabidopsis* plants overexpressing N-end rule insensitive forms of ERF-VII displayed changes in leaf development (180, 394) and photomorphogenesis (2). During leaf development, maturation of chloroplasts regulates transition from cell proliferation to cell expansion (14). Chloroplast development is regulated by NTRC and FDX–TRXs (382), leading to changes in the production of oxidation signals such as oxygen, NO, and ROS that will control the transition in leaf development by acting as retrograde signals (Fig. 17) (14). During cell expansion, the transcription factor KUODA1 inhibits the expression of cell wall peroxidases, lowering the levels of apoplastic ROS to restrict cell wall tightening and promote growth (308).

G. Redox regulation in plant physiology: a brief conclusion

There is a balance of oxidation and reduction signals integrating photosynthesis, development, and stress responses, allowing plants to cope with fluctuating changes in their biotic and abiotic environment. This involves intraorganellar cross talk of redox systems as well as redox communication within and between cells. In this context, NTRC acts as an important hub to control the redox balance between oxidation and reduction pathways within the chloroplast of C3 plants, thereby influencing retrograde signals such as ROS to control light acclimation, abiotic and biotic stress responses, and plant development. There is also an emerging role of gaseous signals such as oxygen and NO, which modulate proteasomal degradation of proteins containing an N-terminal Cys *via* the N-end rule pathway. Although research into hypoxia usually emphasized stress responses, there are also developmental transitions in the oxygen status, which conversely contribute to the regulation of plant development. Further studies are needed to dissect this complex redox signaling network and its integration with other signals related to metabolites, antioxidants, redoxins, phytohormones, and genetic control elements.

VIII. Concluding Remarks and Future Perspectives

The importance and pervasiveness of redox regulation and signaling in plant biology have currently reached a level that probably Bob Buchanan and collaborators could not even vaguely imagine when they first discovered the principles of TRX-mediated regulation of photosynthetic metabolism in plants >50 years ago. This comprehensive review tries to account for the fact that we now know that redox regulation involves not only one but many different types of PTMs of protein Cys, different RMS, a large number of redoxins (TRXs, GRXs, and NTRC), and an enormous number of protein targets belonging to virtually every metabolic or signaling pathway and located in virtually every subcellular compartment, either of photosynthetic and nonphotosynthetic plant cells. As a result, redox homeostasis infiltrates all aspects of plant physiology. The recent development of plant redox biology has provided the material of this comprehensive review, but also opened many questions that need to be answered in the future.

Combination of traditional biochemical approaches and redox proteomics is showing that redox-regulated proteins are organized in complex networks that we are just beginning to understand. A large part of the redox targets that have been identified by proteomics still have to be analyzed to understand the effect, if any, of the redox modification. Moreover, most of our knowledge is derived from nonquantitative studies performed under conditions that favor the redox modification of the proteome. We have little information of the real status of the redox proteome under different physiological or pathological conditions, and even for the best characterized targets, we rarely know which is the relative abundance of the redox-modified proteins in the cell. To this end, quantitative proteomic methods are being developed and will allow determining the stoichiometry and dynamics of multiple redox PTMs in few or even a single cell, under diverse physiological conditions and time scales. The final goal will be to understand, besides the pervasiveness, the relevance of redox regulation and signaling for plant physiology, thereby digging below the surface that we have just started to scratch.

Beyond quantitative proteomics, a field of redox biology that will hopefully grow more and more in the future regards the genetically encoded redox sensors. At the moment, we have powerful tools to determine the dynamics of the glutathione redox state. Other important redox players (NADPH, ascorbate, TRXs, GRXs, and RMS) are still waiting to be assayed *in vivo* by similar methods. In the absence of accurate information on their localization, dynamics, and redox state, we will hardly get a comprehensive picture of how redox homeostasis influences plant's life. Basic research and genetic engineering will have a fundamental role in the development of new genetically encoded sensors, and the continuous improvement of fluorescent microscopy imaging techniques will likely provide further support to this field in the future.

Structural biology is also promising to contribute significantly to our global understanding of plant redox homeostasis. Once discovered that plants contain tens of different redoxins coexisting in the same subcellular compartment, which, in the same time, also contains hundreds of proteins potentially targeted by different redox PTMs, we still have only a vague idea of which are the principles that govern specificity in all possible interactions. Such principles will be derived from computational analyses of atomic structures of interacting partners and redox-modified proteins. Our available repertoire of complex structures is still limited in number. Solving the tridimensional structure of large complexes of interacting proteins proved difficult in the past because of the intrinsic limitations in obtaining crystals of sufficient quality for X-ray diffraction analysis, but cryoelectron microscopy techniques allow to bypass the crystallization step and permit to unravel large complex structures at atomic resolution.

At the end, what we really would like to know best is how redox regulation and signaling works in the context of plant physiology. Whereas past research into redox regulation was mainly focused on biochemical studies, a recent boost of genetic studies elucidated the organization and biological significance of the redox network *in planta*. These recent studies have fully confirmed the original model of light-dependent regulation of the CB cycle as mediated by TRXs, but have also opened new fields of research and new levels of understanding.

Results from reverse genetic studies clearly indicate that redox regulatory and signaling pathways contain multiple branches and interconnections. Although reverse genetic

approaches are the most powerful way to currently demonstrate the function of a protein *in vivo*, complex networks may hinder a clear-cut interpretation of the results. This is particularly true when a hub element of the network, like, for example, a TRX, is knocked out. Indeed, TRX knock out mutants are likely to show pleiotropic effects. Moreover, the cross talk between redox signaling pathways requires the combination of different knock out mutations to obtain a reliable interpretation of the emerging phenotypes.

Besides the master redox regulators, also the targets should be investigated *in vivo* and mutagenic approaches specifically directed to the redox-active Cys are arguably the best way to tackle this problem. Also, this approach has its own limitation, and in some cases, the substitution of a single Cys was found to affect protein stability *in vivo* besides redox regulation, thereby significantly complicating the emerging picture (204, 476). Nevertheless, this approach seems promising and will possibly be boosted by genome editing techniques that are becoming available. Overall, we firmly believe that the integration of *in vitro* biochemical data with *in vivo* physiological evidence will provide the strongest basis to a general understanding of plant redox homeostasis.

Fifty years after germination, thiol-based redox biology in photosynthetic organisms has developed into a deeply rooted well-established plant that grows and expands its foliage in all directions: it is still in its infancy but the future looks bright and full of opportunities.

Downloaded by LI CO SA/50127/MI from www.liebertpub.com at 07/22/19. For personal use only.

Acknowledgments

The author M.Z. gratefully acknowledges support of this work from the University of Bologna (Alma Idea Grant). P.G. thanks the Deutsche Forschungsgemeinschaft (SFB-TR 175 B02) for funding. The authors thank Dr. Stephan Wagner, Prof. Bruce Morgan, and Prof. Markus Schwarzländer for providing the original for Figure 16A.

References

1. Abat JK and Deswal R. Differential modulation of S-nitrosoproteome of *Brassica juncea* by low temperature: change in S-nitrosylation of Rubisco is responsible for the inactivation of its carboxylase activity. *Proteomics* 9: 4368–4380, 2009.
2. Abbas M, Berckhan S, Rooney D, Gibbs D, Vicente Conde J, Sousa Correia C, Bassel G, Marín-de la Rosa N, León J, Alabadí D, Blázquez M, and Holdsworth M. Oxygen sensing coordinates photomorphogenesis to facilitate seedling survival. *Curr Biol* 25: 1483–1488, 2015.
3. Akter S, Huang J, Bodra N, De Smet B, Wahni K, Rombaut D, Pauwels J, Gevaert K, Carroll K, Van Breusegem F, and Messens J. DYn-2 based identification of arabidopsis sulfenomes. *Mol Cell Proteom* 14: 1183–1200, 2015.
4. Akter S, Huang J, Waszczak C, Jacques S, Gevaert K, Van Breusegem F, and Messens J. Cysteines under ROS attack in plants: a proteomics view. *J Exp Bot* 66: 2935–2944, 2015.
5. Albrecht SC, Barata AG, Großhans J, Teleman AA, and Dick TP. In vivo mapping of hydrogen peroxide and oxidized glutathione reveals chemical and regional specificity of redox homeostasis. *Cell Metab* 14: 819–829, 2011.
6. Alkhalfioui F, Renard M, Vensel WH, Wong J, Tanaka CK, Hurkman WJ, Buchanan BB, and Montrichard F. Thioredoxin-linked proteins are reduced during germination of *Medicago truncatula* seeds. *Plant Physiol* 144: 1559–1579, 2007.
7. Aller I and Meyer AJ. The oxidative protein folding machinery in plant cells. *Protoplasma* 250: 799–816, 2013.
8. Aller I, Rouhier N, and Meyer AJ. Development of roGFP2-derived redox probes for measurement of the glutathione redox potential in the cytosol of severely glutathione-deficient rml1 seedlings. *Front Plant Sci* 4: 506, 2013.
9. Alvarez C, Calo L, Romero LC, Garcia I, and Gotor C. An O-acetylserine(thiol)lyase homolog with L-cysteine desulfhydrase activity regulates cysteine homeostasis in Arabidopsis. *Plant Physiol* 152: 656–669, 2010.
10. Alvarez C, Garcia I, Moreno I, Perez-Perez ME, Crespo JL, Romero LC, and Gotor C. Cysteine-generated sulfide in the cytosol negatively regulates autophagy and modulates the transcriptional profile in Arabidopsis. *Plant Cell* 24: 4621–4634, 2012.
11. Álvarez C, García I, Romero LC, and Gotor C. Mitochondrial sulfide detoxification requires a functional isoform O-acetylserine(thiol)lyase C in *Arabidopsis thaliana*. *Mol Plant* 5: 1217–1226, 2012.
12. Anderson LE. Activation of pea leaf chloroplast sedoheptulose 1,7-diphosphate phosphatase by light and dithiothreitol. *Biochem Biophys Res Commun* 59: 907–913, 1974.
13. Anderson LE and Lim TC. Chloroplast glyceraldehyde 3-phosphate dehydrogenase: light-dependent change in the enzyme. *FEBS Lett* 27: 189–191, 1972.
14. Andriankaja M, Dhondt S, De Bodt S, Vanhaeren H, Coppens F, De Milde L, Mühlenbock P, Skirycz A, Gonzalez N, Beemster GS, and Inzé D. Exit from Proliferation during Leaf Development in *Arabidopsis thaliana*: A Not-So-Gradual Process. *Dev Cell* 22: 64–78, 2012.
15. Armstrong DA. Applications of pulse radiolysis for the study of short-lived sulphur species. In: *Sulfur-Centered Reactive Intermediates in Chemistry and Biology*, edited by Chatgilialoglu C, and Asmus KD. Berlin: Springer, 1990, pp. 121–134.
16. Aroca A, Benito JM, Gotor C, and Romero LC. Persulfidation proteome reveals the regulation of protein function by hydrogen sulfide in diverse biological processes in Arabidopsis. *J Exp Bot* 68: 4915–4927, 2017.
17. Aroca A, Serna A, Gotor C, and Romero LC. S-sulfhydration: a cysteine posttranslational modification in plant systems. *Plant Physiol* 168: 334–342, 2015.
18. Arsova B, Hoja U, Wimmelbacher M, Greiner E, Üstün S, Melzer M, Petersen K, Lein W, and Börnke F. Plastidial thioredoxin z interacts with two fructokinase-like proteins in a thiol-dependent manner: evidence for an essential role in chloroplast development in Arabidopsis and *Nicotiana benthamiana*. *Plant Cell* 22: 1498–1515, 2010.
19. Asard H, Barbaro R, Trost P, and Bérczi A. Cytochromes b561: ascorbate-mediated trans-membrane electron transport. *Antioxid Redox Signal* 19: 1026–1035, 2013.
20. Astier J, Besson-Bard A, Lamotte O, Bertoldo J, Bourque S, Terenzi H, and Wendehenne D. Nitric oxide inhibits the ATPase activity of the chaperone-like AAA+ ATPase CDC48, a target for S-nitrosylation in cryptogein signalling in tobacco cells. *Biochem J* 447: 249–260, 2012.
21. Astier J, Gross I, and Durner J. Nitric oxide production in plants: an update. *J Exp Bot* 69: 3401–3411, 2018.
22. Awad J, Stotz HU, Fekete A, Krischke M, Engert C, Havaux M, Berger S, and Mueller MJ. 2-cysteine peroxiredoxins and thylakoid ascorbate peroxidase create a water-water cycle that is essential to protect the photosynthetic

Downloaded by LI CO SA/50127/MI from www.liebertpub.com at 07/22/19. For personal use only.

apparatus under high light stress conditions. *Plant Physiol* 167: 1592–1603, 2015.
23. Baier D and Latzko E. Properties and regulation of C-1-fructose-1,6-diphosphatase from spinach chloroplasts. *Biochim Biophys Acta* 396: 141–147, 1975.
24. Balmer Y, Koller A, del Val G, Manieri W, Schürmann P, and Buchanan BB. Proteomics gives insight into the regulatory function of chloroplast thioredoxins. *Proc Natl Acad Sci U S A* 100: 370–375, 2003.
25. Balmer Y, Vensel WH, Cai N, Manieri W, Schürmann P, Hurkman WJ, and Buchanan BB. A complete ferredoxin/thioredoxin system regulates fundamental processes in amyloplasts. *Proc Natl Acad Sci U S A* 103: 2988–2993, 2006.
26. Balmer Y, Vensel WH, DuPont FM, Buchanan BB, and Hurkman WJ. Proteome of amyloplasts isolated from developing wheat endosperm presents evidence of broad metabolic capability. *J Exp Bot* 57: 1591–1602, 2006.
27. Balmer Y, Vensel WH, Hurkman WJ, and Buchanan BB. Thioredoxin target proteins in chloroplast thylakoid membranes. *Antioxid Redox Signal* 8: 1829–1834, 2006.
28. Balmer Y, Vensel WH, Tanaka CK, Hurkman WJ, Gelhaye E, Rouhier N, Jacquot J-P, Manieri W, Schürmann P, Droux M, and Buchanan BB. Thioredoxin links redox to the regulation of fundamental processes of plant mitochondria. *Proc Natl Acad Sci U S A* 101: 2642–2647, 2004.
29. Balsera M, Soll J, and Buchanan BB. Redox extends its regulatory reach to chloroplast protein import. *Trends Plant Sci* 15: 515–521, 2010.
30. Bandyopadhyay S, Gama F, Molina-Navarro MM, Gualberto JM, Claxton R, Naik SG, Huynh BH, Herrero E, Jacquot JP, Johnson MK, and Rouhier N. Chloroplast monothiol glutaredoxins as scaffold proteins for the assembly and delivery of [2Fe-2S] clusters. *EMBO J* 27: 1122–1133, 2008.
31. Baniulis D, Hasan SS, Stofleth JT, and Cramer WA. Mechanism of enhanced superoxide production in the cytochrome b (6)f complex of oxygenic photosynthesis. *Biochemistry* 52: 8975–8983, 2013.
32. Bartsch S, Monnet J, Selbach K, Quigley F, Gray J, von Wettstein D, Reinbothe S, and Reinbothe C. Three thioredoxin targets in the inner envelope membrane of chloroplasts function in protein import and chlorophyll metabolism. *Proc Natl Acad Sci U S A* 105: 4933–4938, 2008.
33. Bashandy T, Guilleminot J, Vernoux T, Caparros-Ruiz D, Ljung K, Meyer Y, and Reichheld J-P. Interplay between the NADP-Linked Thioredoxin and Glutathione Systems in Arabidopsis Auxin Signaling. *Plant Cell* 22: 376–391, 2010.
34. Baxter A, Mittler R, and Suzuki N. ROS as key players in plant stress signalling. *J Exp Bot* 65: 1229–1240, 2014.
35. Bechtold U, Rabbani N, Mullineaux PM, and Thornalley PJ. Quantitative measurement of specific biomarkers for protein oxidation, nitration and glycation in Arabidopsis leaves. *Plant J* 59: 661–671, 2009.
36. Bedhomme M, Adamo M, Marchand CH, Couturier J, Rouhier N, Lemaire SD, Zaffagnini M, and Trost P. Glutathionylation of cytosolic glyceraldehyde-3-phosphate dehydrogenase from the model plant *Arabidopsis thaliana* is reversed by both glutaredoxins and thioredoxins in vitro. *Biochem J* 445: 337–347, 2012.
37. Bedhomme M, Zaffagnini M, Marchand CH, Gao XH, Moslonka-Lefebvre M, Michelet L, Decottignies P, and Lemaire SD. Regulation by glutathionylation of isocitrate lyase from *Chlamydomonas reinhardtii*. *J Biol Chem* 284: 36282–36291, 2009.
38. Beer SM, Taylor ER, Brown SE, Dahm CC, Costa NJ, Runswick MJ, and Murphy MP. Glutaredoxin 2 catalyzes the reversible oxidation and glutathionylation of mitochondrial membrane thiol proteins: implications for mitochondrial redox regulation and antioxidant defense. *J Biol Chem* 279: 47939–47951, 2004.
39. Begas P, Liedgens L, Moseler A, Meyer AJ, and Deponte M. Glutaredoxin catalysis requires two distinct glutathione interaction sites. *Nat Commun* 8: 14835, 2017.
40. Beneloujaephajri E, Costa A, L'Haridon F, Métraux JP, and Binda M. Production of reactive oxygen species and wound-induced resistance in *Arabidopsis thaliana* against *Botrytis cinerea* are preceded and depend on a burst of calcium. *BMC Plant Biol* 13: 160, 2013.
41. Benhar M. Nitric oxide and the thioredoxin system: a complex interplay in redox regulation. *Biochim Biophys Acta* 1850: 2476–2484, 2015.
42. Benhar M, Forrester MT, Hess DT, and Stamler JS. Regulated protein denitrosylation by cytosolic and mitochondrial thioredoxins. *Science* 320: 1050–1054, 2008.
43. Benhar M, Forrester MT, and Stamler JS. Protein denitrosylation: enzymatic mechanisms and cellular functions. *Nat Rev Mol Cell Biol* 10: 721–732, 2009.
44. Benhar M, Thompson JW, Moseley MA, and Stamler JS. Identification of S-nitrosylated targets of thioredoxin using a quantitative proteomic approach. *Biochemistry* 49: 6963–6969, 2010.
45. Benitez-Alfonso Y, Cilia M, Roman AS, Thomas C, Maule A, Hearn S, and Jackson D. Control of Arabidopsis meristem development by thioredoxin-dependent regulation of intercellular transport. *Proc Natl Acad Sci U S A* 106: 3615–3620, 2009.
46. Berger H, De Mia M, Morisse S, Marchand CH, Lemaire SD, Wobbe L, and Kruse O. A light switch based on protein S-Nitrosylation Fine-Tunes Photosynthetic Light Harvesting in Chlamydomonas. *Plant Physiol* 171: 821–832, 2016.
47. Bernal-Bayard P, Hervás M, Cejudo FJ, and Navarro JA. Electron Transfer Pathways and Dynamics of Chloroplast NADPH-dependent Thioredoxin Reductase C (NTRC). *J Biol Chem* 287: 33865–33872, 2012.
48. Berndt C, Schwenn JD, and Lillig CH. The specificity of thioredoxins and glutaredoxins is determined by electrostatic and geometric complementarity. *Chem Sci* 6: 7049–7058, 2015.
49. Bianco CL, Toscano JP, Bartberger MD, and Fukuto JM. The chemical biology of HNO signaling. *Arch Biochem Biophys* 617: 129–136, 2017.
50. Bienert GP and Chaumont F. Aquaporin-facilitated transmembrane diffusion of hydrogen peroxide. *Biochim Biophys Acta* 1840: 1596–1604, 2014.
51. Bohrer AS, Massot V, Innocenti G, Reichheld JP, Issakidis-Bourguet E, and Vanacker H. New insights into the reduction systems of plastidial thioredoxins point out the unique properties of thioredoxin z from Arabidopsis. *J Exp Bot* 63: 6315–6323, 2012.
52. Broin M, Cuine S, Eymery F, and Rey P. The plastidic 2-cysteine peroxiredoxin is a target for a thioredoxin involved in the protection of the photosynthetic apparatus against oxidative damage. *Plant Cell* 14: 1417–1432, 2002.
53. Brunkard JO, Runkel AM, and Zambryski PC. Chloroplasts extend stromules independently and in response to

internal redox signals. *Proc Natl Acad Sci U S A* 112: 10044–10049, 2015.
54. Buchanan BB. The path to thioredoxin and redox regulation in chloroplasts. *Annu Rev Plant Biol* 67: 1–24, 2016.
55. Buchanan BB and Balmer Y. Redox regulation: a broadening horizon. *Annu Rev Plant Biol* 56: 187–220, 2005.
56. Buchanan BB, Holmgren A, Jacquot JP, and Scheibe R. Fifty years in the thioredoxin field and a bountiful harvest. *Biochim Biophys Acta* 1820: 1822–1829, 2012.
57. Buchanan BB, Kalberer PP, and Arnon DI. Ferredoxin-activated fructose diphosphatase in isolated chloroplasts. *Biochem Biophys Res Commun* 29: 74–79, 1967.
58. Buchanan BB, Schürmann P, and Kalberer PP. Ferredoxin-activated fructose diphosphatase of spinach chloroplasts. Resolution of the system, properties of the alkaline fructose diphosphatase component, and physiological significance of the ferredoxin-linked activation. *J Biol Chem* 246: 5952–5959, 1971.
59. Buey RM, Arellano JB, López-Maury L, Galindo-Trigo S, Velázquez-Campoy A, Revuelta JL, de Pereda JM, Florencio FJ, Schürmann P, Buchanan BB, and Balsera M. Unprecedented pathway of reducing equivalents in a diflavin-linked disulfide oxidoreductase. *Proc Natl Acad Sci U S A* 114: 12725–12730, 2017.
60. Bushweller JH, Billeter M, Holmgren A, and Wüthrich K. The nuclear magnetic resonance solution structure of the mixed disulfide between *Escherichia coli* glutaredoxin (C14S) and glutathione. *J Mol Biol* 235: 1585–1597, 1994.
61. Cain P, Hall M, Schröder WP, Kieselbach T, and Robinson C. A novel extended family of stromal thioredoxins. *Plant Mol Biol* 70: 273–281, 2009.
62. Cairns NG, Pasternak M, Wachter A, Cobbett CS, and Meyer AJ. Maturation of arabidopsis seeds is dependent on glutathione biosynthesis within the embryo. *Plant Physiol* 141: 446–455, 2006.
63. Calderón A, Ortiz-Espín A, Iglesias-Fernández R, Carbonero P, Pallardó FV, Sevilla F, and Jiménez A. Thioredoxin (Trxo1) interacts with proliferating cell nuclear antigen (PCNA) and its overexpression affects the growth of tobacco cell culture. *Redox Biol* 11: 688–700, 2017.
64. Camejo D, Romero-Puertas MdC, Rodríguez-Serrano M, Sandalio LM, Lázaro JJ, Jiménez A, and Sevilla F. Salinity-induced changes in S-nitrosylation of pea mitochondrial proteins. *J Proteom* 79: 87–99, 2013.
65. Capitani G, Marković-Housley Z, DelVal G, Morris M, Jansonius JN, and ürmann P. Crystal structures of two functionally different thioredoxins in spinach chloroplasts. *J Mol Biol* 302: 135–154, 2000.
66. Caplan JL, Kumar AS, Park E, Padmanabhan MS, Hoban K, Modla S, Czymmek K, and Dinesh-Kumar SP. Chloroplast stromules function during innate immunity. *Dev Cell* 34: 45–57, 2015.
67. Caplan JL, Mamillapalli P, Burch-Smith TM, Czymmek K, and Dinesh-Kumar SP. Chloroplastic protein NRIP1 mediates innate immune receptor recognition of a viral effector. *Cell* 132: 449–462, 2008.
68. Cardi M, Zaffagnini M, De Lillo A, Castiglia D, Chibani K, Gualberto JM, Rouhier N, Jacquot J-P, and Esposito S. Plastidic P2 glucose-6P dehydrogenase from poplar is modulated by thioredoxin m-type: distinct roles of cysteine residues in redox regulation and NADPH inhibition. *Plant Sci* 252: 257–266, 2016.
69. Carrillo LR, Froehlich JE, Cruz JA, Savage LJ, and Kramer DM. Multi-level regulation of the chloroplast ATP synthase: the chloroplast NADPH thioredoxin reductase C (NTRC) is required for redox modulation specifically under low irradiance. *Plant J* 87: 654–663, 2016.
70. Cavallini D, Federici G, and Barboni E. Interaction of proteins with sulfide. *Eur J Biochem* 14: 169–174, 1970.
71. Centeno DC, Osorio S, Nunes-Nesi A, Bertolo ALF, Carneiro RT, Araújo WL, Steinhauser M-C, Michalska J, Rohrmann J, Geigenberger P, Oliver SN, Stitt M, Carrari F, Rose JKC, and Fernie AR. Malate Plays a Crucial Role in Starch Metabolism, Ripening, and Soluble Solid Content of Tomato Fruit and Affects Postharvest Softening. *Plant Cell* 23: 162–184, 2011.
72. Chacinska A, Pfannschmidt S, Wiedemann N, Kozjak V, Sanjuán Szklarz LK, Schulze-Specking A, Truscott KN, Guiard B, Meisinger C, and Pfanner N. Essential role of Mia40 in import and assembly of mitochondrial intermembrane space proteins. *Embo J* 23: 3735–3746, 2004.
73. Chaki M, Shekariesfahlan A, Ageeva A, Mengel A, von Toerne C, Durner J, and Lindermayr C. Identification of nuclear target proteins for S-nitrosylation in pathogen-treated *Arabidopsis thaliana* cell cultures. *Plant Sci* 238: 115–126, 2015.
74. Chamizo-Ampudia A, Sanz-Luque E, Llamas Á, Ocaña-Calahorro F, Mariscal V, Carreras A, Barroso JB, Galván A, and Fernández E. A dual system formed by the ARC and NR molybdoenzymes mediates nitrite-dependent NO production in Chlamydomonas. *Plant Cell Environ* 39: 2097–2107, 2016.
75. Chang CCC, Ślesak I, Jordá L, Sotnikov A, Melzer M, Miszalski Z, Mullineaux PM, Parker JE, Karpińska B, and Karpiński S. Arabidopsis chloroplastic glutathione peroxidases play a role in cross talk between photooxidative stress and immune responses. *Plant Physiol* 150: 670–683, 2009.
76. Chardonnet S, Sakr S, Cassier-Chauvat C, Le Maréchal P, Chauvat F, Lemaire SD, and Decottignies P. First proteomic study of S-glutathionylation in cyanobacteria. *J Proteome Res* 14: 59–71, 2015.
77. Charles RL, Schröder E, May G, Free P, Gaffney PRJ, Wait R, Begum S, Heads RJ, and Eaton P. Protein sulfenation as a redox sensor: proteomics studies using a novel biotinylated dimedone analogue. *Mol Cell Proteomics* 6: 1473–1484, 2007.
78. Chartron J, Shiau C, Stout CD, and Carroll KS. 3′-Phosphoadenosine-5′-phosphosulfate Reductase in Complex with Thioredoxin: A Structural Snapshot in the Catalytic Cycle. *Biochemistry* 46: 3942–3951, 2007.
79. Chen J, Wu FH, Wang WH, Zheng CJ, Lin GH, Dong XJ, He JX, Pei ZM, and Zheng HL. Hydrogen sulphide enhances photosynthesis through promoting chloroplast biogenesis, photosynthetic enzyme expression, and thiol redox modification in *Spinacia oleracea* seedlings. *J Exp Bot* 62: 4481–4493, 2011.
80. Chen KY and Morris JC. Kinetics of oxidation of aqueous sulfide by oxygen. *Environ Sci Technol* 6: 529–537, 1972.
81. Cheng NH, Liu JZ, Brock A, Nelson RS, and Hirschi KD. AtGRXcp, an Arabidopsis chloroplastic glutaredoxin, is critical for protection against protein oxidative damage. *J Biol Chem* 281: 26280–26288, 2006.
82. Cheng NH, Liu JZ, Liu X, Wu Q, Thompson SM, Lin J, Chang J, Whitham SA, Park S, Cohen JD, and Hirschi KD. Arabidopsis monothiol glutaredoxin, AtGRXS17, is critical for temperature-dependent postembryonic growth and development via modulating auxin response. *J Biol Chem* 286: 20398–20406, 2011.

Downloaded by LI CO SA/50127/MI from www.liebertpub.com at 07/22/19. For personal use only.

Downloaded by LI CO SA/50127/MI from www.liebertpub.com at 07/22/19. For personal use only.

83. Cheng T, Chen J, Ef AA, Wang P, Wang G, Hu X and Shi J. Quantitative proteomics analysis reveals that S-nitrosoglutathione reductase (GSNOR) and nitric oxide signaling enhance poplar defense against chilling stress. Planta 242: 1361–1390, 2015.
84. Chibani K, Saul F, Didierjean C, Rouhier N, and Haouz A. Structural snapshots along the reaction mechanism of the atypical poplar thioredoxin-like2.1. *FEBS Lett* 592: 1030–1041, 2018.
85. Chibani K, Tarrago L, Gualberto JM, Wingsle G, Rey P, Jacquot J-P, and Rouhier N. Atypical thioredoxins in poplar: the glutathione-dependent thioredoxin-like 2.1 supports the activity of target enzymes possessing a single redox active cysteine. *Plant Physiol* 159: 592–605, 2012.
86. Chibani K, Tarrago L, Schürmann P, Jacquot JP, and Rouhier N. Biochemical properties of poplar thioredoxin z. *FEBS Lett* 585: 1077–1081, 2011.
87. Chibani K, Wingsle G, Jacquot JP, Gelhaye E, and Rouhier N. Comparative genomic study of the thioredoxin family in photosynthetic organisms with emphasis on *Populus trichocarpa*. *Mol Plant* 2: 308–322, 2009.
88. Chivers PT, Prehoda KE, Volkman BF, Kim B-M, Markley JL, and Raines RT. Microscopic p K a values of *Escherichia coli* thioredoxin. *Biochemistry* 36: 14985–14991, 1997.
89. Chivers PT and Raines RT. General acid/base catalysis in the active site of *Escherichia coli* thioredoxin. *Biochemistry* 36: 15810–15816, 1997.
90. Choudhury FK, Rivero RM, Blumwald E, and Mittler R. Reactive oxygen species, abiotic stress and stress combination. *Plant J* 90: 856–867, 2017.
91. Cobessi D, Tête-Favier F, Marchal S, Azza S, Branlant G, and Aubry A. Apo and holo crystal structures of an NADP-dependent aldehyde dehydrogenase from *Streptococcus mutans*. *J Mol Biol* 290: 161–173, 1999.
92. Collin V, Issakidis-Bourguet E, Marchand C, Hirasawa M, Lancelin JM, Knaff DB, and Miginiac-Maslow M. The Arabidopsis plastidial thioredoxins: new functions and new insights into specificity. *J Biol Chem* 278: 23747–23752, 2003.
93. Collin V, Lamkemeyer P, Miginiac-Maslow M, Hirasawa M, Knaff DB, Dietz KJ, and Issakidis-Bourguet E. Characterization of plastidial thioredoxins from Arabidopsis belonging to the new y-type. *Plant Physiol* 136: 4088–4095, 2004.
94. Considine MJ, Diaz-Vivancos P, Kerchev P, Signorelli S, Agudelo-Romero P, Gibbs DJ, and Foyer CH. Learning to breathe: developmental phase transitions in oxygen status. *Trends Plant Sci* 22: 140–153, 2017.
95. Considine MJ and Foyer CH. Redox regulation of plant development. *Antioxid Redox Signal* 21: 1305–1326, 2014.
96. Copley SD, Novak WRP, and Babbitt PC. Divergence of function in the thioredoxin fold suprafamily: evidence for evolution of peroxiredoxins from a thioredoxin-like ancestor. *Biochemistry* 43: 13981–13995, 2004.
97. Corpas FJ, Alché JD, and Barroso JB. Current overview of S-nitrosoglutathione (GSNO) in higher plants. *Front Plant Sci* 4: 126, 2013.
98. Coudevylle N, Thureau A, Hemmerlin C, Gelhaye E, Jacquot JP, and Cung MT. Solution structure of a natural CPPC active site variant, the reduced form of thioredoxin h1 from poplar. *Biochemistry* 44: 2001–2008, 2005.
99. Courteille A, Vesa S, Sanz-Barrio R, Cazale A-C, Becuwe-Linka N, Farran I, Havaux M, Rey P, and Rumeau D. Thioredoxin m4 Controls Photosynthetic Alternative Electron Pathways in Arabidopsis. *Plant Physiol* 161: 508–520, 2013.
100. Couturier J, Jacquot JP, and Rouhier N. Evolution and diversity of glutaredoxins in photosynthetic organisms. *Cell Mol Life Sci* 66: 2539–2557, 2009.
101. Couturier J, Jacquot JP, and Rouhier N. Toward a refined classification of class I dithiol glutaredoxins from poplar: biochemical basis for the definition of two subclasses. *Front Plant Sci* 4: 518, 2013.
102. Couturier J, Koh CS, Zaffagnini M, Winger AM, Gualberto JM, Corbier C, Decottignies P, Jacquot JP, Lemaire SD, Didierjean C, and Rouhier N. Structure-function relationship of the chloroplastic glutaredoxin S12 with an atypical WCSYS active site. *J Biol Chem* 284: 9299–9310, 2009.
103. Couturier J, Przybyla-Toscano J, Roret T, Didierjean C, and Rouhier N. The roles of glutaredoxins ligating Fe-S clusters: sensing, transfer or repair functions? *Biochim Biophys Acta* 1853: 1513–1527, 2015.
104. Couturier J, Ströher E, Albetel AN, Roret T, Muthuramalingam M, Tarrago L, Seidel T, Tsan P, Jacquot JP, Johnson MK, Dietz KJ, Didierjean C, and Rouhier N. Arabidopsis chloroplastic glutaredoxin C5 as a model to explore molecular determinants for iron–sulfur cluster binding into glutaredoxins. *J Biol Chem* 286: 27515–27527, 2011.
105. Couvertier SM, Zhou Y, and Weerapana E. Chemical-proteomic strategies to investigate cysteine posttranslational modifications. *Biochim Biophys Acta* 1844: 2315–2330, 2014.
106. Cuevasanta E, Lange M, Bonanata J, Coitiño EL, Ferrer-Sueta G, Filipovic MR, and Alvarez B. Reaction of Hydrogen Sulfide with Disulfide and Sulfenic Acid to Form the Strongly Nucleophilic Persulfide. *J Biol Chem* 290: 26866–26880, 2015.
107. Czapski G and Goldstein S. The role of the reactions of.NO with superoxide and oxygen in biological systems: a kinetic approach. *Free Radic Biol Med* 19: 785–794, 1995.
108. Da Q, Wang P, Wang M, Sun T, Jin H, Liu B, Wang J, Grimm B, and Wang H-B. Thioredoxin and NADPH-dependent thioredoxin reductase C regulation of Tetrapyrrole Biosynthesis. *Plant Physiol* 175: 652–666, 2017.
109. Daloso DM, Müller K, Obata T, Florian A, Tohge T, Bottcher A, Riondet C, Bariat L, Carrari F, Nunes-Nesi A, Buchanan BB, Reichheld J-P, Araújo WL, and Fernie AR. Thioredoxin, a master regulator of the tricarboxylic acid cycle in plant mitochondria. *Proc Natl Acad Sci U S A* 112: E1392–E1400, 2015.
110. Dangoor I, Peled-Zehavi H, Levitan A, Pasand O, and Danon A. A small family of chloroplast atypical thioredoxins. *Plant Physiol* 149: 1240–1250, 2009.
111. Dangoor I, Peled-Zehavi H, Wittenberg G, and Danon A. A chloroplast light-regulated oxidative sensor for moderate light intensity in Arabidopsis. *Plant Cell* 24: 1894–1906, 2012.
112. Danon A. Environmentally-induced oxidative stress and its signaling. In: *Photosynthesis*, edited by Eaton-Rye J, Tripathy B, and Sharkey T. Dordrecht: Springer, 2012, pp. 319–330, 2012.
113. Davies MJ. Protein oxidation and peroxidation. *Biochem J* 473: 805–825, 2016.
114. Declercq JP, Evrard C, Clippe A, Stricht DV, Bernard A, and Knoops B. Crystal structure of human peroxiredoxin 5, a novel type of mammalian peroxiredoxin at 1.5 A resolution. *J Mol Biol* 311: 751–759, 2001.

115. del Río LA and López-Huertas E. ROS generation in peroxisomes and its role in cell signaling. *Plant Cell Physiol* 57: 1364–1376, 2016.
116. Delaunay A, Pflieger D, Barrault MB, Vinh J, and Toledano MB. A thiol peroxidase is an H2O2 receptor and redox-transducer in gene activation. *Cell* 111: 471–481, 2002.
117. Delledonne M, Xia Y, Dixon RA, and Lamb C. Nitric oxide functions as a signal in plant disease resistance. *Nature* 394: 585–588, 1998.
118. Delorme-Hinoux V, Bangash SAK, Meyer AJ, and Reichheld JP. Nuclear thiol redox systems in plants. *Plant Sci* 243: 84–95, 2016.
119. Delprato ML, Krapp AR, and Carrillo N. Green light to plant responses to pathogens: the role of chloroplast light-dependent signaling in biotic stress. *Photochem Photobiol* 91: 1004–1011, 2015.
120. Diaz-Vivancos P, de Simone A, Kiddle G, and Foyer CH. Glutathione–linking cell proliferation to oxidative stress. *Free Radic Biol Med* 89: 1154–1164, 2015.
121. Diaz Vivancos P, Wolff T, Markovic J, Pallardó FV, and Foyer CH. A nuclear glutathione cycle within the cell cycle. *Biochem J* 431: 169–178, 2010.
122. Dietz K-J. Efficient high light acclimation involves rapid processes at multiple mechanistic levels. *J Exp Bot* 66: 2401–2414, 2015.
123. Dietz K-J, Turkan I, and Krieger-Liszkay A. Redox- and reactive oxygen species-dependent signaling into and out of the photosynthesizing chloroplast. *Plant Physiol* 171: 1541–1550, 2016.
124. Dietz KJ. Peroxiredoxins in plants and cyanobacteria. *Antioxid Redox Signal* 15: 1129–1159, 2011.
125. Dissmeyer N, Rivas S, and Graciet E. Life and death of proteins after protease cleavage: protein degradation by the N-end rule pathway. *New Phytol* 218: 929–935, 2018.
126. Dixon DP, Skipsey M, Grundy NM, and Edwards R. Stress-induced protein S-glutathionylation in Arabidopsis. *Plant Physiol* 138: 2233–2244, 2005.
127. Dóka É, Pader I, Bíró A, Johansson K, Cheng Q, Ballagó K, Prigge JR, Pastor-Flores D, Dick TP, Schmidt EE, Arnér ESJ, and Nagy P. A novel persulfide detection method reveals protein persulfide- and polysulfide-reducing functions of thioredoxin and glutathione systems. *Sci Adv* 2: e1500968, 2016.
128. Dooley CT, Dore TM, Hanson GT, Jackson WC, Remington SJ, and Tsien RY. Imaging dynamic redox changes in mammalian cells with green fluorescent protein indicators. *J Biol Chem* 279: 22284–22293, 2004.
129. Doulias P-T, Greene JL, Greco TM, Tenopoulou M, Seeholzer SH, Dunbrack RL, and Ischiropoulos H. Structural profiling of endogenous S-nitrosocysteine residues reveals unique features that accommodate diverse mechanisms for protein S-nitrosylation. *Proc Natl Acad Sci U S A* 107: 16958–16963, 2010.
130. Du H, Kim S, Nam KH, Lee MS, Son O, Lee SH, and Cheon CI. Identification of uricase as a potential target of plant thioredoxin: implication in the regulation of nodule development. *Biochem Biophys Res Commun* 397: 22–26, 2010.
131. Dubreuil-Maurizi C and Poinssot B. Role of glutathione in plant signaling under biotic stress. *Plant Signal Behav* 7: 210–212, 2012.
132. Dubreuil-Maurizi C, Vitecek J, Marty L, Branciard L, Frettinger P, Wendehenne D, Meyer AJ, Mauch F, and Poinssot B. Glutathione deficiency of the Arabidopsis mutant pad2-1 affects oxidative stress-related events, defense gene expression, and the hypersensitive response. *Plant Physiol* 157: 2000–2012, 2011.
133. Eliyahu E, Rog I, Inbal D, and Danon A. ACHT4-driven oxidation of APS1 attenuates starch synthesis under low light intensity in Arabidopsis plants. *Proc Natl Acad Sci U S A* 112: 12876–12881, 2015.
134. Exposito-Rodriguez M, Laissue PP, Yvon-Durocher G, Smirnoff N, and Mullineaux PM. Photosynthesis-dependent H2O2 transfer from chloroplasts to nuclei provides a high-light signalling mechanism. *Nat Commun* 8: 49, 2017.
135. Faccenda A, Bonham CA, Vacratsis PO, Zhang X, and Mutus B. Gold nanoparticle enrichment method for identifying S-nitrosylation and S-glutathionylation sites in proteins. *J Am Chem Soc* 132: 11392–11394, 2010.
136. Fares A, Rossignol M, and Peltier JB. Proteomics investigation of endogenous S-nitrosylation in Arabidopsis. *Biochem Biophys Res Commun* 416: 331–336, 2011.
137. Farmer EE and Mueller MJ. ROS-mediated lipid peroxidation and RES-activated signaling. *Annu Rev Plant Biol* 64: 429–450, 2013.
138. Farnese FS, Menezes-Silva PE, Gusman GS, and Oliveira JA. When bad guys become good ones: the key role of reactive oxygen species and nitric oxide in the plant responses to abiotic stress. *Front Plant Sci* 7: 471, 2016.
139. Feechan A, Kwon E, Yun B-W, Wang Y, Pallas JA, and Loake GJ. A central role for S-nitrosothiols in plant disease resistance. *Proc Natl Acad Sci U S A* 102: 8054–8059, 2005.
140. Feng J, Wang C, Chen Q, Chen H, Ren B, Li X, and Zuo J. S-nitrosylation of phosphotransfer proteins represses cytokinin signaling. *Nat Commun* 4: 1529, 2013.
141. Feng S, Chen Y, Yang F, Zhang L, Gong Y, Adilijiang G, Gao Y, and Deng H. Development of a clickable probe for profiling of protein glutathionylation in the central cellular metabolism of *E. coli* and *Drosophila*. *Chem Biol* 22: 1461–1469, 2015.
142. Feng Y, Zhong N, Rouhier N, Hase T, Kusunoki M, Jacquot JP, Jin C, and Xia B. Structural insight into poplar glutaredoxin C1 with a bridging iron–sulfur cluster at the active site. *Biochemistry* 45: 7998–8008, 2006.
143. Fermani S, Sparla F, Falini G, Martelli PL, Casadio R, Pupillo P, Ripamonti A, and Trost P. Molecular mechanism of thioredoxin regulation in photosynthetic A2B2-glyceraldehyde-3-phosphate dehydrogenase. *Proc Natl Acad Sci U S A* 104: 11109–11114, 2007.
144. Fermani S, Trivelli X, Sparla F, Thumiger A, Calvaresi M, Marri L, Falini G, Zerbetto F, and Trost P. Conformational selection and folding-upon-binding of intrinsically disordered protein CP12 regulate photosynthetic enzymes assembly. *J Biol Chem* 287: 21372–21383, 2012.
145. Fernandes AP, Fladvad M, Berndt C, Andrésen C, Lillig CH, Neubauer P, Sunnerhagen M, Holmgren A, and Vlamis-Gardikas A. A novel monothiol glutaredoxin (Grx4) from *Escherichia coli* can serve as a substrate for thioredoxin reductase. *J Biol Chem* 280: 24544–24552, 2005.
146. Ferrer-Sueta G, Manta B, Botti H, Radi R, Trujillo M, and Denicola A. Factors affecting protein thiol reactivity and specificity in peroxide reduction. *Chem Res Toxicol* 24: 434–450, 2011.
147. Finkemeier I, Goodman M, Lamkemeyer P, Kandlbinder A, Sweetlove LJ, and Dietz KJ. The mitochondrial type II

Downloaded by LI CO SA/50127/MI from www.liebertpub.com at 07/22/19. For personal use only.

peroxiredoxin F is essential for redox homeostasis and root growth of *Arabidopsis thaliana* under stress. *J Biol Chem* 280: 12168–12180, 2005.
148. Fischer BB, Hideg É, and Krieger-Liszkay A. Production, detection, and signaling of singlet oxygen in photosynthetic organisms. *Antioxid Redox Signal* 18: 2145–2162, 2013.
149. Florez-Sarasa I, Flexas J, Rasmusson AG, Umbach AL, Siedow JN, and Ribas-Carbo M. In vivo cytochrome and alternative pathway respiration in leaves of *Arabidopsis thaliana* plants with altered alternative oxidase under different light conditions. *Plant Cell Environ* 34: 1373–1383, 2011.
150. Foloppe N, Sagemark J, Nordstrand K, Berndt KD, and Nilsson L. Structure, dynamics and electrostatics of the active site of glutaredoxin 3 from *Escherichia coli*: comparison with functionally related proteins1. *J Mol Biol* 310: 449–470, 2001.
151. Foresi N, Correa-Aragunde N, Parisi G, Calo G, Salerno G, and Lamattina L. Characterization of a nitric oxide synthase from the plant kingdom: NO generation from the green alga *Ostreococcus tauri* is light irradiance and growth phase dependent. *Plant Cell* 22: 3816–3830, 2010.
152. Forrester MT, Thompson JW, Foster MW, Nogueira L, Moseley MA, and Stamler JS. Proteomic analysis of S-nitrosylation and denitrosylation by resin-assisted capture. *Nat Biotechnol* 27: 557–559, 2009.
153. Foster MW, Forrester MT, and Stamler JS. A protein microarray-based analysis of S-nitrosylation. *Proc Natl Acad Sci U S A* 106: 18948–18953, 2009.
154. Foyer CH, Karpinska B, and Krupinska K. The functions of WHIRLY1 and REDOX-RESPONSIVE TRANSCRIPTION FACTOR 1 in cross tolerance responses in plants: a hypothesis. *Philos Trans R Soc Lond B Biol Sci* 369: 20130226, 2014.
155. Foyer CH and Noctor G. Redox homeostasis and antioxidant signaling: a metabolic interface between stress perception and physiological responses. *Plant Cell* 17: 1866–1875, 2005.
156. Foyer CH and Noctor G. Redox regulation in photosynthetic organisms: signaling, acclimation, and practical implications. *Antioxid Redox Signal* 11: 861–905, 2009.
157. Foyer CH and Noctor G. Ascorbate and glutathione: the heart of the redox hub. *Plant Physiol* 155: 2–18, 2011.
158. Foyer CH and Noctor G. Stress-triggered redox signalling: what's in pROSpect? *Plant Cell Environ* 39: 951–964, 2016.
159. Foyer CH, Ruban AV, and Noctor G. Viewing oxidative stress through the lens of oxidative signalling rather than damage. *Biochem J* 474: 877–883, 2017.
160. Fratelli M, Demol H, Puype M, Casagrande S, Eberini I, Salmona M, Bonetto V, Mengozzi M, Duffieux F, Miclet E, Bachi A, Vandekerckhove J, Gianazza E, and Ghezzi P. Identification by redox proteomics of glutathionylated proteins in oxidatively stressed human T lymphocytes. *Proc Natl Acad Sci U S A* 99: 3505–3510, 2002.
161. Frederickson Matika DE and Loake GJ. Redox regulation in plant immune function. *Antioxid Redox Signal* 21: 1373–1388, 2014.
162. Frungillo L, Skelly MJ, Loake GJ, Spoel SH, and Salgado I. S-nitrosothiols regulate nitric oxide production and storage in plants through the nitrogen assimilation pathway. *Nat Commun* 5: 5401, 2014.
163. Gallogly MM, Starke DW, Leonberg AK, Ospina SME, and Mieyal JJ. Kinetic and mechanistic characterization and versatile catalytic properties of mammalian glutaredoxin 2: implications for intracellular roles. *Biochemistry* 47: 11144–11157, 2008.
164. Gama F, Keech O, Eymery F, Finkemeier I, Gelhaye E, Gardeström P, Dietz KJ, Rey P, Jacquot J-P, and Rouhier N. The mitochondrial type II peroxiredoxin from poplar. *Physiol Plant* 129: 196–206, 2007.
165. Gao XH, Krokowski D, Guan BJ, Bederman I, Majumder M, Parisien M, Diatchenko L, Kabil O, Willard B, Banerjee R, Wang B, Bebek G, Evans CR, Fox PL, Gerson SL, Hoppel CL, Liu M, Arvan P, and Hatzoglou M. Quantitative H2S-mediated protein sulfhydration reveals metabolic reprogramming during the integrated stress response. *Elife* 4: e10067, 2015.
166. Gao XH, Zaffagnini M, Bedhomme M, Michelet L, Cassier-Chauvat C, Decottignies P, and Lemaire SD. Biochemical characterization of glutaredoxins from *Chlamydomonas reinhardtii*: kinetics and specificity in deglutathionylation reactions. *FEBS Lett* 584: 2242–2248, 2010.
167. García-Santamarina S, Boronat S, Domènech A, Ayté J, Molina H, and Hidalgo E. Monitoring in vivo reversible cysteine oxidation in proteins using ICAT and mass spectrometry. *Nat Protoc* 9: 1131–1145, 2014.
168. Gascuel O. BIONJ: an improved version of the NJ algorithm based on a simple model of sequence data. *Mol Biol Evol* 14: 685–695, 1997.
169. Gebicki S and Gebicki JM. Formation of peroxides in amino acids and proteins exposed to oxygen free radicals. *Biochem J* 289: 743–749, 1993.
170. Geigenberger P. Response of plant metabolism to too little oxygen. *Curr Opin Plant Biol* 6: 247–256, 2003.
171. Geigenberger P, Thormählen I, Daloso DM, and Fernie AR. The unprecedented versatility of the plant thioredoxin system. *Trends Plant Sci* 22: 249–262, 2017.
172. Gelhaye E, Rouhier N, Gérard J, Jolivet Y, Gualberto J, Navrot N, Ohlsson P-I, Wingsle G, Hirasawa M, Knaff DB, Wang H, Dizengremel P, Meyer Y, and Jacquot J-P. A specific form of thioredoxin h occurs in plant mitochondria and regulates the alternative oxidase. *Proc Natl Acad Sci U S A* 101: 14545–14550, 2004.
173. Gelhaye E, Rouhier N, and Jacquot JP. Evidence for a subgroup of thioredoxin h that requires GSH/Grx for its reduction. *FEBS Lett* 555: 443–448, 2003.
174. Geng B, Yang J, Qi Y, Zhao J, Pang Y, Du J, and Tang C. H2S generated by heart in rat and its effects on cardiac function. *Biochem Biophys Res Commun* 313: 362–368, 2004.
175. Gergondey R, Garcia C, Marchand CH, Lemaire SD, Camadro JM, and Auchère F. Modulation of the specific glutathionylation of mitochondrial proteins in the yeast *Saccharomyces cerevisiae* under basal and stress conditions. *Biochem J* 474: 1175–1193, 2017.
176. Gibbs DJ, Bailey M, Tedds HM, and Holdsworth MJ. From start to finish: amino-terminal protein modifications as degradation signals in plants. *New Phytol* 211: 1188–1194, 2016.
177. Gibbs DJ, Conde JV, Berckhan S, Prasad G, Mendiondo GM, and Holdsworth MJ. Group VII ethylene response factors coordinate oxygen and nitric oxide signal transduction and stress responses in plants. *Plant Physiol* 169: 23–31, 2015.

Downloaded by LI CO SA/50127/MI from www.liebertpub.com at 07/22/19. For personal use only.

178. Gibbs DJ, Lee SC, Md Isa NM, Gramuglia S, Fukao T, Bassel GW, Correia CS, Corbineau F, Theodoulou FL, Bailey-Serres J, and Holdsworth MJ. Homeostatic response to hypoxia is regulated by the N-end rule pathway in plants. *Nature* 479: 415–418, 2011.
179. Gibbs D, Md Isa N, Movahedi M, Lozano-Juste J, Mendiondo G, Berckhan S, Marín-de la Rosa N, Vicente Conde J, Sousa Correia C, Pearce SP, Bassel G, Hamali B, Talloji P, Tomé DA, Coego A, Beynon J, Alabadí D, Bachmair A, León J, Gray J, Theodoulou F, and Holdsworth M. Nitric oxide sensing in plants is mediated by proteolytic control of group VII ERF transcription factors. *Mol Cell* 53: 369–379, 2014.
180. Giuntoli B, Shukla V, Maggiorelli F, Giorgi FM, Lombardi L, Perata P, and Licausi F. Age-dependent regulation of ERF-VII transcription factor activity in *Arabidopsis thaliana*. *Plant Cell Environ* 40: 2333–2346, 2017.
181. Giustarini D, Milzani A, Aldini G, Carini M, Rossi R, and Dalle-Donne I. S-nitrosation versus S-glutathionylation of protein sulfhydryl groups by S-nitrosoglutathione. *Antioxid Redox Signal* 7: 930–939, 2005.
182. Go YM, Chandler JD, and Jones DP. The cysteine proteome. *Free Radic Biol Med* 84: 227–245, 2015.
183. Go YM and Jones DP. Redox biology: interface of the exposome with the proteome, epigenome and genome. *Redox Biol* 2: 358–360, 2014.
184. Gollan PJ, Tikkanen M, and Aro EM. Photosynthetic light reactions: integral to chloroplast retrograde signalling. *Curr Opin Plant Biol* 27: 180–191, 2015.
185. Gotor C, Álvarez C, Bermúdez MÁ, Moreno I, García I, and Romero LC. Low abundance does not mean less importance in cysteine metabolism. *Plant Signal Behav* 5: 1028–1030, 2010.
186. Gould NS, Evans P, Martínez-Acedo P, Marino SM, Gladyshev VN, Carroll KS, and Ischiropoulos H. Site-specific proteomic mapping identifies selectively modified regulatory cysteine residues in functionally distinct protein networks. *Chem Biol* 22: 965–975, 2015.
187. Goyer A, Haslekås C, Miginiac-Maslow M, Klein U, Le Maréchal P, Jacquot JP, and Decottignies P. Isolation and characterization of a thioredoxin-dependent peroxidase from *Chlamydomonas reinhardtii*. *Eur J Biochem* 269: 272–282, 2002.
188. Graciet E, Walter F, O'Maoileidigh DS, Pollmann S, Meyerowitz EM, Varshavsky A, and Wellmer F. The N-end rule pathway controls multiple functions during Arabidopsis shoot and leaf development. *Proc Natl Acad Sci U S A* 106: 13618–13623, 2009.
189. Greetham D, Vickerstaff J, Shenton D, Perrone GG, Dawes IW, and Grant CM. Thioredoxins function as deglutathionylase enzymes in the yeast *Saccharomyces cerevisiae*. *BMC Biochem* 11: 3, 2010.
190. Gross E, Sevier CS, Heldman N, Vitu E, Bentzur M, Kaiser CA, Thorpe C, and Fass D. Generating disulfides enzymatically: reaction products and electron acceptors of the endoplasmic reticulum thiol oxidase Ero1p. *Proc Natl Acad Sci U S A* 103: 299–304, 2006.
191. Gross F, Durner J, and Gaupels F. Nitric oxide, antioxidants and prooxidants in plant defence responses. *Front Plant Sci* 4: 419, 2013.
192. Gruber CW, Čemažar M, Heras B, Martin JL, and Craik DJ. Protein disulfide isomerase: the structure of oxidative folding. *Trends Biochem Sci* 31: 455–464, 2006.
193. Guerra D, Ballard K, Truebridge I, and Vierling E. S-Nitrosation of Conserved Cysteines Modulates Activity and Stability of S-Nitrosoglutathione Reductase (GSNOR). *Biochemistry* 55: 2452–2464, 2016.
194. Guo J, Nguyen AY, Dai Z, Su D, Gaffrey MJ, Moore RJ, Jacobs JM, Monroe ME, Smith RD, Koppenaal DW, Pakrasi HB, and Qian WJ. Proteome-wide light/dark modulation of thiol oxidation in cyanobacteria revealed by quantitative site-specific redox proteomics. *Mol Cell Proteomics* 13: 3270–3285, 2014.
195. Guo Y, Huang C, Xie Y, Song F, and Zhou X. A tomato glutaredoxin gene SlGRX1 regulates plant responses to oxidative, drought and salt stresses. *Planta* 232: 1499–1509, 2010.
196. Gupta KJ, Fernie AR, Kaiser WM, and van Dongen JT. On the origins of nitric oxide. *Trends Plant Sci* 16: 160–168, 2011.
197. Gupta V and Carroll KS. Sulfenic acid chemistry, detection and cellular lifetime. *Biochim Biophys Acta* 1840: 847–875, 2014.
198. Gupta V, Paritala H, and Carroll KS. Reactivity, selectivity, and stability in sulfenic acid detection: a comparative study of nucleophilic and electrophilic probes. *Bioconjug Chem* 27: 1411–1418, 2016.
199. Gupta V, Yang J, Liebler DC, and Carroll KS. Diverse redoxome reactivity profiles of carbon nucleophiles. *J Am Chem Soc* 139: 5588–5595, 2017.
200. Gütle DD, Roret T, Müller SJ, Couturier J, Lemaire SD, Hecker A, Dhalleine T, Buchanan BB, Reski R, Einsle O, and Jacquot JP. Chloroplast FBPase and SBPase are thioredoxin-linked enzymes with similar architecture but different evolutionary histories. *Proc Natl Acad Sci U S A* 113: 6779–6784, 2016.
201. Gutsche N, Thurow C, Zachgo S, and Gatz C. Plant-specific CC-type glutaredoxins: functions in developmental processes and stress responses. *Biol Chem* 396: 495–509, 2015.
202. Gutscher M, Pauleau AL, Marty L, Brach T, Wabnitz GH, Samstag Y, Meyer AJ, and Dick TP. Real-time imaging of the intracellular glutathione redox potential. *Nat Meth* 5: 553–559, 2008.
203. Gutscher M, Sobotta MC, Wabnitz GH, Ballikaya S, Meyer AJ, Samstag Y, and Dick TP. Proximity-based protein thiol oxidation by H2O2-scavenging peroxidases. *J Biol Chem* 284: 31532–31540, 2009.
204. Hädrich N, Hendriks JHM, Kötting O, Arrivault S, Feil R, Zeeman SC, Gibon Y, Schulze WX, Stitt M, and Lunn JE. Mutagenesis of cysteine 81 prevents dimerization of the APS1 subunit of ADP-glucose pyrophosphorylase and alters diurnal starch turnover in *Arabidopsis thaliana* leaves. *Plant J* 70: 231–242, 2012.
205. Hägglund P, Bunkenborg J, Maeda K, Finnie C, and Svensson B. Identification of thioredoxin target disulfides using isotope-coded affinity tags. *Methods Mol Biol* 1072: 677–685, 2014.
206. Hägglund P, Bunkenborg J, Maeda K, and Svensson B. Identification of thioredoxin disulfide targets using a quantitative proteomics approach based on isotope-coded affinity tags. *J Proteome Res* 7: 5270–5276, 2008.
207. Hall A, Nelson K, Poole LB, and Karplus PA. Structure-based insights into the catalytic power and conformational dexterity of peroxiredoxins. *Antioxid Redox Signal* 15: 795–815, 2011.

Downloaded by LI CO SA/50127/MI from www.liebertpub.com at 07/22/19. For personal use only.

Downloaded by LI CO SA/50127/MI from www.liebertpub.com at 07/22/19. For personal use only.

208. Hall M, Mata-Cabana A, Akerlund HE, Florencio FJ, Schroder WP, Lindahl M, and Kieselbach T. Thioredoxin targets of the plant chloroplast lumen and their implications for plastid function. *Proteomics* 10: 987–1001, 2010.
209. Hamnell-Pamment Y, Lind C, Palmberg C, Bergman T, and Cotgreave IA. Determination of site-specificity of S-glutathionylated cellular proteins. *Biochem Biophys Res Commun* 332: 362–369, 2005.
210. Hao G, Derakhshan B, Shi L, Campagne F, and Gross SS. SNOSID, a proteomic method for identification of cysteine S-nitrosylation sites in complex protein mixtures. *Proc Natl Acad Sci U S A* 103: 1012–1017, 2006.
211. Hao G and Gross SS. Electrospray tandem mass spectrometry analysis of S- and N-nitrosopeptides: facile loss of NO and radical-induced fragmentation. *J Am Soc Mass Spectrom* 17: 1725–1730, 2006.
212. Hara S, Motohashi K, Arisaka F, Romano PGN, Hosoya-Matsuda N, Kikuchi N, Fusada N, and Hisabori T. Thioredoxin-h1 reduces and reactivates the oxidized cytosolic malate dehydrogenase dimer in higher plants. *J Biol Chem* 281: 32065–32071, 2006.
213. Hartmann SK, Stockdreher Y, Wandrey G, Hosseinpour Tehrani H, Zambanini T, Meyer AJ, Büchs J, Blank LM, Schwarzländer M, and Wierckx N. Online in vivo monitoring of cytosolic NAD redox dynamics in *Ustilago maydis*. *Biochim Biophys Acta* 1859: 1015–1024, 2018.
214. Held JM and Gibson BW. Regulatory control or oxidative damage? Proteomic approaches to interrogate the role of cysteine oxidation status in biological processes. *Mol Cell Proteom* 11: 013037, 2012.
215. Heldt HW, Werdan K, Milovancev M, and Geller G. Alkalization of the chloroplast stroma caused by light-dependent proton flux into the thylakoid space. *Biochim Biophys Acta* 314: 224–241, 1973.
216. Heller J, Meyer AJ, and Tudzynski P. Redox-sensitive GFP2: use of the genetically encoded biosensor of the redox status in the filamentous fungus *Botrytis cinerea*. *Mol Plant Pathol* 13: 935–947, 2012.
217. Henard CA, Guarnieri MT, and Knoshaug EP. The Chlorella vulgaris S-Nitrosoproteome under Nitrogen-Replete and -Deplete Conditions. *Front Bioeng Biotechnol* 4: 100, 2016.
218. Herrera-Vásquez A, Salinas P, and Holuigue L. Corrigendum: salicylic acid and reactive oxygen species interplay in the transcriptional control of defense genes expression. *Front Plant Sci* 8: 171, 2015.
219. Heyno E, Innocenti G, Lemaire SD, Issakidis-Bourguet E, and Krieger-Liszkay A. Putative role of the malate valve enzyme NADP–malate dehydrogenase in H(2)O(2) signalling in Arabidopsis. *Philos Trans R Soc Lond B Biol Sci* 369: 20130228, 2014.
220. Hildebrandt T, Knuesting J, Berndt C, Morgan B, and Scheibe R. Cytosolic thiol switches regulating basic cellular functions: GAPDH as an information hub? *Biol Chem* 396: 523–537, 2015.
221. Hind G, Nakatani HY, and Izawa S. Light-dependent redistribution of ions in suspensions of chloroplast thylakoid membranes. *Proc Natl Acad Sci U S A* 71: 1484–1488, 1974.
222. Hirasawa M, Ruelland E, Schepens I, Issakidis-Bourguet E, Miginiac-Maslow M, and Knaff DB. Oxidation–reduction properties of the regulatory disulfides of sorghum chloroplast nicotinamide adenine dinucleotide phosphate-malate dehydrogenase. *Biochemistry* 39: 3344–3350, 2000.
223. Hirasawa M, Schürmann P, Jacquot JP, Manieri W, Jacquot P, Keryer E, Hartman FC, and Knaff DB. Oxidation–reduction properties of chloroplast thioredoxins, ferredoxin:thioredoxin reductase, and thioredoxin f-regulated enzymes. *Biochemistry* 38: 5200–5205, 1999.
224. Holmgren A, Soderberg BO, Eklund H, and Branden CI. Three-dimensional structure of *Escherichia coli* thioredoxin-S2 to 2.8 A resolution. *Proc Natl Acad Sci U S A* 72: 2305–2309, 1975.
225. Horling F, Lamkemeyer P, Konig J, Finkemeier I, Kandlbinder A, Baier M, and Dietz KJ. Divergent light-, ascorbate-, and oxidative stress-dependent regulation of expression of the peroxiredoxin gene family in Arabidopsis. *Plant Physiol* 131: 317–325, 2003.
226. Hoshi T and Heinemann SH. Regulation of cell function by methionine oxidation and reduction. *J Physiol* 531: 1–11, 2001.
227. Hosoya-Matsuda N, Motohashi K, Yoshimura H, Nozaki A, Inoue K, Ohmori M, and Hisabori T. Anti-oxidative stress system in cyanobacteria. Significance of type II peroxiredoxin and the role of 1-Cys peroxiredoxin in Synechocystis sp. strain PCC 6803. *J Biol Chem* 280: 840–846, 2005.
228. Hou X, Hu W-W, Shen L, Lee LYC, Tao Z, Han J-H, and Yu H. Global identification of DELLA target genes during Arabidopsis flower development. *Plant Physiol* 147: 1126–1142, 2008.
229. Hu J, Huang X, Chen L, Sun X, Lu C, Zhang L, Wang Y, and Zuo J. Site-specific nitrosoproteomic identification of endogenously S-nitrosylated proteins in Arabidopsis. *Plant Physiol* 167: 1731–1746, 2015.
230. Huang S, Van Aken O, Schwarzländer M, Belt K, and Millar AH. The roles of mitochondrial reactive oxygen species in cellular signaling and stress response in plants. *Plant Physiol* 171: 1551–1559, 2016.
231. Hung YP, Albeck JG, Tantama M, and Yellen G. Imaging cytosolic NADH-NAD(+) redox state with a genetically encoded fluorescent biosensor. *Cell Metab* 14: 545–554, 2011.
232. Ikegami A, Yoshimura N, Motohashi K, Takahashi S, Romano PGN, Hisabori T, Takamiya K, and Masuda T. The CHLI1 subunit of *Arabidopsis thaliana* magnesium chelatase is a target protein of the chloroplast thioredoxin. *J Biol Chem* 282: 19282–19291, 2007.
233. Inigo S, Durand AN, Ritter A, Le Gall S, Termathe M, Klassen R, Tohge T, De Coninck B, Van Leene J, De Clercq R, Cammue BP, Fernie AR, Gevaert K, De Jaeger G, Leidel SA, Schaffrath R, Van Lijsebettens M, Pauwels L, and Goossens A. Glutaredoxin GRXS17 associates with the cytosolic iron-sulfur cluster assembly pathway. *Plant Physiol* 172: 858–873, 2016.
234. Ishiga Y, Ishiga T, Ikeda Y, Matsuura T, and Mysore KS. NADPH-dependent thioredoxin reductase C plays a role in nonhost disease resistance against *Pseudomonas syringae* pathogens by regulating chloroplast-generated reactive oxygen species. *PeerJ* 4: e1938, 2016.
235. Ishiga Y, Ishiga T, Wangdi T, Mysore KS, and Uppalapati SR. NTRC and chloroplast-generated reactive oxygen species regulate *Pseudomonas syringae* pv. tomato disease development in tomato and Arabidopsis. *Mol Plant Microbe Interact* 25: 294–306, 2012.

236. Ito H, Iwabuchi M, and Ogawa K. The sugar-metabolic enzymes aldolase and triose-phosphate isomerase are targets of glutathionylation in *Arabidopsis thaliana*: detection using biotinylated glutathione. *Plant Cell Physiol* 44: 655–660, 2003.
237. Jacques S, Ghesquière B, De Bock PJ, Demol H, Wahni K, Willems P, Messens J, Van Breusegem F, and Gevaert K. Protein methionine sulfoxide dynamics in *Arabidopsis thaliana* under oxidative stress. *Mol Cell Proteom* 14: 1217–1229, 2015.
238. Jacques S, Ghesquière B, Van Breusegem F, and Gevaert K. Plant proteins under oxidative attack. *Proteomics* 13: 932–940, 2013.
239. Jacquot J-P, Eklund H, Rouhier N, and Schürmann P. Structural and evolutionary aspects of thioredoxin reductases in photosynthetic organisms. *Trends Plant Sci* 14: 336–343, 2009.
240. Jacquot JP and Buchanan BB. Enzyme Regulation in C (4) Photosynthesis: purification and properties of thioredoxin-linked NADP-malate dehydrogenase from corn leaves. *Plant Physiol* 68: 300–304, 1981.
241. Jaffrey SR, Erdjument-Bromage H, Ferris CD, Tempst P, and Snyder SH. Protein S-nitrosylation: a physiological signal for neuronal nitric oxide. *Nat Cell Biol* 3: 193–197, 2001.
242. Jagodnik J, Brosse A, Le Lam TN, Chiaruttini C, and Guillier M. Mechanistic study of base-pairing small regulatory RNAs in bacteria. *Methods* 117: 67–76, 2017.
243. Jeong W, Bae SH, Toledano MB, and Rhee SG. Role of sulfiredoxin as a regulator of peroxiredoxin function and regulation of its expression. *Free Radic Biol Med* 53: 447–456, 2012.
244. Jiang K, Schwarzer C, Lally E, Zhang S, Ruzin S, Machen T, Remington SJ, and Feldman L. Expression and characterization of a redox-sensing green fluorescent protein (reduction-oxidation-sensitive green fluorescent protein) in Arabidopsis. *Plant Physiol* 141: 397–403, 2006.
245. Jiao Y, Sun L, Song Y, Wang L, Liu L, Zhang L, Liu B, Li N, Miao C, and Hao F. AtrbohD and AtrbohF positively regulate abscisic acid-inhibited primary root growth by affecting Ca2+ signalling and auxin response of roots in Arabidopsis. *J Exp Bot* 64: 4183–4192, 2013.
246. Johansson C, Lillig CH, and Holmgren A. Human mitochondrial glutaredoxin reduces S-glutathionylated proteins with high affinity accepting electrons from either glutathione or thioredoxin reductase. *J Biol Chem* 279: 7537–7543, 2004.
247. Juárez-Díaz JA, McClure B, Vázquez-Santana S, Guevara-García A, León-Mejía P, Márquez-Guzmán J, and Cruz-García F. A novel thioredoxin h is secreted in Nicotiana alata and reduces S-RNase in vitro. *J Biol Chem* 281: 3418–3424, 2006.
248. Jubany-Mari T, Alegre-Batlle L, Jiang K, and Feldman LJ. Use of a redox-sensing GFP (c-roGFP1) for real-time monitoring of cytosol redox status in *Arabidopsis thaliana* water-stressed plants. *FEBS Lett* 584: 889–897, 2010.
249. Kabil O and Banerjee R. Redox biochemistry of hydrogen sulfide. *J Biol Chem* 285: 21903–21907, 2010.
250. Kaneko R and Wada Y. Decomposition of protein nitrosothiolsin matrix-assisted laser desorption/ionization and electrospray ionization mass spectrometry. *J Mass Spectrom* 38: 526–530, 2003.
251. Kangasjarvi S, Neukermans J, Li S, Aro E-M, and Noctor G. Photosynthesis, photorespiration, and light signalling in defence responses. *J Exp Bot* 63: 1619–1636, 2012.
252. Kangasjärvi S, Tikkanen M, Durian G, and Aro E-M. Photosynthetic light reactions – An adjustable hub in basic production and plant immunity signaling. *Plant Physiol Biochem* 81: 128–134, 2014.
253. Kehr S, Jortzik E, Delahunty C, Yates JR, 3rd, Rahlfs S, and Becker K. Protein S-glutathionylation in malaria parasites. *Antioxid Redox Signal* 15: 2855–2865, 2011.
254. Kekulandara DN, Samarasinghe KTG, Munkanatta Godage DNP, and Ahn YH. Clickable glutathione using tetrazine-alkene bioorthogonal chemistry for detecting protein glutathionylation. *Org Biomol Chem* 14: 10886–10893, 2016.
255. Kelliher T and Walbot V. Hypoxia triggers meiotic fate acquisition in maize. *Science* 337: 345–348, 2012.
256. Kieselbach T. Oxidative folding in chloroplasts. *Antioxid Redox Signal* 19: 72–82, 2013.
257. Kim MR, Khaleda L, Jung IJ, Kim JY, Lee SY, Cha J-Y, and Kim W-Y. Overexpression of chloroplast-localized NADPH-dependent thioredoxin reductase C (NTRC) enhances tolerance to photo-oxidative and drought stresses in *Arabidopsis thaliana*. *J Plant Biol* 60: 175–180, 2017.
258. Kim SG, Chung JS, Sutton RB, Lee JS, López-Maury L, Lee SY, Florencio FJ, Lin T, Zabet-Moghaddam M, Wood MJ, Nayak K, Madem V, Tripathy JN, Kim SK, and Knaff DB. Redox, mutagenic and structural studies of the glutaredoxin/arsenate reductase couple from the cyanobacterium Synechocystis sp. PCC 6803. *Biochim Biophys Acta* 1824: 392–403, 2012.
259. Kimura H. Signaling molecules: hydrogen sulfide and polysulfide. *Antioxid Redox Signal* 22: 362–376, 2015.
260. Kinoshita H, Nagasaki J, Yoshikawa N, Yamamoto A, Takito S, Kawasaki M, Sugiyama T, Miyake H, Weber APM, and Taniguchi M. The chloroplastic 2-oxoglutarate/malate transporter has dual function as the malate valve and in carbon/nitrogen metabolism. *Plant J* 65: 15–26, 2011.
261. Kirchsteiger K, Ferrández J, Pascual MB, González M, and Cejudo FJ. NADPH thioredoxin reductase c is localized in plastids of photosynthetic and nonphotosynthetic tissues and is involved in lateral root formation in arabidopsis. *Plant Cell* 24: 1534–1548, 2012.
262. Kneeshaw S, Gelineau S, Tada Y, Loake GJ, and Spoel SH. Selective protein denitrosylation activity of Thioredoxin-h5 modulates plant Immunity. *Mol Cell* 56: 153–162, 2014.
263. Knuesting J, Riondet C, Maria C, Kruse I, Bécuwe N, König N, Berndt C, Tourrette S, Guilleminot-Montoya J, Herrero E, Gaymard F, Balk J, Belli G, Scheibe R, Reichheld JP, Rouhier N, and Rey P. Arabidopsis glutaredoxin S17 and its partner, the nuclear factor Y subunit C11/negative cofactor 2alpha, contribute to maintenance of the shoot apical meristem under long-day photoperiod. *Plant Physiol* 167: 1643–1658, 2015.
264. Koh CS, Navrot N, Didierjean C, Rouhier N, Hirasawa M, Knaff DB, Wingsle G, Samian R, Jacquot JP, Corbier C, and Gelhaye E. An atypical catalytic mechanism involving three cysteines of thioredoxin. *J Biol Chem* 283: 23062–23072, 2008.
265. Kolbert Z, Feigl G, Bordé Á, Molnár Á, and Erdei L. Protein tyrosine nitration in plants: present knowledge, computational prediction and future perspectives. *Plant Physiol Biochem* 113: 56–63, 2017.
266. König J, Baier M, Horling F, Kahmann U, Harris G, Schürmann P, and Dietz K-J. The plant-specific function

Downloaded by LI CO SA/50127/MI from www.liebertpub.com at 07/22/19. For personal use only.

of 2-Cys peroxiredoxin-mediated detoxification of peroxides in the redox-hierarchy of photosynthetic electron flux. *Proc Natl Acad Sci U S A* 99: 5738–5743, 2002.
267. König J, Lotte K, Plessow R, Brockhinke A, Baier M, and Dietz KJ. Reaction mechanism of plant 2-Cys peroxiredoxin. Role of the C terminus and the quaternary structure. *J Biol Chem* 278: 24409–24420, 2003.
268. Kovacs I, Holzmeister C, Wirtz M, Geerlof A, Fröhlich T, Römling G, Kuruthukulangarakoola GT, Linster E, Hell R, Arnold GJ, Durner J, and Lindermayr C. ROS-Mediated Inhibition of S-nitrosoglutathione Reductase Contributes to the Activation of Anti-oxidative Mechanisms. *Front Plant Sci* 7: 2016, 1669.
269. Kovacs I and Lindermayr C. Nitric oxide-based protein modification: formation and site-specificity of protein S-nitrosylation. *Front Plant Sci* 4: 137, 2013.
270. Krieger-Liszkay A and Trebst A. Tocopherol is the scavenger of singlet oxygen produced by the triplet states of chlorophyll in the PSII reaction centre. *J Exp Bot* 57: 1677–1684, 2006.
271. Kubienová L, Kopečný D, Tylichová M, Briozzo P, Skopalová J, Šebela M, Navrátil M, Tâche R, Luhová L, Barroso JB, and Petřivalský M. Structural and functional characterization of a plant S-nitrosoglutathione reductase from Solanum lycopersicum. *Biochimie* 95: 889–902, 2013.
272. Kwon E, Feechan A, Yun BW, Hwang BH, Pallas JA, Kang JG, and Loake GJ. AtGSNOR1 function is required for multiple developmental programs in Arabidopsis. *Planta* 236: 887–900, 2012.
273. La Camera S, L'Haridon F, Astier J, Zander M, Abou-Mansour E, Page G, Thurow C, Wendehenne D, Gatz C, Métraux JP, and Lamotte O. The glutaredoxin ATGRXS13 is required to facilitate *Botrytis cinerea* infection of *Arabidopsis thaliana* plants. *Plant J* 68: 507–519, 2011.
274. Lallement P-A, Brouwer B, Keech O, Hecker A, and Rouhier N. The still mysterious roles of cysteine-containing glutathione transferases in plants. *Front Pharmacol* 5: 192, 2014.
275. Laloi C, Rayapuram N, Chartier Y, Grienenberger J-M, Bonnard G, and Meyer Y. Identification and characterization of a mitochondrial thioredoxin system in plants. *Proc Natl Acad Sci U S A* 98: 14144–14149, 2001.
276. Laloi C, Stachowiak M, Pers-Kamczyc E, Warzych E, Murgia I, and Apel K. Cross-talk between singlet oxygen- and hydrogen peroxide-dependent signaling of stress responses in *Arabidopsis thaliana*. *Proc Natl Acad Sci U S A* 104: 672–677, 2007.
277. Lancelin JM, Guilhaudis L, Krimm I, Blackledge MJ, Marion D, and Jacquot JP. NMR structures of thioredoxin m from the green alga *Chlamydomonas reinhardtii*. *Proteins* 41: 334–349, 2000.
278. Laporte D, Olate E, Salinas P, Salazar M, Jordana X, and Holuigue L. Glutaredoxin GRXS13 plays a key role in protection against photooxidative stress in Arabidopsis. *J Exp Bot* 63: 503–515, 2012.
279. Latzko E, von Garnier R, and Gibbs M. Effect of photosynthesis, photosynthetic inhibitors and oxygen on the activity of ribulose 5-phosphate kinase. *Biochem Biophys Res Commun* 39: 1140–1144, 1970.
280. Laugier E, Tarrago L, Courteille A, Innocenti G, Eymery F, Rumeau D, Issakidis-Bourguet E, and Rey P. Involvement of thioredoxin y2 in the preservation of leaf methionine sulfoxide reductase capacity and growth under high light. *Plant Cell Environ* 36: 670–682, 2013.
281. Lee U, Wie C, Fernandez BO, Feelisch M, and Vierling E. Modulation of nitrosative stress by S-nitrosoglutathione reductase is critical for thermotolerance and plant growth in Arabidopsis. *Plant Cell* 20: 786–802, 2008.
282. Lehmann S, Serrano M, L'Haridon F, Tjamos SE, and Metraux J-P. Reactive oxygen species and plant resistance to fungal pathogens. *Phytochemistry* 112: 54–62, 2015.
283. Leichert LI, Gehrke F, Gudiseva HV, Blackwell T, Ilbert M, Walker AK, Strahler JR, Andrews PC, and Jakob U. Quantifying changes in the thiol redox proteome upon oxidative stress in vivo. *Proc Natl Acad Sci U S A* 105: 8197–8202, 2008.
284. Lemaire SD. The glutaredoxin family in oxygenic photosynthetic organisms. *Photosynth Res* 79: 305–318, 2004.
285. Lemaire SD, Guillon B, Le Maréchal P, Keryer E, Miginiac-Maslow M, and Decottignies P. New thioredoxin targets in the unicellular photosynthetic eukaryote *Chlamydomonas reinhardtii*. *Proc Natl Acad Sci U S A* 101: 7475–7480, 2004.
286. Lemaire SD, Michelet L, Zaffagnini M, Massot V, and Issakidis-Bourguet E. Thioredoxins in chloroplasts. *Curr Genet* 51: 343–365, 2007.
287. Lemaire SD and Miginiac-Maslow M. The thioredoxin superfamily in *Chlamydomonas reinhardtii*. *Photosynth Res* 82: 203–220, 2004.
288. Lennartz K, Plucken H, Seidler A, Westhoff P, Bechtold N, and Meierhoff K. HCF164 encodes a thioredoxin-like protein involved in the biogenesis of the cytochrome b (6)f complex in Arabidopsis. *Plant Cell* 13: 2539–2551, 2001.
289. Leonard SE, Reddie KG, and Carroll KS. Mining the thiol proteome for sulfenic acid modifications reveals new targets for oxidation in cells. *ACS Chem Biol* 4: 783–799, 2009.
290. Lepistö A, Pakula E, Toivola J, Krieger-Liszkay A, Vignols F, and Rintamäki E. Deletion of chloroplast NADPH-dependent thioredoxin reductase results in inability to regulate starch synthesis and causes stunted growth under short-day photoperiods. *J Exp Bot* 64: 3843–3854, 2013.
291. Li L, Cheng N, Hirschi KD, and Wang X. Structure of Arabidopsis chloroplastic monothiol glutaredoxin AtGRXcp. *Acta Crystallogr D Biol Crystallogr* 66: 725–732, 2010.
292. Li S, Zhu H, Wang J, Wang X, Li X, Ma C, Wen L, Yu B, Wang Y, Li J, and Wang PG. Comparative analysis of Cu(I)-catalyzed alkyne-azide cycloaddition (CuAAC) and strain-promoted alkyne-azide cycloaddition (SPAAC) in O-GlcNAc proteomics. *Electrophoresis* 37: 1431–1436, 2016.
293. Licausi F, Giorgi FM, Schmälzlin E, Usadel B, Perata P, van Dongen JT, and Geigenberger P. HRE-type genes are regulated by growth-related changes in internal oxygen concentrations during the normal development of potato (Solanum tuberosum) tubers. *Plant Cell Physiol* 52: 1957–1972, 2011.
294. Licausi F, Kosmacz M, Weits DA, Giuntoli B, Giorgi FM, Voesenek LA, Perata P, and van Dongen JT. Oxygen sensing in plants is mediated by an N-end rule pathway for protein destabilization. *Nature* 479: 419–422, 2011.
295. Lim CJ, Kim WB, Lee BS, Lee HY, Kwon TH, Park JM, and Kwon SY. Silencing of SlFTR-c, the catalytic subunit of ferredoxin:thioredoxin reductase, induces pathogenesis-

Downloaded by LI CO SA/50127/MI from www.liebertpub.com at 07/22/19. For personal use only.

related genes and pathogen resistance in tomato plants. *Biochem Biophys Res Commun* 399: 750–754, 2010.
296. Lin A, Wang Y, Tang J, Xue P, Li C, Liu L, Hu B, Yang F, Loake GJ, and Chu C. Nitric oxide and protein S-nitrosylation are integral to hydrogen peroxide-induced leaf cell death in rice. *Plant Physiol* 158: 451–464, 2012.
297. Lind C, Gerdes R, Hamnell Y, Schuppe-Koistinen I, von Löwenhielm HB, Holmgren A, and Cotgreave IA. Identification of S-glutathionylated cellular proteins during oxidative stress and constitutive metabolism by affinity purification and proteomic analysis. *Arch Biochem Biophys* 406: 229–240, 2002.
298. Lindahl M and Florencio FJ. Thioredoxin-linked processes in cyanobacteria are as numerous as in chloroplasts, but targets are different. *Proc Natl Acad Sci U S A* 100: 16107–16112, 2003.
299. Lindahl M, Mata-Cabana A, and Kieselbach T. The disulfide proteome and other reactive cysteine proteomes: analysis and functional significance. *Antioxid Redox Signal* 14: 2581–2642, 2011.
300. Lindermayr C. Crosstalk between reactive oxygen species and nitric oxide in plants: key role of S-nitrosoglutathione reductase. *Free Radic Biol Med* 122: 110–115, 2018.
301. Lindermayr C, Saalbach G, and Durner J. Proteomic identification of S-nitrosylated proteins in Arabidopsis. *Plant Physiol* 137: 921–930, 2005.
302. Liu CT and Benkovic SJ. Capturing a sulfenic acid with arylboronic acids and benzoxaborole. *J Am Chem Soc* 135: 14544–14547, 2013.
303. Liu L, Hausladen A, Zeng M, Que L, Heitman J, and Stamler JS. A metabolic enzyme for S-nitrosothiol conserved from bacteria to humans. *Nature* 410: 490–494, 2001.
304. Liu M, Hou J, Huang L, Huang X, Heibeck TH, Zhao R, Pasa-Tolic L, Smith RD, Li Y, Fu K, Zhang Z, Hinrichs SH, and Ding SJ. Site-specific proteomics approach for study protein S-nitrosylation. *Anal Chem* 82: 7160–7168, 2010.
305. Liu X, Liu S, Feng Y, Liu JZ, Chen Y, Pham K, Deng H, Hirschi KD, Wang X, and Cheng N. Structural insights into the N-terminal GIY-YIG endonuclease activity of Arabidopsis glutaredoxin AtGRXS16 in chloroplasts. *Proc Natl Acad Sci U S A* 110: 9565–9570, 2013.
306. Lo Conte M, Lin J, Wilson MA, and Carroll KS. A Chemical Approach for the Detection of Protein Sulfinylation. *ACS Chem Biol* 10: 1825–1830, 2015.
307. Longen S, Richter F, Köhler Y, Wittig I, Beck KF, and Pfeilschifter J. Quantitative Persulfide Site Identification (qPerS-SID) Reveals Protein Targets of H2S Releasing Donors in Mammalian Cells. *Sci Rep* 6: 29808, 2016.
308. Lu D, Wang T, Persson S, Mueller-Roeber B, and Schippers JHM. Transcriptional control of ROS homeostasis by KUODA1 regulates cell expansion during leaf development. *Nat Commun* 5: 3767, 2014.
309. Luo T, Fan T, Liu Y, Rothbart M, Yu J, Zhou S, Grimm B, and Luo M. Thioredoxin redox regulates ATPase activity of magnesium chelatase CHLI subunit and modulates redox-mediated signaling in tetrapyrrole biosynthesis and homeostasis of reactive oxygen species in pea plants. *Plant Physiol* 159: 118–130, 2012.
310. Lüthje S, Möller B, Perrineau FC, and Wöltje K. Plasma membrane electron pathways and oxidative stress. *Antioxid Redox Signal* 18: 2163–2183, 2013.
311. Maeda K, Finnie C, and Svensson B. Cy5 maleimide labelling for sensitive detection of free thiols in native protein extracts: identification of seed proteins targeted by barley thioredoxin h isoforms. *Biochem J* 378: 497–507, 2004.
312. Maeda K, Finnie C, and Svensson B. Identification of thioredoxin h-reducible disulphides in proteomes by differential labelling of cysteines: insight into recognition and regulation of proteins in barley seeds by thioredoxin h. *Proteomics* 5: 1634–1644, 2005.
313. Maeda K, Hägglund P, Finnie C, Svensson B, and Henriksen A. Structural basis for target protein recognition by the protein disulfide reductase thioredoxin. *Structure* 14: 1701–1710, 2006.
314. Maeda K, Hägglund P, Finnie C, Svensson B, and Henriksen A. Crystal structures of barley thioredoxin h isoforms HvTrxh1 and HvTrxh2 reveal features involved in protein recognition and possibly in discriminating the isoform specificity. *Protein Sci* 17: 1015–1024, 2008.
315. Mammarella ND, Cheng Z, Fu ZQ, Daudi A, Bolwell GP, Dong X, and Ausubel FM. Apoplastic peroxidases are required for salicylic acid-mediated defense against *Pseudomonas syringae*. *Phytochemistry* 112: 110–121, 2015.
316. Marchal C, Delorme-Hinoux V, Bariat L, Siala W, Belin C, Saez-Vasquez J, Riondet C, and Reichheld J-P. NTR/NRX define a new thioredoxin system in the nucleus of *Arabidopsis thaliana* cells. *Mol Plant* 7: 30–44, 2014.
317. Marchand C, Le Maréchal P, Meyer Y, and Decottignies P. Comparative proteomic approaches for the isolation of proteins interacting with thioredoxin. *Proteomics* 6: 6528–6537, 2006.
318. Marchand C, Le Maréchal P, Meyer Y, Miginiac-Maslow M, Issakidis-Bourguet E, and Decottignies P. New targets of Arabidopsis thioredoxins revealed by proteomic analysis. *Proteomics* 4: 2696–2706, 2004.
319. Marchand CH, Vanacker H, Collin V, Issakidis-Bourguet E, Maréchal PL, and Decottignies P. Thioredoxin targets in Arabidopsis roots. *Proteomics* 10: 2418–2428, 2010.
320. Marino SM and Gladyshev VN. Structural analysis of cysteine S-nitrosylation: a modified acid-based motif and the emerging role of trans-nitrosylation. *J Mol Biol* 395: 844–859, 2010.
321. Marino SM and Gladyshev VN. Proteomics: mapping reactive cysteines. *Nat Chem Biol* 7: 72–73, 2011.
322. Marri L, Zaffagnini M, Collin V, Issakidis-Bourguet E, Lemaire SD, Pupillo P, Sparla F, Miginiac-Maslow M, and Trost P. Prompt and easy activation by specific thioredoxins of Calvin cycle enzymes of *Arabidopsis thaliana* associated in the GAPDH/CP12/PRK supramolecular complex. *Mol Plant* 2: 259–269, 2009.
323. Martin BR and Cravatt BF. Large-scale profiling of protein palmitoylation in mammalian cells. *Nat Methods* 6: 135–138, 2009.
324. Marty L, Siala W, Schwarzlander M, Fricker MD, Wirtz M, Sweetlove LJ, Meyer Y, Meyer AJ, Reichheld J-P, and Hell R. The NADPH-dependent thioredoxin system constitutes a functional backup for cytosolic glutathione reductase in Arabidopsis. *Proc Natl Acad Sci U S A* 106: 9109–9114, 2009.
325. Marx C, Wong JH, and Buchanan BB. Thioredoxin and germinating barley: targets and protein redox changes. *Planta* 216: 454–460, 2003.
326. Mastrobuoni G, Irgang S, Pietzke M, Assmus HE, Wenzel M, Schulze WX, and Kempa S. Proteome dynamics and early salt stress response of the photosynthetic organism

Downloaded by LI CO SA/50127/MI from www.liebertpub.com at 07/22/19. For personal use only.

Downloaded by LI CO SA/50127/MI from www.liebertpub.com at 07/22/19. For personal use only.

Chlamydomonas reinhardtii. *BMC Genomics* 13: 215, 2012.
327. Mata-Pérez C, Begara-Morales JC, Chaki M, Sánchez-Calvo B, Valderrama R, Padilla MN, Corpas FJ, and Barroso JB. Protein tyrosine nitration during development and abiotic stress response in plants. *Front Plant Sci* 7: 1699, 2016.
328. Matern S, Peskan-Berghoefer T, Gromes R, Kiesel RV, and Rausch T. Imposed glutathione-mediated redox switch modulates the tobacco wound-induced protein kinase and salicylic acid-induced protein kinase activation state and impacts on defence against *Pseudomonas syringae*. *J Exp Bot* 66: 1935–1950, 2015.
329. Menchise V, Corbier C, Didierjean C, Saviano M, Benedetti E, Jacquot JP, and Aubry A. Crystal structure of the wild-type and D30A mutant thioredoxin h of *Chlamydomonas reinhardtii* and implications for the catalytic mechanism. *Biochem J* 359: 65–75, 2001.
330. Meng L, Wong JH, Feldman LJ, Lemaux PG, and Buchanan BB. A membrane-associated thioredoxin required for plant growth moves from cell to cell, suggestive of a role in intercellular communication. *Proc Natl Acad Sci U S A* 107: 3900–3905, 2010.
331. Merksamer PI, Trusina A, and Papa FR. Real-time redox measurements during endoplasmic reticulum stress reveal interlinked protein folding functions. *Cell* 135: 933–947, 2008.
332. Meyer AJ, Brach T, Marty L, Kreye S, Rouhier N, Jacquot JP, and Hell R. Redox-sensitive GFP in *Arabidopsis thaliana* is a quantitative biosensor for the redox potential of the cellular glutathione redox buffer. *Plant J* 52: 973–986, 2007.
333. Meyer AJ and Dick TP. Fluorescent protein-based redox probes. *Antioxid Redox Signal* 13: 621–650, 2010.
334. Meyer AJ, Riemer J, and Rouhier N. Oxidative protein folding: state-of-the-art and current avenues of research in plants. *New Phytol* 221: 1230–1246, 2019.
335. Meyer Y, Belin C, Delorme-Hinoux V, Reichheld JP, and Riondet C. Thioredoxin and glutaredoxin systems in plants: molecular mechanisms, crosstalks, and functional significance. *Antioxid Redox Signal* 17: 1124–1160, 2012.
336. Meyer Y, Siala W, Bashandy T, Riondet C, Vignols F, and Reichheld JP. Glutaredoxins and thioredoxins in plants. *Biochim Biophys Acta* 1783: 589–600, 2008.
337. Mhamdi A, Noctor G, and Baker A. Plant catalases: peroxisomal redox guardians. *Arch Biochem Biophys* 525: 181–194, 2012.
338. Michelet L, Zaffagnini M, Marchand C, Collin V, Decottignies P, Tsan P, Lancelin J-M, Trost P, Miginiac-Maslow M, Noctor G, and Lemaire SD. Glutathionylation of chloroplast thioredoxin f is a redox signaling mechanism in plants. *Proc Natl Acad Sci U S A* 102: 16478–16483, 2005.
339. Michelet L, Zaffagnini M, Morisse S, Sparla F, Pérez-Pérez ME, Francia F, Danon A, Marchand CH, Fermani S, Trost P, and Lemaire SD. Redox regulation of the Calvin-Benson cycle: something old, something new. *Front Plant Sci* 4: 470, 2013.
340. Michelet L, Zaffagnini M, Vanacker H, Le Maréchal P, Marchand C, Schroda M, Lemaire SD, and Decottignies P. In vivo targets of S-thiolation in *Chlamydomonas reinhardtii*. *J Biol Chem* 283: 21571–21578, 2008.
341. Mignolet-Spruyt L, Xu E, Idänheimo N, Hoeberichts FA, Mühlenbock P, Brosché M, Van Breusegem F, and Kangasjärvi J. Spreading the news: subcellular and organellar reactive oxygen species production and signalling. *J Exp Bot* 67: 3831–3844, 2016.
342. Mikkelsen R, Mutenda KE, Mant A, Schürmann P, and Blennow A. Alpha-glucan, water dikinase (GWD): a plastidic enzyme with redox-regulated and coordinated catalytic activity and binding affinity. *Proc Natl Acad Sci U S A* 102: 1785–1790, 2005.
343. Mishanina TV, Libiad M, and Banerjee R. Biogenesis of reactive sulfur species for signaling by hydrogen sulfide oxidation pathways. *Nat Chem Biol* 11: 457–464, 2015.
344. Mittard V, Blackledge MJ, Stein M, Jacquot JP, Marion D, and Lancelin JM. NMR solution structure of an oxidised thioredoxin h from the eukaryotic green alga *Chlamydomonas reinhardtii*. *Eur J Biochem* 243: 374–383, 1997.
345. Mittler R. ROS are good. *Trends Plant Sci* 22: 11–19, 2017.
346. Mittler R, Vanderauwera S, Suzuki N, Miller G, Tognetti VB, Vandepoele K, Gollery M, Shulaev V, and Van Breusegem F. ROS signaling: the new wave? *Trends Plant Sci* 16: 300–309, 2011.
347. Mock HP and Dietz KJ. Redox proteomics for the assessment of redox-related posttranslational regulation in plants. *Biochim Biophys Acta* 1864: 967–973, 2016.
348. Morgan B and Schwarzländer M. Fluoreszierende Proteinsensoren für die Redoxregulation in lebenden Zellen. *BIOspektrum* 22: 260–263, 2016.
349. Morisse S, Michelet L, Bedhomme M, Marchand CH, Calvaresi M, Trost P, Fermani S, Zaffagnini M, and Lemaire SD. Thioredoxin-dependent redox regulation of chloroplastic phosphoglycerate kinase from *Chlamydomonas reinhardtii*. *J Biol Chem* 289: 30012–30024, 2014.
350. Morisse S, Zaffagnini M, Gao XH, Lemaire SD, and Marchand CH. Insight into protein S-nitrosylation in *Chlamydomonas reinhardtii*. *Antioxid Redox Signal* 21: 1271–1284, 2014.
351. Moseler A, Aller I, Wagner S, Nietzel T, Przybyla-Toscano J, Mühlenhoff U, Lill R, Berndt C, Rouhier N, Schwarzländer M, and Meyer AJ. The mitochondrial monothiol glutaredoxin S15 is essential for iron–sulfur protein maturation in *Arabidopsis thaliana*. *Proc Natl Acad Sci U S A* 112: 13735–13740, 2015.
352. Motohashi K and Hisabori T. HCF164 receives the reducing equivalents from stroma thioredoxin across thylakoid membrane and mediates reduction of target proteins in thylakoid lumen. *J Biol Chem* 281: 35039–35047, 2006.
353. Motohashi K, Kondoh A, Stumpp MT, and Hisabori T. Comprehensive survey of proteins targeted by chloroplast thioredoxin. *Proc Natl Acad Sci U S A* 98: 11224–11229, 2001.
354. Mou Z, Fan W, and Dong X. Inducers of plant systemic acquired resistance regulate NPR1 function through redox changes. *Cell* 113: 935–944, 2003.
355. Mubarakshina MM, Ivanov BN, Naydov IA, Hillier W, Badger MR, and Krieger-Liszkay A. Production and diffusion of chloroplastic H2O2 and its implication to signalling. *J Exp Bot* 61: 3577–3587, 2010.
356. Mur LAJ, Mandon J, Persijn S, Cristescu SM, Moshkov IE, Novikova GV, Hall MA, Harren FJM, Hebelstrup KH, and Gupta KJ. Nitric oxide in plants: an assessment of the current state of knowledge. *AoB Plants* 5: pls052, 2013.

357. Murmu J, Bush MJ, DeLong C, Li S, Xu M, Khan M, Malcolmson C, Fobert PR, Zachgo S, and Hepworth SR. Arabidopsis basic leucine-zipper transcription factors TGA9 and TGA10 interact with floral glutaredoxins ROXY1 and ROXY2 and are redundantly required for anther development. *Plant Physiol* 154: 1492–1504, 2010.
358. Murphy MP. How mitochondria produce reactive oxygen species. *Biochem J* 417: 1–13, 2009.
359. Murray CI, Uhrigshardt H, O'Meally RN, Cole RN, and Van Eyk JE. Identification and quantification of S-nitrosylation by cysteine reactive tandem mass tag switch assay. *Mol Cell Proteom* 11: 013441, 2012.
360. Murray RW and Jindal SL. The photosensitized oxidation of disulfides related to cystine. *Photochem Photobiol* 16: 147–151, 1972.
361. Mustafa AK, Gadalla MM, Sen N, Kim S, Mu W, Gazi SK, Barrow RK, Yang G, Wang R, and Snyder SH. H2S signals through protein S-sulfhydration. *Sci Signal* 2: ra72, 2009.
362. Nagy P, Karton A, Betz A, Peskin AV, Pace P, O'Reilly RJ, Hampton MB, Radom L, and Winterbourn CC. Model for the exceptional reactivity of peroxiredoxins 2 and 3 with hydrogen peroxide: a kinetic and computational study. *J Biol Chem* 286: 18048–18055, 2011.
363. Naranjo B, Diaz-Espejo A, Lindahl M, and Cejudo FJ. Type-f thioredoxins have a role in the short-term activation of carbon metabolism and their loss affects growth under short-day conditions in *Arabidopsis thaliana*. *EXBOTJ* 67: 1951–1964, 2016.
364. Naranjo B, Mignée C, Krieger-Liszkay A, Hornero-Méndez D, Gallardo-Guerrero L, Cejudo FJ, and Lindahl M. The chloroplast NADPH thioredoxin reductase C, NTRC, controls non-photochemical quenching of light energy and photosynthetic electron transport in Arabidopsis. *Plant Cell Environ* 39: 804–822, 2016.
365. Nawrocki WJ, Tourasse NJ, Taly A, Rappaport F, and Wollman FA. The plastid terminal oxidase: its elusive function points to multiple contributions to plastid physiology. *Annu Rev Plant Biol* 66: 49–74, 2015.
366. Ndamukong I, Abdallat AA, Thurow C, Fode B, Zander M, Weigel R, and Gatz C. SA-inducible Arabidopsis glutaredoxin interacts with TGA factors and suppresses JA-responsive PDF1.2 transcription. *Plant J* 50, 128–139, 2007.
367. Née G, Zaffagnini M, Trost P, and Issakidis-Bourguet E. Redox regulation of chloroplastic glucose-6-phosphate dehydrogenase: a new role for f-type thioredoxin. *FEBS Lett* 583: 2827–2832, 2009.
368. Nelson KJ, Parsonage D, Hall A, Karplus PA, and Poole LB. Cysteine pK(a) values for the bacterial peroxiredoxin AhpC. *Biochemistry* 47: 12860–12868, 2008.
369. Nikitovic D and Holmgren A. S-nitrosoglutathione is cleaved by the thioredoxin system with liberation of glutathione and redox regulating nitric oxide. *J Biol Chem* 271: 19180–19185, 1996.
370. Nikkanen L, Toivola J, Diaz MG, and Rintamäki E. Chloroplast thioredoxin systems: prospects for improving photosynthesis. *Phil Trans R Soc B* 372: 20160474, 2017.
371. Nikkanen L, Toivola J, and Rintamäki E. Crosstalk between chloroplast thioredoxin systems in regulation of photosynthesis. *Plant Cell Environ* 39: 1691–1705, 2016.
372. Nilsson T, Mann M, Aebersold R, Yates JR, 3rd, Bairoch A, and Bergeron JJM. Mass spectrometry in high-throughput proteomics: ready for the big time. *Nat Methods* 7: 681–685, 2010.
373. Noctor G. Metabolic signalling in defence and stress: the central roles of soluble redox couples. *Plant Cell Environ* 29: 409–425, 2006.
374. Noctor G and Foyer CH. Intracellular Redox Compartmentation and ROS-Related Communication in Regulation and Signaling. *Plant Physiol* 171: 1581–1592, 2016.
375. Noctor G, Lelarge-Trouverie C, and Mhamdi A. The metabolomics of oxidative stress. *Phytochemistry* 112: 33–53, 2015.
376. Noctor G, Mhamdi A, and Foyer CH. Oxidative stress and antioxidative systems: recipes for successful data collection and interpretation. *Plant Cell Environ* 39: 1140–1160, 2016.
377. Noctor G, Reichheld JP, and Foyer CH. ROS-related redox regulation and signaling in plants. *Semin Cell Dev Biol* 80: 3–12, 2018.
378. Noctor G, Veljovic-Jovanovic S, Driscoll S, Novitskaya L, and Foyer CH. Drought and oxidative load in the leaves of C3 plants: a predominant role for photorespiration? *Ann Bot* 89: 841–850, 2002.
379. Nordstrand K, Åslund F, Holmgren A, Otting G, and Berndt KD. NMR structure of *Escherichia coli* glutaredoxin 3-glutathione mixed disulfide complex: implications for the enzymatic mechanism. *J Mol Biol* 286: 541–552, 1999.
380. Oelze M-L, Kandlbinder A, and Dietz K-J. Redox regulation and overreduction control in the photosynthesizing cell: complexity in redox regulatory networks. *Biochim Biophys Acta* 1780: 1261–1272, 2008.
381. Oger E, Marino D, Guigonis JM, Pauly N, and Puppo A. Sulfenylated proteins in the *Medicago truncatula-Sinorhizobium meliloti* symbiosis. *J Proteom* 75: 4102–4113, 2012.
382. Ojeda V, Pérez-Ruiz JM, González M, Nájera VA, Sahrawy M, Serrato AJ, Geigenberger P, and Cejudo FJ. NADPH Thioredoxin Reductase C and thioredoxins act concertedly in seedling development. *Plant Physiol* 174: 1436–1448, 2017.
383. Okegawa Y and Motohashi K. Chloroplastic thioredoxin m functions as a major regulator of Calvin cycle enzymes during photosynthesis in vivo. *Plant J* 84: 900–913, 2015.
384. Onda Y. Oxidative protein-folding systems in plant cells. *Int J Cell Biol* 2013: 1–15, 2013.
385. Ortega-Galisteo AP, Rodríguez-Serrano M, Pazmiño DM, Gupta DK, Sandalio LM, and Romero-Puertas MC. S-Nitrosylated proteins in pea (Pisum sativum L.) leaf peroxisomes: changes under abiotic stress. *J Exp Bot* 63: 2089–2103, 2012.
386. Ostergaard H, Henriksen A, Hansen FG, and Winther JR. Shedding light on disulfide bond formation: engineering a redox switch in green fluorescent protein. *EMBO J* 20: 5853–5862, 2001.
387. Østergaard H, Tachibana C, and Winther JR. Monitoring disulfide bond formation in the eukaryotic cytosol. *J Cell Biol* 166: 337–345, 2004.
388. Paige JS, Xu G, Stancevic B, and Jaffrey SR. Nitrosothiol reactivity profiling identifies S-nitrosylated proteins with unexpected stability. *Chem Biol* 15: 1307–1316, 2008.
389. Palmieri MC, Lindermayr C, Bauwe H, Steinhauser C, and Durner J. Regulation of plant glycine decarboxylase by s-nitrosylation and glutathionylation. *Plant Physiol* 152: 1514–1528, 2010.
390. Pan J and Carroll KS. Persulfide reactivity in the detection of protein s-sulfhydration. *ACS Chem Biol* 8: 1110–1116, 2013.

Downloaded by LI CO SA/50127/MI from www.liebertpub.com at 07/22/19. For personal use only.

Downloaded by LI CO SA/50127/MI from www.liebertpub.com at 07/22/19. For personal use only.

391. Pattison DI, Rahmanto AS, and Davies MJ. Photo-oxidation of proteins. *Photochem Photobiol Sci* 11: 38–53, 2012.
392. Paul BD and Snyder SH. H(2)S signalling through protein sulfhydration and beyond. *Nat Rev Mol Cell Biol* 13: 499–507, 2012.
393. Paul BD and Snyder SH. H2S: A Novel Gasotransmitter that Signals by Sulfhydration. *Trends Biochem Sci* 40: 687–700, 2015.
394. Paul MV, Iyer S, Amerhauser C, Lehmann M, van Dongen JT, and Geigenberger P. Oxygen Sensing via the Ethylene Response Transcription Factor RAP2.12 Affects Plant Metabolism and Performance under Both Normoxia and Hypoxia. *Plant Physiol* 172: 141–153, 2016.
395. Paulsen CE and Carroll KS. Cysteine-mediated redox signaling: chemistry, biology, and tools for discovery. *Chem Rev* 113: 4633–4679, 2013.
396. Paulsen CE, Truong TH, Garcia FJ, Homann A, Gupta V, Leonard SE, and Carroll KS. Peroxide-dependent sulfenylation of the EGFR catalytic site enhances kinase activity. *Nat Chem Biol* 8: 57–64, 2012.
397. Pedersen TA, Kirk M, and Bassham JA. Light-dark transients in levels of intermediate compounds during photosynthesis in air-adapted Chlorella. *Physiol Plant* 19: 219–231, 1966.
398. Pérez-Martín M, Blaby-Haas CE, Pérez-Pérez ME, Andrés-Garrido A, Blaby IK, Merchant SS, and Crespo JL. Activation of autophagy by metals in *Chlamydomonas reinhardtii*. *Eukaryot Cell* 14: 964–973, 2015.
399. Perez-Martin M, Perez-Perez ME, Lemaire SD, and Crespo JL. Oxidative stress contributes to autophagy induction in response to endoplasmic reticulum stress in *Chlamydomonas reinhardtii*. *Plant Physiol* 166: 997–1008, 2014.
400. Pérez-Pérez ME, Couso I, and Crespo JL. Carotenoid deficiency triggers autophagy in the model green alga *Chlamydomonas reinhardtii*. *Autophagy* 8: 376–388, 2012.
401. Pérez-Pérez ME, Florencio FJ, and Crespo JL. Inhibition of target of rapamycin signaling and stress activate autophagy in *Chlamydomonas reinhardtii*. *Plant Physiol* 152: 1874–1888, 2010.
402. Pérez-Pérez ME, Florencio FJ, and Lindahl M. Selecting thioredoxins for disulphide proteomics: target proteomes of three thioredoxins from the cyanobacterium *Synechocystis sp.* PCC 6803. *Proteomics* 6: S186–S195, 2006.
403. Pérez-Pérez ME, Lemaire SD, and Crespo JL. Reactive oxygen species and autophagy in plants and algae. *Plant Physiol* 160: 156–164, 2012.
404. Pérez-Pérez ME, Martín-Figueroa E, and Florencio FJ. Photosynthetic regulation of the cyanobacterium Synechocystis sp. PCC 6803 thioredoxin system and functional analysis of TrxB (Trx x) and TrxQ (Trx y) thioredoxins. *Mol Plant* 2: 270–283, 2009.
405. Pérez-Pérez ME, Mauriès A, Maes A, Tourasse NJ, Hamon M, Lemaire SD, and Marchand CH. The Deep Thioredoxome in *Chlamydomonas reinhardtii*: new insights into redox regulation. *Mol Plant* 10: 1107–1125, 2017.
406. Pérez-Pérez ME, Zaffagnini M, Marchand CH, Crespo JL, and Lemaire SD. The yeast autophagy protease Atg4 is regulated by thioredoxin. *Autophagy* 10: 1953–1964, 2014.
407. Pérez-Ruiz JM, Guinea M, Puerto-Galán L, and Cejudo FJ. NADPH thioredoxin reductase C is involved in redox regulation of the Mg-chelatase I subunit in *Arabidopsis thaliana* chloroplasts. *Mol Plant* 7: 1252–1255, 2014.
408. Pérez-Ruiz JM, Naranjo B, Ojeda V, Guinea M, and Cejudo FJ. NTRC-dependent redox balance of 2-Cys peroxiredoxins is needed for optimal function of the photosynthetic apparatus. *Proc Natl Acad Sci U S A* 114: 12069–12074, 2017.
409. Perez-Ruiz JM, Spinola MC, Kirchsteiger K, Moreno J, Sahrawy M, and Cejudo FJ. Rice NTRC is a high-efficiency redox system for chloroplast protection against oxidative damage. *Plant Cell* 18: 2356–2368, 2006.
410. Peterson FC, Lytle BL, Sampath S, Vinarov D, Tyler E, Shahan M, Markley JL, and Volkman BF. Solution structure of thioredoxin h1 from *Arabidopsis thaliana*. *Protein Sci* 14: 2195–2200, 2005.
411. Pierella Karlusich JJ, Zurbriggen MD, Shahinnia F, Sonnewald S, Sonnewald U, Hosseini SA, Hajirezaei MR, and Carrillo N. Chloroplast Redox Status Modulates Genome-Wide Plant Responses during the Non-host Interaction of Tobacco with the Hemibiotrophic Bacterium *Xanthomonas campestris* pv. vesicatoria. *Front Plant Sci* 8: 1158, 2017.
412. Plomion C, Aury JM, Amselem J, Leroy T, Murat F, Duplessis S, Faye S, Francillonne N, Labadie K, Le Provost G, Lesur I, Bartholomé J, Faivre-Rampant P, Kohler A, Leplé JC, Chantret N, Chen J, Diévart A, Alaeitabar T, Barbe V, Belser C, Bergès H, Bodénès C, Bogeat-Triboulot MB, Bouffaud ML, Brachi B, Chancerel E, Cohen D, Couloux A, Da Silva C, Dossat C, Ehrenmann F, Gaspin C, Grima-Pettenati J, Guichoux E, Hecker A, Herrmann S, Hugueney P, Hummel I, Klopp C, Lalanne C, Lascoux M, Lasserre E, Lemainque A, Desprez-Loustau ML, Luyten I, Madoui MA, Mangenot S, Marchal C, Maumus F, Mercier J, Michotey C, Panaud O, Picault N, Rouhier N, Rué O, Rustenholz C, Salin F, Soler M, Tarkka M, Velt A, Zanne AE, Martin F, Wincker P, Quesneville H, Kremer A, and Salse J. Oak genome reveals facets of long lifespan. *Nat Plants* 4: 440–452, 2018.
413. Poole LB, Klomsiri C, Knaggs SA, Furdui CM, Nelson KJ, Thomas MJ, Fetrow JS, Daniel LW, and King SB. Fluorescent and affinity-based tools to detect cysteine sulfenic acid formation in proteins. *Bioconjug Chem* 18: 2004–2017, 2007.
414. Poole LB and Schöneich C. Introduction: what we do and do not know regarding redox processes of thiols in signaling pathways. *Free Radic Biol Med* 80: 145–147, 2015.
415. Poole LB, Zeng BB, Knaggs SA, Yakubu M, and King SB. Synthesis of chemical probes to map sulfenic acid modifications on proteins. *Bioconjug Chem* 16: 1624–1628, 2005.
416. Poole TH, Reisz JA, Zhao W, Poole LB, Furdui CM, and King SB. Strained cycloalkynes as new protein sulfenic acid traps. *J Am Chem Soc* 136: 6167–6170, 2014.
417. Prescher JA and Bertozzi CR. Chemistry in living systems. *Nat Chem Biol* 1: 13–21, 2005.
418. Pucciariello C and Perata P. New insights into reactive oxygen species and nitric oxide signalling under low oxygen in plants. *Plant Cell Environ* 40: 473–482, 2017.
419. Pulido P, Spínola MC, Kirchsteiger K, Guinea M, Pascual MB, Sahrawy M, Sandalio LM, Dietz KJ, González M, and Cejudo FJ. Functional analysis of the pathways for 2-Cys peroxiredoxin reduction in *Arabidopsis thaliana* chloroplasts. *J Exp Bot* 61: 4043–4054, 2010.
420. Puyaubert J and Baudouin E. New clues for a cold case: nitric oxide response to low temperature. *Plant Cell Environ* 37: 2623–2630, 2014.

421. Puyaubert J, Fares A, Rézé N, Peltier JB, and Baudouin E. Identification of endogenously S-nitrosylated proteins in Arabidopsis plantlets: effect of cold stress on cysteine nitrosylation level. *Plant Sci* 215–216: 150–156, 2014.
422. Qu Z, Meng F, Bomgarden RD, Viner RI, Li J, Rogers JC, Cheng J, Greenlief CM, Cui J, Lubahn DB, Sun GY, and Gu Z. Proteomic quantification and site-mapping of S-nitrosylated proteins using isobaric iodoTMT reagents. *J Proteome Res* 13: 3200–3211, 2014.
423. Raja V, Majeed U, Kang H, Andrabi KI, and John R. Abiotic stress: interplay between ROS, hormones and MAPKs. *Environ Exp Bot* 137: 142–157, 2017.
424. Reddie KG and Carroll KS. Expanding the functional diversity of proteins through cysteine oxidation. *Curr Opin Chem Biol* 12: 746–754, 2008.
425. Reichheld JP, Meyer E, Khafif M, Bonnard G, and Meyer Y. AtNTRB is the major mitochondrial thioredoxin reductase in *Arabidopsis thaliana*. *FEBS Lett* 579: 337–342, 2005.
426. Reisz JA, Bechtold E, King SB, Poole LB, and Furdui CM. Thiol-blocking electrophiles interfere with labeling and detection of protein sulfenic acids. *FEBS J* 280: 6150–6161, 2013.
427. Rey P, Becuwe N, Tourrette S, and Rouhier N. Involvement of Arabidopsis glutaredoxin S14 in the maintenance of chlorophyll content. *Plant Cell Environ* 40: 2319–2332, 2017.
428. Ribeiro CW, Baldacci-Cresp F, Pierre O, Larousse M, Benyamina S, Lambert A, Hopkins J, Castella C, Cazareth J, Alloing G, Boncompagni E, Couturier J, Mergaert P, Gamas P, Rouhier N, Montrichard F, and Frendo P. Regulation of differentiation of nitrogen-fixing bacteria by microsymbiont targeting of plant thioredoxin s1. *Curr Biol* 27: 250–256, 2017.
429. Richter AS, Peter E, Rothbart M, Schlicke H, Toivola J, Rintamaki E, and Grimm B. Posttranslational Influence of NADPH-Dependent Thioredoxin Reductase C on Enzymes in Tetrapyrrole Synthesis. *Plant Physiol* 162: 63–73, 2013.
430. Riemer J, Bulleid N, and Herrmann JM. Disulfide formation in the ER and mitochondria: two solutions to a common process. *Science* 324: 1284–1287, 2009.
431. Riondet C, Desouris JP, Montoya JG, Chartier Y, Meyer Y, and Reichheld J-P. A dicotyledon-specific glutaredoxin GRXC1 family with dimer-dependent redox regulation is functionally redundant with GRXC2. *Plant Cell Environ* 35: 360–373, 2012.
432. Romero-Puertas MC, Campostrini N, Mattè A, Righetti PG, Perazzolli M, Zolla L, Roepstorff P, and Delledonne M. Proteomic analysis of S-nitrosylated proteins in *Arabidopsis thaliana* undergoing hypersensitive response. *Proteomics* 8: 1459–1469, 2008.
433. Romero JM and Bizzozero OA. Intracellular glutathione mediates the denitrosylation of protein nitrosothiols in the rat spinal cord. *J Neurosci Res* 87: 701–709, 2009.
434. Roos G, Foloppe N, and Messens J. Understanding the pKa of redox cysteines: the key role of hydrogen bonding. *Antioxid Redox Signal* 18: 94–127, 2013.
435. Roos G, Loverix S, and Geerlings P. Origin of the pKa Perturbation of N-Terminal Cysteine in α-and 310-Helices: A Computational DFT Study. *J Phys Chem B* 110: 557–562, 2006.
436. Rosenwasser S, Graff van Creveld S, Schatz D, Malitsky S, Tzfadia O, Aharoni A, Levin Y, Gabashvili A, Feldmesser E, and Vardi A. Mapping the diatom redox-sensitive proteome provides insight into response to nitrogen stress in the marine environment. *Proc Natl Acad Sci U S A* 111: 2740–2745, 2014.
437. Rosenwasser S, Rot I, Sollner E, Meyer AJ, Smith Y, Leviatan N, Fluhr R, and Friedman H. Organelles contribute differentially to reactive oxygen species-related events during extended darkness. *Plant Physiol* 156: 185–201, 2011.
438. Rouhier N, Cerveau D, Couturier J, Reichheld JP, and Rey P. Involvement of thiol-based mechanisms in plant development. *Biochim Biophys Acta* 1850: 1479–1496, 2015.
439. Rouhier N, Gelhaye E, and Jacquot J-P. Plant glutaredoxins: still mysterious reducing systems. *Cell Mol Life Sci* 61: 1266–1277, 2004.
440. Rouhier N, Lemaire SD, and Jacquot JP. The role of glutathione in photosynthetic organisms: emerging functions for glutaredoxins and glutathionylation. *Annu Rev Plant Biol* 59: 143–166, 2008.
441. Rouhier N, Unno H, Bandyopadhyay S, Masip L, Kim SK, Hirasawa M, Gualberto JM, Lattard V, Kusunoki M, Knaff DB, Georgiou G, Hase T, Johnson MK, and Jacquot JP. Functional, structural, and spectroscopic characterization of a glutathione-ligated [2Fe-2S] cluster in poplar glutaredoxin C1. *Proc Natl Acad Sci U S A* 104: 7379–7384, 2007.
442. Ruban AV. Nonphotochemical chlorophyll fluorescence quenching: mechanism and effectiveness in protecting plants from photodamage. *Plant Physiol* 170: 1903–1916, 2016.
443. Rusterucci C, Espunya MC, Diaz M, Chabannes M, and Martinez MC. S-nitrosoglutathione reductase affords protection against pathogens in Arabidopsis, both locally and systemically. *Plant Physiol* 143: 1282–1292, 2007.
444. Saarinen M, Gleason FK, and Eklund H. Crystal structure of thioredoxin-2 from Anabaena. *Structure* 3: 1097–1108, 1995.
445. Samarasinghe KTG, Munkanatta Godage DNP, VanHecke GC, and Ahn YH. Metabolic synthesis of clickable glutathione for chemoselective detection of glutathionylation. *J Am Chem Soc* 136: 11566–11569, 2014.
446. Samarasinghe KTG, Munkanatta Godage DNP, Zhou Y, Ndombera FT, Weerapana E, and Ahn YH. A clickable glutathione approach for identification of protein glutathionylation in response to glucose metabolism. *Mol Biosyst* 12: 2471–2480, 2016.
447. Scheibe R. Malate valves to balance cellular energy supply. *Physiol Plant* 120: 21–26, 2004.
448. Scheibe R and Anderson LE. Dark modulation of NADP-dependent malate dehydrogenase and glucose-6-phosphate dehydrogenase in the chloroplast. *Biochim Biophys Acta* 636: 58–64, 1981.
449. Scheibe R and Dietz KJ. Reduction-oxidation network for flexible adjustment of cellular metabolism in photoautotrophic cells. *Plant Cell Environ* 35: 202–216, 2012.
450. Scheler C, Durner J, and Astier J. Nitric oxide and reactive oxygen species in plant biotic interactions. *Curr Opin Plant Biol* 16: 534–539, 2013.
451. Schippers JHM, Foyer CH, and van Dongen JT. Redox regulation in shoot growth, SAM maintenance and flowering. *Curr Opin Plant Biol* 29: 121–128, 2016.
452. Schmidt R and Schippers JHM. ROS-mediated redox signaling during cell differentiation in plants. *Biochim Biophys Acta* 1850: 1497–1508, 2015.

Downloaded by LI CO SA/50127/MI from www.liebertpub.com at 07/22/19. For personal use only.

453. Schöneich C. Methionine oxidation by reactive oxygen species: reaction mechanisms and relevance to Alzheimer's disease. *Biochim Biophys Acta* 1703: 111–119, 2005.
454. Schöneich C. Mechanisms of protein damage induced by cysteine thiyl radical formation. *Chem Res Toxicol* 21: 1175–1179, 2008.
455. Schürmann P and Buchanan BB. Role of ferredoxin in the activation of sedoheptulose diphosphatase in isolated chloroplasts. *Biochim Biophys Acta* 376: 189–192, 1975.
456. Schürmann P and Buchanan BB. The ferredoxin/thioredoxin system of oxygenic photosynthesis. *Antioxid Redox Signal* 10: 1235–1274, 2008.
457. Schürmann P, Wolosiuk RA, Breazeale VD, and Buchanan BB. Two proteins function in the regulation of photosynthetic CO2 assimilation in chloroplasts. *Nature* 263: 257–258, 1976.
458. Schwarzländer M, Dick TP, Meyer AJ, and Morgan B. Dissecting Redox Biology Using Fluorescent Protein Sensors. *Antioxid Redox Signal* 24: 680–712, 2016.
459. Schwarzländer M, Fricker MD, Müller C, Marty L, Brach T, Novak J, Sweetlove LJ, Hell R, and Meyer AJ. Confocal imaging of glutathione redox potential in living plant cells. *J Microsc* 231: 299–316, 2008.
460. Schwarzländer M, Fricker MD, and Sweetlove LJ. Monitoring the in vivo redox state of plant mitochondria: effect of respiratory inhibitors, abiotic stress and assessment of recovery from oxidative challenge. *Biochim Biophys Acta* 1787: 468–475, 2009.
461. Scuffi D, Nietzel T, Di Fino LM, Meyer AJ, Lamattina L, Schwarzländer M, Laxalt AM, and García-Mata C. Hydrogen sulfide increases production of NADPH oxidase-dependent hydrogen peroxide and phospholipase D-derived phosphatidic acid in guard cell signaling. *Plant Physiol* 176: 2532–2542, 2018.
462. Sehrawat A, Abat JK, and Deswal R. RuBisCO depletion improved proteome coverage of cold responsive S-nitrosylated targets in *Brassica juncea*. *Front Plant Sci* 4: 342, 2013.
463. Sehrawat A and Deswal R. S-nitrosylation analysis in *Brassica juncea* apoplast highlights the importance of nitric oxide in cold-stress signaling. *J Proteome Res* 13: 2599–2619, 2014.
464. Selga T, Selga M, and Ozoliņa A. Plastid-nuclear complexes in the photosynthesizing cells from their mitosis up to programmed death. *Photosynthetica* 51: 474–476, 2013.
465. Selles B, Jacquot JP, and Rouhier N. Comparative genomic study of protein disulfide isomerases from photosynthetic organisms. *Genomics* 97: 37–50, 2011.
466. Seo YH and Carroll KS. Profiling protein thiol oxidation in tumor cells using sulfenic acid-specific antibodies. *Proc Natl Acad Sci U S A* 106: 16163–16168, 2009.
467. Serrano I, Audran C, and Rivas S. Chloroplasts at work during plant innate immunity. *J Exp Bot* 67: 3845–3854, 2016.
468. Serrato AJ, Pérez-Ruiz JM, Spínola MC, and Cejudo FJ. A novel NADPH thioredoxin reductase, localized in the chloroplast, which deficiency causes hypersensitivity to abiotic stress in *Arabidopsis thaliana*. *J Biol Chem* 279: 43821–43827, 2004.
469. Seth D and Stamler JS. The SNO-proteome: causation and classifications. *Curr Opin Chem Biol* 15: 129–136, 2011.
470. Sethuraman M, McComb ME, Heibeck T, Costello CE, and Cohen RA. Isotope-coded affinity tag approach to identify and quantify oxidant-sensitive protein thiols. *Mol Cell Proteom* 3: 273–278, 2004.
471. Sevilla F, Camejo D, Ortiz-Espín A, Calderón A, Lázaro JJ, and Jiménez A. The thioredoxin/peroxiredoxin/sulfiredoxin system: current overview on its redox function in plants and regulation by reactive oxygen and nitrogen species. *J Exp Bot* 66: 2945–2955, 2015.
472. Sewelam N, Kazan K, and Schenk PM. Global Plant Stress Signaling: Reactive Oxygen Species at the Cross-Road. *Front Plant Sci* 7: 187, 2016.
473. Shaikhali J, Heiber I, Seidel T, Stroher E, Hiltscher H, Birkmann S, Dietz KJ, and Baier M. The redox-sensitive transcription factor Rap2.4a controls nuclear expression of 2-Cys peroxiredoxin A and other chloroplast antioxidant enzymes. *BMC Plant Biol* 8: 48, 2008.
474. Shakir S, Vinh J, and Chiappetta G. Quantitative analysis of the cysteine redoxome by iodoacetyl tandem mass tags. *Anal Bioanal Chem* 409: 3821–3830, 2017.
475. Simionato D, Basso S, Zaffagnini M, Lana T, Marzotto F, Trost P, and Morosinotto T. Protein redox regulation in the thylakoid lumen: the importance of disulfide bonds for violaxanthin de-epoxidase. *FEBS Lett* 589: 919–923, 2015.
476. Skryhan K, Gurrieri L, Sparla F, Trost P, and Blennow A. Redox Regulation of Starch Metabolism. *Front Plant Sci* 9: 2018, 1344.
477. Sonntag C. *The Chemical Basis of Radiation Biology*. London: Taylor & Francis, 1987.
478. Sparla F, Costa A, Lo Schiavo F, Pupillo P, and Trost P. Redox regulation of a novel plastid-targeted beta-amylase of Arabidopsis. *Plant Physiol* 141: 840–850, 2006.
479. Sparla F, Pupillo P, and Trost P. The C-terminal extension of glyceraldehyde-3-phosphate dehydrogenase subunit B acts as an autoinhibitory domain regulated by thioredoxins and nicotinamide adenine dinucleotide. *J Biol Chem* 277: 44946–44952, 2002.
480. Sparla F, Zaffagnini M, Wedel N, Scheibe R, Pupillo P, and Trost P. Regulation of photosynthetic GAPDH dissected by mutants. *Plant Physiol* 138: 2210–2219, 2005.
481. Ströher E, Grassl J, Carrie C, Fenske R, Whelan J, and Millar AH. Glutaredoxin S15 is involved in Fe-S cluster transfer in mitochondria influencing lipoic acid-dependent enzymes, plant growth and arsenic tolerance in Arabidopsis. *Plant Physiol* 170: 1284–1299, 2015.
482. Subramani J, Kundumani-Sridharan V, Hilgers RHP, Owens C, and Das KC. Thioredoxin Uses a GSH-independent Route to Deglutathionylate Endothelial Nitric-oxide Synthase and Protect against Myocardial Infarction. *J Biol Chem* 291: 23374–23389, 2016.
483. Sullivan DM, Wehr NB, Fergusson MM, Levine RL, and Finkel T. Identification of oxidant-sensitive proteins: TNF-alpha induces protein glutathiolation. *Biochemistry* 39: 11121–11128, 2000.
484. Suzuki N, Miller G, Morales J, Shulaev V, Torres MA, and Mittler R. Respiratory burst oxidases: the engines of ROS signaling. *Curr Opin Plant Biol* 14: 691–699, 2011.
485. Szabó C. Hydrogen sulphide and its therapeutic potential. *Nat Rev Drug Discov* 6: 917–935, 2007.
486. Szabó C, Ischiropoulos H, and Radi R. Peroxynitrite: biochemistry, pathophysiology and development of therapeutics. *Nat Rev Drug Discov* 6: 662–680, 2007.
487. Tada Y, Spoel SH, Pajerowska-Mukhtar K, Mou Z, Song J, Wang C, Zuo J, and Dong X. Plant immunity requires conformational changes [corrected] of NPR1 via S-

Downloaded by LI CO SA/50127/MI from www.liebertpub.com at 07/22/19. For personal use only.

Downloaded by LI CO SA/50127/MI from www.liebertpub.com at 07/22/19. For personal use only.

nitrosylation and thioredoxins. *Science* 321: 952–956, 2008.
488. Takahashi H, Kopriva S, Giordano M, Saito K, and Hell R. Sulfur assimilation in photosynthetic organisms: molecular functions and regulations of transporters and assimilatory enzymes. *Annu Rev Plant Biol* 62: 157–184, 2011.
489. Takanishi CL, Ma LH, and Wood MJ. A genetically encoded probe for cysteine sulfenic acid protein modification in vivo. *Biochemistry* 46: 14725–14732, 2007.
490. Takanishi CL and Wood MJ. A genetically encoded probe for the identification of proteins that form sulfenic acid in response to H_2O_2 in *Saccharomyces cerevisiae*. *J Proteome Res* 10: 2715–2724, 2011.
491. Tanou G, Filippou P, Belghazi M, Job D, Diamantidis G, Fotopoulos V, and Molassiotis A. Oxidative and nitrosative-based signaling and associated post-translational modifications orchestrate the acclimation of citrus plants to salinity stress. *Plant J* 72: 585–599, 2012.
492. Tanou G, Ziogas V, Belghazi M, Christou A, Filippou P, Job D, Fotopoulos V, and Molassiotis A. Polyamines reprogram oxidative and nitrosative status and the proteome of citrus plants exposed to salinity stress. *Plant Cell Environ* 37: 864–885, 2014.
493. Tao R, Zhao Y, Chu H, Wang A, Zhu J, Chen X, Zou Y, Shi M, Liu R, Su N, Du J, Zhou HM, Zhu L, Qian X, Liu H, Loscalzo J, and Yang Y. Genetically encoded fluorescent sensors reveal dynamic regulation of NADPH metabolism. *Nat Methods* 14: 720–728, 2017.
494. Tarrago L, Laugier E, Zaffagnini M, Marchand C, Le Maréchal P, Rouhier N, Lemaire SD, and Rey P. Regeneration mechanisms of *Arabidopsis thaliana* methionine sulfoxide reductases B by glutaredoxins and thioredoxins. *J Biol Chem* 284: 18963–18971, 2009.
495. Tarrago L, Laugier E, Zaffagnini M, Marchand CH, Le Maréchal P, Lemaire SD, and Rey P. Plant thioredoxin CDSP32 regenerates 1-cys methionine sulfoxide reductase B activity through the direct reduction of sulfenic acid. *J Biol Chem* 285: 14964–14972, 2010.
496. Teo CF and Wells L. Monitoring protein O-linked beta-N-acetylglucosamine status via metabolic labeling and copper-free click chemistry. *Anal Biochem* 464: 70–72, 2014.
497. Terrile MC, París R, Calderón-Villalobos LIA, Iglesias MJ, Lamattina L, Estelle M, and Casalongué CA. Nitric oxide influences auxin signaling through S-nitrosylation of the Arabidopsis TRANSPORT INHIBITOR RESPONSE 1 auxin receptor. *Plant J* 70: 492–500, 2012.
498. Thormählen I, Meitzel T, Groysman J, Öchsner AB, von Roepenack-Lahaye E, Naranjo B, Cejudo FJ, and Geigenberger P. Thioredoxin f1 and NADPH-Dependent Thioredoxin Reductase C have overlapping functions in regulating photosynthetic metabolism and plant growth in response to varying light conditions. *Plant Physiol* 169: 1766–1786, 2015.
499. Thormählen I, Naranjo B, Trujillo-Hernandez JA, Reichheld J-P, Cejudo FJ, and Geigenberger P. On the Elaborate Network of Thioredoxins in Higher Plants. In: *Progress in Botany*, edited by Cánovas FM, Lüttge U, and Matyssek R. Berlin, Heidelberg: Springer, 2018.
500. Thormählen I, Ruber J, Von Roepenack-Lahaye E, Ehrlich S-M, Massot V, Hümmer C, Tezycka J, Issakidis-Bourguet E, and Geigenberger P. Inactivation of thioredoxin f1 leads to decreased light activation of ADP-glucose pyrophosphorylase and altered diurnal starch turnover in leaves of Arabidopsis plants. *Plant Cell Environ* 36: 16–29, 2013.
501. Thormählen I, Zupok A, Rescher J, Leger J, Weissenberger S, Groysman J, Orwat A, Chatel-Innocenti G, Issakidis-Bourguet E, Armbruster U, and Geigenberger P. Thioredoxins play a crucial role in dynamic acclimation of photosynthesis in fluctuating light. *Mol Plant* 10: 168–182, 2017.
502. Thurlkill RL, Grimsley GR, Scholtz JM, and Pace CN. pK values of the ionizable groups of proteins. *Protein Sci* 15: 1214–1218, 2006.
503. Tikhonov AN. pH-dependent regulation of electron transport and ATP synthesis in chloroplasts. *Photosynth Res* 116: 511–534, 2013.
504. Tognetti VB, Bielach A, and Hrtyan M. Redox regulation at the site of primary growth: auxin, cytokinin and ROS crosstalk. *Plant Cell Environ* 40: 2586–2605, 2017.
505. Toohey JI. Sulfur signaling: is the agent sulfide or sulfane? *Anal Biochem* 413: 1–7, 2011.
506. Trapet P, Kulik A, Lamotte O, Jeandroz S, Bourque S, Nicolas-Francès V, Rosnoblet C, Besson-Bard A, and Wendehenne D. NO signaling in plant immunity: a tale of messengers. *Phytochemistry* 112: 72–79, 2015.
507. Traverso JA, Micalella C, Martinez A, Brown SC, Satiat-Jeunemaître B, Meinnel T, and Giglione C. Roles of N-terminal fatty acid acylations in membrane compartment partitioning: arabidopsis h-type thioredoxins as a case study. *Plant Cell* 25: 1056–1077, 2013.
508. Trost P, Fermani S, Calvaresi M, and Zaffagnini M. Biochemical basis of sulphenomics: how protein sulphenic acids may be stabilized by the protein microenvironment. *Plant Cell Environ* 40: 483–490, 2017.
509. van Dongen JT and Licausi F. Oxygen sensing and signaling. *Annu Rev Plant Biol* 66: 345–367, 2015.
510. Vandenabeele S, Vanderauwera S, Vuylsteke M, Rombauts S, Langebartels C, Seidlitz HK, Zabeau M, Van Montagu M, Inzé D, and Van Breusegem F. Catalase deficiency drastically affects gene expression induced by high light in *Arabidopsis thaliana*. *Plant J* 39: 45–58, 2004.
511. Vandiver MS, Paul BD, Xu R, Karuppagounder S, Rao F, Snowman AM, Ko HS, Lee YI, Dawson VL, Dawson TM, Sen N, and Snyder SH. Sulfhydration mediates neuroprotective actions of parkin. *Nat Commun* 4, 1626, 2013.
512. Vanzo E, Ghirardo A, Merl-Pham J, Lindermayr C, Heller W, Hauck SM, Durner J, and Schnitzler JP. S-nitrosoproteome in poplar leaves in response to acute ozone stress. *PLoS One* 9: e106886, 2014.
513. Verma PK, Verma S, Pande V, Mallick S, Deo Tripathi R, Dhankher OP, and Chakrabarty D. Overexpression of rice glutaredoxin OsGrx_C7 and OsGrx_C2. 1 reduces intracellular arsenic accumulation and increases tolerance in *Arabidopsis thaliana*. *Front Plant Sci* 7: 740, 2016.
514. Vernoux T, Wilson RC, Seeley KA, Reichheld JP, Muroy S, Brown S, Maughan SC, Cobbett CS, Van Montagu M, Inze D, May MJ, and Sung ZR. The ROOT MERISTEMLESS1/CADMIUM SENSITIVE2 gene defines a glutathione-dependent pathway involved in initiation and maintenance of cell division during postembryonic root development. *Plant Cell* 12: 97–110, 2000.
515. Vescovi M, Zaffagnini M, Festa M, Trost P, Lo Schiavo F, and Costa A. Nuclear accumulation of cytosolic glyceraldehyde-3-phosphate dehydrogenase in cadmium-stressed Arabidopsis roots. *Plant Physiol* 162: 333–346, 2013.
516. Vetoshkina DV, Ivanov BN, Khorobrykh SA, Proskuryakov II, and Borisova-Mubarakshina MM. Involvement

of the chloroplast plastoquinone pool in the Mehler reaction. *Physiol Plant* 161: 45–55, 2017.
517. Vieira Dos Santos C, Cuine S, Rouhier N, and Rey P. The Arabidopsis plastidic methionine sulfoxide reductase B proteins. Sequence and activity characteristics, comparison of the expression with plastidic methionine sulfoxide reductase A, and induction by photooxidative stress. *Plant Physiol* 138: 909–922, 2005.
518. Vogel MO, Moore M, König K, Pecher P, Alsharafa K, Lee J, and Dietz K-J. Fast Retrograde Signaling in Response to High Light Involves Metabolite Export, Mitogen-Activated Protein Kinase 6, and AP2/ERF Transcription Factors in Arabidopsis. *Plant Cell* 26: 1151–1165, 2014.
519. von Sonntag C. Free-radical reactions involving thiols and disulphides. In: *Sulfur-Centered Reactive Intermediates in Chemistry and Biology*, edited by Chatgilialoglu C, and Asmus KD. Berlin: Springer, 1990, pp. 359–366.
520. Wang H and Xian M. Chemical methods to detect S-nitrosation. *Curr Opin Chem Biol* 15: 32–37, 2011.
521. Wang L, Li Y, Jacquot JP, Rouhier N, and Xia B. Characterization of poplar GrxS14 in different structural forms. *Protein Cell* 5: 329–333, 2014.
522. Wang P, Du Y, Hou YJ, Zhao Y, Hsu CC, Yuan F, Zhu X, Tao WA, Song CP, and Zhu JK. Nitric oxide negatively regulates abscisic acid signaling in guard cells by S-nitrosylation of OST1. *Proc Natl Acad Sci U S A* 112: 613–618, 2015.
523. Wang P, Liu J, Liu B, Feng D, Da Q, Wang P, Shu S, Su J, Zhang Y, Wang J, and Wang H-B. Evidence for a role of chloroplastic m-type thioredoxins in the biogenesis of photosystem II in arabidopsis. *Plant Physiol* 163: 1710–1728, 2013.
524. Wang W, He E, Chen J, Guo Y, Chen J, Liu X, and Zheng H. The reduced state of the plastoquinone pool is required for chloroplast-mediated stomatal closure in response to calcium stimulation. *Plant J* 86: 132–144, 2016.
525. Wang Y, Liu T, Wu C, and Li H. A strategy for direct identification of protein S-nitrosylation sites by quadrupole time-of-flight mass spectrometry. *J Am Soc Mass Spectrom* 19: 1353–1360, 2008.
526. Wang Z, Xing S, Birkenbihl RP, and Zachgo S. Conserved functions of arabidopsis and rice CC-type glutaredoxins in flower development and pathogen response. *Mol Plant* 2: 323–335, 2009.
527. Waszczak C, Akter S, Eeckhout D, Persiau G, Wahni K, Bodra N, Van Molle I, De Smet B, Vertommen D, Gevaert K, De Jaeger G, Van Montagu M, Messens J, and Van Breusegem F. Sulfenome mining in *Arabidopsis thaliana*. *Proc Natl Acad Sci U S A* 111: 11545–11550, 2014.
528. Waszczak C, Akter S, Jacques S, Huang J, Messens J, and Van Breusegem F. Oxidative post-translational modifications of cysteine residues in plant signal transduction. *J Exp Bot* 66: 2923–2934, 2015.
529. Wedel N and Soll J. Evolutionary conserved light regulation of Calvin cycle activity by NADPH-mediated reversible phosphoribulokinase/CP12/ glyceraldehyde-3-phosphate dehydrogenase complex dissociation. *Proc Natl Acad Sci U S A* 95: 9699–9704, 1998.
530. Weerapana E, Wang C, Simon GM, Richter F, Khare S, Dillon MBD, Bachovchin DA, Mowen K, Baker D, and Cravatt BF. Quantitative reactivity profiling predicts functional cysteines in proteomes. *Nature* 468: 790–795, 2010.
531. Weits DA, Giuntoli B, Kosmacz M, Parlanti S, Hubberten HM, Riegler H, Hoefgen R, Perata P, Van Dongen JT, and Licausi F. Plant cysteine oxidases control the oxygen-dependent branch of the N-end-rule pathway. *Nat Commun* 5: 3425, 2014.
532. White MD, Kamps JJAG, East S, Taylor Kearney LJ, and Flashman E. The plant cysteine oxidases from *Arabidopsis thaliana* are kinetically tailored to act as oxygen sensors. *J Biol Chem* 293: 11786–11795, 2018.
533. White MD, Klecker M, Hopkinson RJ, Weits DA, Mueller C, Naumann C, O'Neill R, Wickens J, Yang J, Brooks-Bartlett JC, Garman EF, Grossmann TN, Dissmeyer N, and Flashman E. Plant cysteine oxidases are dioxygenases that directly enable arginyl transferase-catalysed arginylation of N-end rule targets. *Nat Commun* 8: 14690, 2017.
534. Whiteman M and Moore PK. Hydrogen sulfide and the vasculature: a novel vasculoprotective entity and regulator of nitric oxide bioavailability? *J Cell Mol Med* 13: 488–507, 2009.
535. Wimmelbacher M and Börnke F. Redox activity of thioredoxin z and fructokinase-like protein 1 is dispensable for autotrophic growth of *Arabidopsis thaliana*. *J Exp Bot* 65: 2405–2413, 2014.
536. Winterbourn CC and Hampton MB. Thiol chemistry and specificity in redox signaling. *Free Radic Biol Med* 45: 549–561, 2008.
537. Winterbourn CC and Metodiewa D. Reactivity of biologically important thiol compounds with superoxide and hydrogen peroxide. *Free Radic Biol Med* 27: 322–328, 1999.
538. Wolosiuk RA and Buchanan BB. Thioredoxin and glutathione regulate photosynthesis in chloroplasts. *Nature* 266: 565–567, 1977.
539. Wolosiuk RA and Buchanan BB. Activation of Chloroplast NADP-linked Glyceraldehyde-3-Phosphate Dehydrogenase by the Ferredoxin/Thioredoxin System. *Plant Physiol* 61: 669–671, 1978.
540. Wolosiuk RA and Buchanan BB. Regulation of chloroplast phosphoribulokinase by the ferredoxin/thioredoxin system. *Arch Biochem Biophys* 189: 97–101, 1978.
541. Wolosiuk RA, Buchanan BB, and Crawford NA. Regulation of NADP-malate dehydrogenase by the light-actuated ferredoxin/thioredoxin system of chloroplasts. *FEBS Lett* 81: 253–258, 1977.
542. Wong JH, Balmer Y, Cai N, Tanaka CK, Vensel WH, Hurkman WJ, and Buchanan BB. Unraveling thioredoxin-linked metabolic processes of cereal starchy endosperm using proteomics. *FEBS Lett* 547: 151–156, 2003.
543. Wong JH, Cai N, Balmer Y, Tanaka CK, Vensel WH, Hurkman WJ, and Buchanan BB. Thioredoxin targets of developing wheat seeds identified by complementary proteomic approaches. *Phytochemistry* 65: 1629–1640, 2004.
544. Wood MJ, Storz G, and Tjandra N. Structural basis for redox regulation of Yap1 transcription factor localization. *Nature* 430: 917–921, 2004.
545. Wright MH, Paape D, Price HP, Smith DF, and Tate EW. Global Profiling and Inhibition of Protein Lipidation in Vector and Host Stages of the Sleeping Sickness Parasite Trypanosoma brucei. *ACS Infect Dis* 2: 427–441, 2016.
546. Wu Q, Hu Y, Sprague SA, Kakeshpour T, Park J, Nakata PA, Cheng N, Hirschi KD, White FF, and Park S. Expression of a monothiol glutaredoxin, AtGRXS17, in tomato (Solanum lycopersicum) enhances drought tolerance. *Biochem Biophys Res Commun* 491: 1034–1039, 2017.

Downloaded by LI CO SA/50127/MI from www.liebertpub.com at 07/22/19. For personal use only.

547. Wu Q, Lin J, Liu JZ, Wang X, Lim W, Oh M, Park J, Rajashekar CB, Whitham SA, Cheng NH, Hirschi KD, and Park S. Ectopic expression of Arabidopsis glutaredoxin AtGRXS17 enhances thermotolerance in tomato. *Plant Biotechnol J* 10: 945–955, 2012.
548. Xia XJ, Fang PP, Guo X, Qian XJ, Zhou J, Shi K, Zhou YH, and Yu JQ. Brassinosteroid-mediated apoplastic H2O2-glutaredoxin 12/14 cascade regulates antioxidant capacity in response to chilling in tomato. *Plant Cell Environ* 41: 1052–1064, 2017.
549. Xing S, Rosso MG, and Zachgo S. ROXY1, a member of the plant glutaredoxin family, is required for petal development in *Arabidopsis thaliana*. *Development* 132: 1555–1565, 2005.
550. Xing S and Zachgo S. ROXY1 and ROXY2, two Arabidopsis glutaredoxin genes, are required for anther development. *Plant J* 53: 790–801, 2008.
551. Xu S, Guerra D, Lee U, and Vierling E. S-nitrosoglutathione reductases are low-copy number, cysteine-rich proteins in plants that control multiple developmental and defense responses in Arabidopsis. *Front Plant Sci* 4: 430, 2013.
552. Yamazaki D, Motohashi K, Kasama T, Hara Y, and Hisabori T. Target proteins of the cytosolic thioredoxins in Arabidopsis thaliana. *Plant Cell Physiol* 45: 18–27, 2004.
553. Yang F, Bui HT, Pautler M, Llaca V, Johnston R, Lee B-H, Kolbe A, Sakai H, and Jackson D. A Maize Glutaredoxin Gene, Abphyl2, regulates shoot meristem size and phyllotaxy. *Plant Cell* 27: 121–131, 2015.
554. Yang J, Carroll KS, and Liebler DC. The expanding landscape of the thiol redox proteome. *Mol Cell Proteom* 15: 1–11, 2016.
555. Yang J, Gupta V, Carroll KS, and Liebler DC. Site-specific mapping and quantification of protein S-sulphenylation in cells. *Nat Commun* 5: 4776, 2014.
556. Yang J, Gupta V, Tallman KA, Porter NA, Carroll KS, and Liebler DC. Global, in situ, site-specific analysis of protein S-sulfenylation. *Nat Protoc* 10: 1022–1037, 2015.
557. Yang SS and Zhai QH. Cytosolic GAPDH: a key mediator in redox signal transduction in plants. *Biol Plant* 61: 417–426, 2017.
558. Yano H and Kuroda M. Disulfide proteome yields a detailed understanding of redox regulations: a model study of thioredoxin-linked reactions in seed germination. *Proteomics* 6: 294–300, 2006.
559. Yano H, Wong JH, Lee YM, Cho M-J, and Buchanan BB. A strategy for the identification of proteins targeted by thioredoxin. *Proc Natl Acad Sci U S A* 98: 4794–4799, 2001.
560. Yao Y, He RJ, Xie QL, Zhao Xh, Deng XM, He JB, Song L, He J, Marchant A, Chen X, and Wu A. Ethylene response factor 74 (ERF74) plays an essential role in controlling a respiratory burst oxidase homolog D (RbohD)-dependent mechanism in response to different stresses in Arabidopsis. *New Phytol* 213: 1667–1681, 2017.
561. Yoshida K, Hara A, Sugiura K, Fukaya Y, and Hisabori T. Thioredoxin-like2/2-Cys peroxiredoxin redox cascade supports oxidative thiol modulation in chloroplasts. *Proc Natl Acad Sci U S A* 115: E8296–E8304, 2018.
562. Yoshida K, Hara S, and Hisabori T. Thioredoxin Selectivity for Thiol-based redox regulation of target proteins in chloroplasts. *J Biol Chem* 290: 14278–14288, 2015.
563. Yoshida K and Hisabori T. Two distinct redox cascades cooperatively regulate chloroplast functions and sustain plant viability. *Proc Natl Acad Sci U S A* 113: E3967–E3976, 2016.
564. Yoshida K and Hisabori T. Distinct electron transfer from ferredoxin-thioredoxin reductase to multiple thioredoxin isoforms in chloroplasts. *Biochem J* 474: 1347–1360, 2017.
565. Yoshida K, Noguchi K, Motohashi K, and Hisabori T. Systematic exploration of thioredoxin target proteins in plant mitochondria. *Plant Cell Physiol* 54: 875–892, 2013.
566. Yoshida K, Terashima I, and Noguchi K. Up-regulation of mitochondrial alternative oxidase concomitant with chloroplast over-reduction by excess light. *Plant Cell Physiol* 48: 606–614, 2007.
567. Yu M, Yun BW, Spoel SH, and Loake GJ. A sleigh ride through the SNO: regulation of plant immune function by protein S-nitrosylation. *Curr Opin Plant Biol* 15: 424–430, 2012.
568. Yu Q, Tian H, Yue K, Liu J, Zhang B, Li X, and Ding Z. A P-Loop NTPase regulates quiescent center cell division and distal stem cell identity through the regulation of ROS homeostasis in arabidopsis root. *PLoS Genet* 12: e1006175, 2016.
569. Yu X, Pasternak T, Eiblmeier M, Ditengou F, Kochersperger P, Sun J, Wang H, Rennenberg H, Teale W, Paponov I, Zhou W, Li C, Li X, and Palme K. Plastid-localized glutathione reductase2-regulated glutathione redox status is essential for Arabidopsis root apical meristem maintenance. *Plant Cell* 25: 4451–4468, 2013.
570. Yun BW, Feechan A, Yin M, Saidi NBB, Le Bihan T, Yu M, Moore JW, Kang JG, Kwon E, Spoel SH, Pallas JA, and Loake GJ. S-nitrosylation of NADPH oxidase regulates cell death in plant immunity. *Nature* 478: 264–268, 2011.
571. Zaffagnini M, Bedhomme M, Groni H, Marchand CH, Puppo C, Gontero B, Cassier-Chauvat C, Decottignies P, and Lemaire SD. Glutathionylation in the photosynthetic model organism *Chlamydomonas reinhardtii*: a proteomic survey. *Mol Cell Proteom* 11: 014142, 2012.
572. Zaffagnini M, Bedhomme M, Lemaire SD, and Trost P. The emerging roles of protein glutathionylation in chloroplasts. *Plant Sci* 185–186: 86–96, 2012.
573. Zaffagnini M, Bedhomme M, Marchand CH, Couturier JR, Gao XH, Rouhier N, Trost P, and Lemaire SD. Glutaredoxin S12: unique properties for redox signaling. *Antioxid Redox Signal* 16: 17–32, 2012.
574. Zaffagnini M, Bedhomme M, Marchand CH, Morisse S, Trost P, and Lemaire SD. Redox regulation in photosynthetic organisms: focus on glutathionylation. *Antioxid Redox Signal* 16: 567–586, 2012.
575. Zaffagnini M, De Mia M, Morisse S, Di Giacinto N, Marchand CH, Maes A, Lemaire SD, and Trost P. Protein S-nitrosylation in photosynthetic organisms: a comprehensive overview with future perspectives. *Biochim Biophys Acta* 1864: 952–966, 2016.
576. Zaffagnini M, Fermani S, Calvaresi M, Orrù R, Iommarini L, Sparla F, Falini G, Bottoni A, and Trost P. Tuning Cysteine Reactivity and Sulfenic Acid Stability by Protein Microenvironment in Glyceraldehyde-3-Phosphate Dehydrogenases of *Arabidopsis thaliana*. *Antioxid Redox Signal* 24: 502–517, 2016.
577. Zaffagnini M, Fermani S, Costa A, Lemaire SD, and Trost P. Plant cytoplasmic GAPDH: redox post-translational modifications and moonlighting properties. *Front Plant Sci* 4: 450, 2013.

Downloaded by LI CO SA/50127/MI from www.liebertpub.com at 07/22/19. For personal use only.

578. Zaffagnini M, Michelet L, Massot V, Trost P, and Lemaire SD. Biochemical characterization of glutaredoxins from *Chlamydomonas reinhardtii* reveals the unique properties of a chloroplastic CGFS-type glutaredoxin. *J Biol Chem* 283: 8868–8876, 2008.
579. Zaffagnini M, Michelet L, Sciabolini C, Di Giacinto N, Morisse S, Marchand CH, Trost P, Fermani S, and Lemaire SD. High-resolution crystal structure and redox properties of chloroplastic triosephosphate isomerase from *Chlamydomonas reinhardtii*. *Mol Plant* 7: 101–120, 2014.
580. Zaffagnini M, Morisse S, Bedhomme M, Marchand CH, Festa M, Rouhier N, Lemaire SD, and Trost P. Mechanisms of nitrosylation and denitrosylation of cytoplasmic glyceraldehyde-3-phosphate dehydrogenase from *Arabidopsis thaliana*. *J Biol Chem* 288: 22777–22789, 2013.
581. Zannini F, Roret T, Przybyla-Toscano J, Dhalleine T, Rouhier N, and Couturier J. Mitochondrial *Arabidopsis thaliana* TRXo Isoforms Bind an Iron(-)Sulfur Cluster and Reduce NFU Proteins In Vitro. *Antioxidants (Basel)* 7, 2018.
582. Zechmann B. Compartment-specific importance of glutathione during abiotic and biotic stress. *Front Plant Sci* 5: 566, 2014.
583. Zechmann B. Compartment-Specific Importance of Ascorbate During Environmental Stress in Plants. *Antioxid Redox Signal* 29: 1488–1501, 2018.
584. Zeida A, González Lebrero MC, Radi R, Trujillo M, and Estrin DA. Mechanism of cysteine oxidation by peroxynitrite: an integrated experimental and theoretical study. *Arch Biochem Biophys* 539: 81–86, 2013.
585. Zhang D, Macinkovic I, Devarie-Baez NO, Pan J, Park CM, Carroll KS, Filipovic MR, and Xian M. Detection of protein S-sulfhydration by a tag-switch technique. *Angew Chem Int Ed Engl* 53: 575–581, 2014.
586. Zhang DW, Yuan S, Xu F, Zhu F, Yuan M, Ye HX, Guo HQ, Lv X, Yin Y, and Lin HH. Light intensity affects chlorophyll synthesis during greening process by metabolite signal from mitochondrial alternative oxidase in Arabidopsis. *Plant Cell Environ* 39: 12–25, 2016.
587. Zhang N and Portis AR, Jr. Mechanism of light regulation of Rubisco: a specific role for the larger Rubisco activase isoform involving reductive activation by thioredoxin-f. *Proc Natl Acad Sci U S A* 96: 9438–9443, 1999.
588. Zhang T, Zhu M, Zhu N, Strul JM, Dufresne CP, Schneider JD, Harmon AC, and Chen S. Identification of thioredoxin targets in guard cell enriched epidermal peels using cysTMT proteomics. *J Proteom* 133: 48–53, 2016.
589. Zhang X, Huang B, and Chen C. SNO spectral counting (SNOSC), a label-free proteomic method for quantification of changes in levels of protein S-nitrosation. *Free Radic Res* 46: 1044–1050, 2012.
590. Zhang X, Wang W, Li C, Zhao Y, Yuan H, Tan X, Wu L, Wang Z, and Wang H. Structural insights into the binding of buckwheat glutaredoxin with GSH and regulation of its catalytic activity. *J Inorg Biochem* 173: 21–27, 2017.
591. Zhao Y, Wei T, Yin KQ, Chen Z, Gu H, Qu LJ, and Qin G. Arabidopsis RAP2.2 plays an important role in plant resistance to *Botrytis cinerea* and ethylene responses. *New Phytol* 195: 450–460, 2012.
592. Zheng B, Zhu S, and Wu X. Clickable analogue of cerulenin as chemical probe to explore protein palmitoylation. *ACS Chem Biol* 10: 115–121, 2015.
593. Zhou X, Han P, Li J, Zhang X, Huang B, Ruan HQ, and Chen C. ESNOQ, proteomic quantification of endogenous S-nitrosation. *PLoS One* 5: e10015, 2010.
594. Zhu XG, Long SP, and Ort DR. What is the maximum efficiency with which photosynthesis can convert solar energy into biomass? *Curr Opin Biotechnol* 19: 153–159, 2008.
595. Ziegler H and Ziegler I. Der Einfluss der Belichtung auf Die $NADP^+$-Abhängige Glycerinaldehyd-3-Phosphat-Dehydrogenase. *Planta* 65: 369–380, 1965.

Addresses correspondence to:
Dr. Mirko Zaffagnini
Department of Pharmacy and Biotechnology
University of Bologna
Via Irnerio 42
Bologna 40126
Italy

E-mail: mirko.zaffagnini3@unibo.it

Prof. Paolo Trost
Department of Pharmacy and Biotechnology
University of Bologna
Via Irnerio 42
Bologna 40126
Italy

E-mail: paolo.trost@unibo.it

Date of first submission to ARS Central, July 23, 2018; date of final revised submission, November 15, 2018; date of acceptance, November 26, 2018.

Abbreviations Used

ACHT = atypical Cys histidine-rich thioredoxin
APX = ascorbate peroxidase
BASI = barley alpha-amylase/subtilisin inhibitor
BST = biotin switch technique
CAT = catalase
CB = Calvin–Benson
CDSP32 = chloroplastic drought-induced stress protein
cICAT = cleavable isotope-coded affinity tag reagents
Cys = cysteines
DTT = dithiothreitol
ERF-VII = group VII ethylene response factors
FBPase = fructose-1,6-bisphosphate phosphatase
FDX = ferredoxin
Fe-S = iron–sulfur
FTR = ferredoxin:thioredoxin reductase
GAPC = glyceraldehyde-3-phosphate dehydrogenase C (cytoplasmic isoform)
GAPDH = glyceraldehyde-3-phosphate dehydrogenase
GFP = green fluorescent protein
GOX = glycolate oxidase
GPLXs = glutathione peroxidases-like
GRX = glutaredoxin
GSH = reduced glutathione
GSNO = nitrosoglutathione
GSNOR = nitrosoglutathione reductase

Downloaded by LI CO SA/50127/MI from www.liebertpub.com at 07/22/19. For personal use only.

Abbreviations Used (Cont.)

GSSG = oxidized glutathione
GST = glutathione-S-transferase
H_2O_2 = hydrogen peroxide
H_2S = hydrogen sulfide
iTRAQ = isobaric tag for relative and absolute quantification
MMTS = methyl methanethiosulfonate
MS = mass spectrometry
MSBT = methylsulfonyl benzothiazole
NADP-MDH = NADP-malate dehydrogenase
NEM = N-ethyl maleimide
NOFNiR = NO-forming nitrate reductase
NPQ = nonphotochemical quenching
NR = nitrate reductase
NRX = nucleoredoxins
NTR = NADPH:thioredoxin reductase
NTRC = NADPH:thioredoxin reductase C
PCO = plant cysteine oxidase
PDI = protein disulfide isomerase
PET = photosynthetic electron transport
PRK = phosphoribulokinase
PRX = peroxiredoxin
PS1 = photosystem 1
PTM = post-translational modification
QY = quantum yield
RBOH = respiratory burst oxidase homologue
RMS = reactive molecular species
RNS = reactive nitrogen species
ROS = reactive oxygen species
RSS = reactive sulfur species
RubisCO = ribulose-1,5-bisphosphate carboxylase/oxygenase
SBPase = sedoheptulose-1,7-biphosphate phosphatase
SiR = sulfite reductase
SNOSID = SNO site identification
SOD = superoxide dismutase
TGA = TGACG motif-binding
TDX = tetratricopeptide domain-containing thioredoxin
TMT = tandem mass tag
TR = thioredoxin reductase
TRX = thioredoxin
TRXL2 = thioredoxin-like2
YFP = yellow fluorescent protein
WCGPC = tryptophan-cysteine-glycine-proline-cysteine
WCPPC = tryptophan-cysteine-proline-proline-cysteine

Downloaded by LI CO SA/50127/MI from www.liebertpub.com at 07/22/19. For personal use only.